1971

Static and dynamic flexural behavior of a prestressed concrete i-beam bridge - bartonsville bridge, January 1971

C. H. Chen

David A. VanHorn

COMMONWEALTH OF PENNSYLVANIA

Department of Transportation

Bureau of Materials, Testing and Research

Leo D. Sandvig - Director
Wade L. Gramling - Research Engineer
Kenneth L. Heilman - Research Coordinator

Project 67-12: Lateral Distribution of Load for Bridges constructed with Prestressed Concrete I-Beams

STATIC AND DYNAMIC FLEXURAL BEHAVIOR of a PRESTRESSED CONCRETE I-BEAM BRIDGE

BARTONSVILLE BRIDGE

by

Chiou-Horng Chen
David A. VanHorn

This work was sponsored by the Pennsylvania Department of Transportation; U. S. Department of Transportation, Federal Highway Administration; and the Reinforced Concrete Research Council. The opinions, findings, and conclusions expressed in this publication are those of the authors, and not necessarily those of the sponsors.

LEHIGH UNIVERSITY

Office of Research

Bethlehem, Pennsylvania

January, 1971

Fritz Engineering Laboratory Report No. 349.2

TABLE OF CONTENTS

ABSTRACT

This report describes the field testing of an existing beam-slab highway bridge constructed with prestressed concrete I-beams as the main longitudinal girders. The maximum moment cross-section (near midspan), and a cross-section near quarter-span, were selected as the test sections. The principal objectives of the testing were: (1) to evaluate the lateral distribution of live load, and (2) to establish the amplification characteristics of crawl run response under dynamic and controlled impact loading.

It was found that the experimental distribution factors for the interior girders were near the design value, as specified in the PennDOT Bridge Division Standards[1], and in the AASHO Specifications[2]. For the exterior girders, the experimental values were greater than the design values. Considering the over-all behavior of the entire superstructure (subsequently termed total-bridge behavior), the dynamic load factors at the maximum moment section were found to be less than the factor $(1 + \frac{50}{125 + L})$, while at the quarter-span section, the factors were slightly greater than $(1 + \frac{50}{125 + L})$. In the controlled impact tests (test vehicle at 10 mph, passing over a 2-inch ramp at the test section), the experimental impact factors for the total bridge behavior ranged from 1.59 to 1.95, in all cases greater than $(1 + \frac{50}{L + 125})$.

For single-vehicle loading, the distribution coefficients at the maximum moment section were more uniform than the

coefficients at the quarter-span section. However, because of the compensating effect resulting from multi-lane loading, the distribution factors at both sections were nearly equal. For the present, it is recommended that the use of current design specifications for live load distribution in I-beam bridges be continued. However, it is strongly recommended that further work be devoted to the development of new provisions which parallel the proposed provisions for the spread box-beam superstructure.

1. INTRODUCTION

1.1 Background

Since the completion of the first prestressed concrete bridge in the United States in 1951, design engineers have been confronted with the problem of distribution of live loads in prestressed concrete beam-slab type bridges. At that time, the provisions for lateral distribution in the then current AASHO Standard Specifications for highway bridges made no differentiation between the various types of beams used in supporting reinforced concrete decks. Since that time, the specifications have been expanded to include more shapes and types of beams. In the 1969 edition[2], one distribution factor was listed to cover all prestressed concrete girders. However, since there are several kinds of prestressed concrete girders which have been used in highway bridge construction, it is felt that the one distribution factor cannot accurately represent all shapes.

In Pennsylvania, precast prestressed concrete beams have been used since 1951. In 1956, the I-beam shape was added to the existing box-beam shape, and same distribution factor for interior girders has been used for both shapes in I-beam or spread box-beam superstructures. This factor specified in the PennDOT Standards for Prestressed Concrete Bridges[1], is identical to that given in the AASHO Specifications, Section 3, governing the distribution of wheel loads to interior steel I-beam stringers and prestressed

concrete girders. The distribution of live load for the exterior girders is based on the assumption that the slab acts as a simple span between girders, in transmitting wheel loads laterally. See Fig. 1.

Since 1964, an investigation has been underway at Lehigh University to evaluate the structural behavior of bridges of the spread box-beam type, including the development of an analytical method[1a] for the determination of distribution factors.

Realizing that one of the basic differences between the structural behavior of the I-beam and that of the box-beam is the result of torsional rigidity, and that this characteristic is an important factor in the distribution of live load, it was felt that a similar investigation should be directed toward the beam-slab system supported with prestressed concrete I-beams. Therefore a parallel investigation was initiated in 1968 to develop information on several aspects of the structural behavior of I-beam bridges.

1.2 Objectives

Following a literature survey[20], a field test of an in-service I-beam bridge was planned with the following objectives:

1. To establish information on lateral distribution of design vehicle loading at crawl speed.
2. To establish (1) critical speed(s) at which maximum amplification of crawl-run response is achieved, and (2) the magnitude of the maximum amplification.

3. To establish the amplification of crawl-run response, under impact loading.

4. To develop information on stresses on the surface of the slab in both lateral and longitudinal directions.

5. To develop information on stresses in slab reinforcement.

6. To compare the structural behavior of I-beam bridges with that of spread box-beam bridges previously tested.

Items 1, 2, 3, and 6 will be covered in this report.

2. TESTING

2.1 Test Bridge

The test bridge (S-3724), as shown in Fig. 2, is located near Bartonsville, Monroe County, Pennsylvania, and carries L.R. 1002 over Pocono Creek and over L.R. 45033.

The sixth span of the ten-span bridge, as illustrated in Fig. 3, was chosen as the test span. The test span is simply supported with a length of 68 feet 6 inches center-to-center of bearings, and with a skew of 90°.

The cross-section of the test bridge, as shown in Fig. 4, consists of five identical prestressed I-beams, covered with a cast-in-place reinforced concrete deck. The I-beams which are of the standard AASHO Type III cross-section shown in Fig. 5, are spaced at 8 feet, center-to-center. The reinforced concrete deck provides a roadway width of 32 feet. The specified minimum thickness of the slab is 7-1/2 inches. However, measurements indicated that the actual slab thickness at Section M ranges from 6.1 to 7.3 inches, and at Section Q from 5.7 to 7.7 inches, as shown in Fig. 6.

The dimensions of the curb and parapet sections are shown in Fig. 4. There is a construction joint between the slab and the curb section, and vertical reinforcement extends from the slab into the curb and parapet sections. Diaphragms between the beams are located at the ends of the span above the end supports

and at midspan. Dimensions of the diaphragms are shown in Fig. 5. Additional details are given in the PennDOT Standards For Prestressed Concrete Bridges[1].

The girders were designed for AASHO HS 20-44 loading. A distribution factor of S/5.5 = 1.455 was used for the interior girders, while the factor of 0.75 was used for the exterior girders. The impact factor was computed as $\frac{50}{125 + L} = 0.258$. The specified minimum 28-day cylinder strength of the girder concrete was 5000 psi. Each of the girders was pretensioned with 34 7/16-in. seven-wire strands.

2.2 Gage Sections and Locations

As shown in Fig. 3, two cross-sections, M and Q, were selected for the location of strain gages. Section M was 3.55 feet east of midspan, while Section Q was located 16.75 feet west of the east support. Theoretically, the maximum girder moment would occur at Section M, as the drive axle passed over the section with the load vehicle moving eastward. Section Q was selected as a section relatively unaffected by the midspan diaphragms. The locations of all strain gages are shown in Fig. 7. Also shown are the locations of the deflection gages mounted at Section M used to measure both vertical deflections and rotations.

2.3 Instrumentation

All strain gages used in the testing were of the SR-4 electrical resistance type, manufactured by the Baldwin-Lima-

Hamilton Corporation. Initially, each gage location was ground smooth, cleaned with acetone, and sealed with diluted SR-4 cement. The strain gages were mounted in position with undiluted SR-4 cement after the initial coat had cured. Gages applied to the top surface of the slab were waterproofed.

Each deflection gage consisted of four strain gages bonded to a flexible, triangular aluminum plate. The aluminum plate was attached to a bar which was clamped along the bottom edge of the girder, perpendicular to the longitudinal axis of the girder. At the apex of the aluminum plate, a wire was connected to a weight resting on the ground surface. The wire was adjusted to impose an initial downward deflection of the plate. Each deflection gage was calibrated so that changes of flexural strain in the plate occurring when the girder was deflected, could be converted to deflections. With the deflection gages mounted in this manner, the vertical deflection of each beam was equal to the average of the two deflections at the ends of the bar, while the rotation was equal to the difference between the two end deflections divided by the bar length.

2.4 Timing and Position Indicators

Three air hoses were used as position indicators. These hoses were placed normal to the center-line of the roadway at Section M, 40 feet east of Section M, and 40 feet west of Section M. An abrupt offset was produced on the oscillograph traces from

the strain gages as the wheels of the vehicle passed over one of the hoses. These offsets were used to correlate the truck position with strain values from the individual gages. Two additional hoses, located 90 feet east and west of Section M, were used to monitor the speed of the vehicle. A timer was actuated as the front axle of an approaching vehicle passed over the first hose, and was shut off as the front axle passed over the other hose.

2.5 Test Vehicle

The vehicle used for testing was a diesel-powered tractor and semi-trailer unit, provided by the Federal Highway Administration. The truck was loaded with crushed stone to approximate the AASHO HS 20-44 design loading[2]. A photograph of the test vehicle, along with the wheel spacing and the actual axle loading, is shown in Fig. 8.

2.6 Loading Lanes

Seven loading lanes were located on the roadway, as shown in Fig. 9, such that the center-line of the truck would coincide with the center-line of the girder or with a line located midway between two girders.

2.7 Test Runs

A total of 136 runs were divided into two series, as shown in Table 1. Crawl runs, conducted at approximated 2 mph, were considered as representing the static load condition.

Dynamic runs and impact runs were also conducted in this field investigation. The nominal speed of the dynamic runs was varied from 5 mph to 60 mph in 2-1/2 mph increments, while the nominal speed of the impact runs was 10 mph. For the impact runs, wooden ramps were located near Section Q or near Section M such that the wheels of the truck would have a 2-inch drop at one of the test sections.

In the first test series, all strain gages were recorded, except those at locations 46, 47, 49, and 50, as shown in Fig. 7. In the second series, the gages recorded included all of the beam gages at Section Q and all deflection gages at Section M.

Before and after a sequence of test runs, the gages were calibrated with no live load on the bridge, to relate the relationship of the oscillograph traces to base values. Generally, the time interval between consecutive calibrations was not more than two hours.

3. DATA REDUCTION AND EVALUATION

3.1 Oscillograph Trace Readings

In the data reduction process, the first step was to relate each oscillograph trace to a particular strain or deflection gage, based on relative positions of a series of breaks in the traces. This procedure was termed editing. After the editing was completed, the no-load readings were taken. Next, the excursions at the peaks of the tracings and the calibration values for each gage were measured with an accuracy of 0.01 inch. The vertical excursions were then calculated by subtracting the no-load readings from the peak values.

3.2 Deflections and Primary Strains

In order to obtain the deflections and strains, two fortran IV computer programs were developed for use with the CDC 6400 computer. The program inputs consisted of the beam numbers, gage numbers, test sections, locations of the gages, connecting cable lengths, lengths of deflection gage anchorage wires, deflection-strain ratios, gage resistances, gage factors, operation attenuations, vertical excursions of the traces, and equivalent calibration values. The outputs from the computer program for deflections were deflections and rotations of the girders. For the strain program, primary strains were first calculated. Since the locations of the gages were not in one vertical plane, the least-square method could not be directly applied

Therefore, a different method was developed to obtain the strain distribution, as described in Section 3.3.

3.3 Evaluation of Strains and Location of Neutral Axes

In evaluating the magnitudes of the longitudinal strains and the locations of the neutral axes in the beams, the basic assumption was made that the distribution of normal strains across the face of a beam cross-section is planar. With reference to Fig. 10, gages 1, 2, 3, and 4 were used to locate the position of the plane, the location of the neutral axes, and the strain distribution along the vertical axis of symmetry. In locating the plane, it was first assumed that the plane passed through three of the gage readings. The offset of the fourth reading from the resulting plane was then computed. This process was then repeated three times, in each case using a different combination of three gages to locate the plane. The plane finally selected was the one for which the offset of the fourth reading was a minimum.

With reference to Fig. 11, the neutral axis under biaxial bending, shown as IKTN, intersects the y-axis at the point T. By rotating the theoretical strain lines (Fig. 10) into the plane of the cross-section, the strains ϵ_1, ϵ_2, ϵ_3, and ϵ_4 are represented in Fig. 11 by lines 1A, 2H, 3P, and 4E respectively. Strain distribution lines IA, KP, TE, and NH intersect the vertical lines at I, K, T, and N, respectively, to form the neutral axis IKTN.

Lines JC, MG, and QL were drawn parallel to the original strain lines such that strains 1A, 2H, and 3P are equal to BC, FG,

and QS, respectively. Then, the theoretical strain distribution is represented by the line RTDE, and the general equation for the straight line is of the form:

$$\epsilon = ay + b \tag{1}$$

where ϵ is the strain along the y-axis, a is the slope, and b is the strain at point U ($y = 0$). Therefore, b is equal to UE and a is equal to $-(UE)/(UT)$. The deviations of the measured strains ϵ_1, ϵ_2, and ϵ_3 are CD, VG, and QR, respectively.

From the parallely diagonal lines in Fig. 11, $CD = JJ'$, $VG = MM'$, and $QR = TT'$. Next, let $D_1 = -CD$, $D_2 = +VG$, $D_3 = -QR$, and $D_4 = 0$, where the negative and positive signs indicate deviations in opposite directions from the theoretical line RTDE. Then, the distances of the gages from the y-axis are represented by $d_1 = 1B$, $d_2 = F2$, $d_3 = 3S$, and $d_4 = 0$,

$$D_1 = \epsilon_1 - (ay_1 + b) \tag{2}$$

$$D_2 = \epsilon_2 - (ay_2 + b) \tag{3}$$

$$D_3 = \epsilon_3 - (ay_3 + b) \tag{4}$$

From similar triangles,

$$-\frac{D_1}{D_2} = \frac{CD}{VG} = \frac{JJ'}{MM'} = \frac{JT}{MT} = \frac{IJ}{MN} = \frac{d_1}{d_2}$$

Likewise,

$$-\frac{D_2}{D_3} = \frac{d_2}{d_3} \quad \text{and} \quad \frac{D_1}{D_3} = \frac{d_1}{d_3}$$

Then

$$\frac{D_1}{D_2} = \frac{\epsilon_1 - (ay_1 + b)}{\epsilon_2 - (ay_2 + b)} = -\frac{d_1}{d_2} \tag{5}$$

$$\frac{D_2}{D_3} = \frac{\epsilon_2 - (ay_2 + b)}{\epsilon_3 - (ay + b)} = -\frac{d_2}{d_3} \tag{6}$$

$$\frac{D_1}{D_3} = \frac{\epsilon_1 - (ay_1 + b)}{\epsilon_3 - (ay_3 + b)} = \frac{d_1}{d_3} \tag{7}$$

Simplfying equations (5), (6), and (7),

$$(d_1y_2 + d_2y_1)\ a + (d_2 + d_1)\ b = d_1\epsilon_2 + d_2\epsilon_1 \tag{8}$$

$$(d_3y_2 + d_2y_3)\ a + (d_2 + d_3)\ b = d_3\epsilon_2 + d_2\epsilon_3 \tag{9}$$

$$(d_1y_3 - d_3y_1)\ a + (d_1 - d_3)\ b = d_1\epsilon_3 - d_3\epsilon_1 \tag{10}$$

Now, the only unknowns are a and b, and any two of the three equations, (8), (9), and (10), may be used to determine the two values. If equations (9) and (10) are used,

$$a = \frac{(d_1\epsilon_3 - d_3\epsilon_1)\ (d_1 - d_3) - (d_1\epsilon_2 + d_2\epsilon_1)\ (d_2 + d_1)}{(d_1y_2 + d_2y_1)\ (d_1 - d_3) - (d_1y_3 - d_3y_1)\ (d_2 + d_1)} \tag{11}$$

$$b = \frac{(d_1\epsilon_3 - d_3\epsilon_1)\ (d_1y_2 + d_2y_1) - (d_1\epsilon_2 + d_2\epsilon_1)\ (d_1y_3 - d_3y_1)}{(d_1y_2 + d_2y_1)\ (d_1 - d_3) - (d_1y_3 - d_3y_1)\ (d_2 + d_1)} \tag{12}$$

Utilizing equation (1) with these calculated values of a and b, a value of ϵ_4 can be calculated. Next, the absolute deviation of the strain at location 4 is defined and calculated as

$$DD_4 = \left| \epsilon_4 \text{ (experimental)} - \epsilon_4 \text{ (calculated)} \right|$$

This value of DD_4 is based on an analysis assuming that the measured strains ϵ_1, ϵ_2, and ϵ_3 were correct. A similar analysis was then used to establish absolute deviation values DD_1, DD_2, and DD_3. The analysis which yielded the smallest value of the absolute deviation was then selected as representative of the strain distribution for the I-beam cross-section, as shown in Fig. 10.

3.4 Effective Slab Widths, Moment Coefficients, Distribution Coefficients, and Modulus of Elasticity

After the data had been processed through the computer program described in Section 3.2, the principal output included the strains at the bottom face of each girder (ϵ_b), and the slopes of the linear strain distribution along the y-axis for each girder. A second program was then developed to utilize the output from the first program, along with supporting information (modular ratio, total bending moment produced by the test vehicle, dimensions of the cross-section of the superstructure, etc.) to compute the effective slab widths, moment coefficients, and distribution coefficients for each of the beams. In addition, the flexural modulus of elasticity was computed for each of the crawl runs.

In the first step, the transformed effective slab and curb widths were determined by equating first moments of the compressive and tensile areas of each composite beam, with respect to the computed location of the neutral axis. In this step it was assumed that the curb section acted compositely with the slab and the exterior beam, and that there was no longitudinal end-restraint in the beams.

After the moment of inertia had been calculated for each beam, the moment coefficients were determined from

$$\frac{M}{E} = \frac{I\epsilon_b}{c} \tag{13}$$

where $\frac{M}{E}$ is the moment coefficient, I is the moment of inertia of the composite beam, ϵ_b is the fiber strain at the bottom face of the beam, and c is distance from the neutral axis to the bottom face of the beam.

Finally, the distribution coefficients for the beams were computed. The distribution coefficient for a beam was defined and calculated as the ratio of the moment coefficient for that beam to the sum of the moment coefficients for all five beams, for the load vehicle in a particular loading lane. At Section Q, since only girders A, B, and C were gaged, the moment coefficients for girders D and E were taken as the values from girders A and B, when the truck was located in a symmetric lane on the opposite side of the bridge. For Section M, the same procedure was followed. The calculated flexural modulus of elasticity of the beam

concrete was obtained by dividing the total bending moment produced by the load vehicle at the test section, by the sum of the experimentally determined composite beam moment coefficients.

3.5 Influence Lines

Influence lines were developed for bending moment at Sections M and Q in Beams A, B, and C. These influence lines represent the moment coefficients as a function of the lateral location of the load vehicle on the roadway.

Also, influence lines for the vertical deflection of the individual beams were prepared, based on measurements at Section M.

3.6 Distribution Factors

Design provisions for the lateral distribution of live load in beam-slab superstructures are provided in the AASHO Specifications[2] in the form of distribution factors. These factors are defined as the fraction of each wheel load in a design vehicle to be applied to the individual beams. No longitudinal distribution is assumed. Basically, for girders, this fraction is of the form S/K where S is the center-to-center beam spacing (in feet) and K is specified as 5.5 for prestressed concrete beams. For exterior girders the fraction is determined by calculating the reactions of the wheel loads obtained by assuming the flooring to act as a simple span between beams.

In addition, the Specifications list the number of

design load lanes as a function of roadway width. In the Bartonsville test bridge, the roadway width is 32 feet, and the bridge carries two lanes of traffic. However, since the AASHO Specifications specify that three lanes of traffic should be considered for a width of 32 feet, experimental values for the distribution factors were developed for both two- and three-lane loading. For the two-lane case, the bridge was divided into two equal lanes, 16 feet in width. Therefore, in developing the experimental values, the vehicle positions could be laterally shifted over a width of six feet since the design vehicle is considered to occupy a width of ten feet. These values were determined by adding the maximum coefficients produced by vehicles in the two lanes. The sum was then multiplied by two since the distribution factor is defined as a factor applicable to the wheel loads. For the three-lane case, each design lane was 10 feet 8 inches in width, reducing the allowable lateral shifting of the vehicle in each lane to 8 inches. The same general procedure was used to determine the three-lane values.

3.7 Dynamic Load Factors and Impact Factors

The dynamic load factor $(DLF)_m$ was defined as the ratio of the bending moment produced by the load vehicle moving at a particular speed in a particular load lane, to the moment produced by the vehicle at crawl speed in the same lane. Values were computed for individual beams and for the entire bridge considered as

a unit. Similar factors $(DLF)_d$ were defined and computed on the basis of deflections at Section M. These dynamic load factors serve as indices of the amplification of static live load response produced by moving vehicles.

In an attempt to compare values of $(DLF)_m$ and $(DLF)_d$, based on the behavior of the total superstructure, the following equation was used to determine $(DLF)_d$:

$$(DLF)_d = \frac{[1.25\ (\delta_A + \delta_E) + \delta_B + \delta_C + \delta_D] \text{ at speed}}{[1.25\ (\delta_A + \delta_E) + \delta_B + \delta_C + \delta_D] \text{ at crawl}} \qquad (14)$$

where δ_A, δ_B, δ_C, δ_D, and δ_E are the deflections of the individual beams. The factor 1.25 represents the ratio of the moment of inertia (I) of the composite exterior beam to the I of a composite interior beam. Therefore, with the weighted values of I, the $(DLF)_d$ should provide a reasonable approximation of the $(DLF)_m$[17].

Impact factors $(IF)_m$ were also developed, based on the ratios of moments at Section M in the controlled impact runs (See Section 2.7) to moments in the crawl runs.

3.8 Vibration Frequency

Two frequencies of vibration were evaluated from the test data. First, the natural frequency of the superstructure was determined, utilizing the deflection data from the impact runs. After the vehicle had passed over the bridge, a decaying pattern of oscillation was reflected in the deflection gage traces. The

natural frequency was determined as the number of vibration cycles in a one-second period (See Fig. 12). Next, the loaded frequencies were determined for all of the speed runs. The gage traces with the vehicle on the structure were non-uniform, as would be expected. Therefore, the loaded frequency was defined as the frequency when the vehicle was at the test section, and calculated based on the time interval between the two successive peak values nearest the point at which the vehicle was at the test section (See Fig. 12). The results presented are based on average values from the six beam-deflection gages.

4. PRESENTATION OF TEST RESULTS

4.1 Moment Coefficients and Modulus of Elasticity

The moment coefficients are presented in Tables 2 - 8. Each moment coefficient represents the flexural moment carried by each girder at one of the test sections, with the vehicle in a designated loading lane. In Table 2, moment coefficients from the crawl runs are presented, representing the behavior of the bridge under static loading.

To obtain the values in Table 2, the data from the test runs were paired in all possible combinations to yield the individual values. Therefore, each value represents the average of from six to thirteen experimental values. The experimental values of modulus of elasticity, shown in Table 2 for each loading lane, were determined by dividing the total vehicle moment at the specified section by the summation of moment coefficients of the five girders. Tables 3 - 6 list the moment coefficients for the speed runs from 5 mph up to 63.8 mph, while Tables 7 and 8 list values for the impact runs.

4.2 Distribution Coefficients

Distribution coefficients, expressed as percentages of the total vehicle moment distributed to the individual girders, are presented in Tables 10 - 14 and Figs. 13 - 16. Distribution coefficients based on deflections are shown in Table 14.

Table 10 lists the distribution coefficients at Sections M and Q, resulting from the crawl runs. These coefficients are graphically presented in Figs. 13 - 16. The speed runs are covered in Tables 11 and 12, and the impact runs in Table 13.

4.3 Influence Lines

Influence lines for the crawl-run distribution coefficients for each girder are shown in Figs. 17 and 18. Actually, the influence lines in the two figures are identical, but each figure portrays a different loading condition. For each girder, there are two influence lines. The solid line represents the variation in coefficient at Section M, while the dashed line represents the variation at Section Q.

The influence lines for deflections of the girders at Section M are shown in Fig. 19.

4.4 Distribution Factors

The distribution factors were determined as explained in Section 3.6. Table 15 lists the distribution coefficients determined from the influence lines, for both two and three traffic lanes. In Table 16, the experimental distribution factor at Sections M and Q for both two and three traffic lanes, are tabulated, along with PennDOT design values. In the last two columns, the ratios of experimental values to design values are given.

Graphical comparisons of the distribution factors listed in Table 16 are shown in Figs. 20 and 21. The numbers shown in

the bars representing experimentally based values, refer to the contributions by vehicles in the indicated load lanes.

4.5 Girder Deflections and Rotations

Girder deflections and rotations are given in Tables 17 - 24. Tables 17 and 21 list the crawl-run deflections and rotations of the girders at Section M. Tables 18, 19, 22, and 23 list the deflections and rotations for the speed runs in Lanes 2 and 4, respectively, while Tables 20 and 24 list the girder deflections and rotations at Section M under impact runs. As mentioned previously, influence lines for deflections are given in Fig. 19. The comparison of maximum deflections of each beam for crawl, speed, and impact runs is presented in Table 31, to illustrate the deflection fluctuations due to vehicle speed and impact load.

4.6 Neutral Axes and Effective Slab Widths

The locations of the neutral axes and the effective slab widths, obtained as explained in Sections 3.3 and 3.4, are shown in Tables 25 - 30. The locations of the neutral axes and effective slab widths at Sections M and Q, for crawl runs and impact runs under various lane loadings, are tabulated in Tables 25 and 28, respectively. Typical examples of girder deflections and rotations for various lane loadings are shown in Fig. 22. For speed runs of the vehicle in Lane 2, the locations of neutral axes and effective slab widths at Section M are shown in Tables 26 and 29, respectively. Tables 27 and 30 tabulate the same information, for the vehicle moving in Lane 4.

4.7 Dynamic Load Factors and Impact Factors

Dynamic load factors $(DLF)_m$ and impact factors $(IF)_m$ were determined as explained in Section 3.7. Tables 3 and 4 list the dynamic load factors at Section M for the vehicle in Lanes 2 and 4, respectively, and Tables 5 and 6 list the factors at Section Q. The dynamic load factors based on deflections $(DLF)_d$ are shown in Tables 18 and 19.

Several figures were plotted to illustrate the amplification of static moments, and the fluctuation of girder deflections, produced in the speed runs. Figures 23 - 25 were used to illustrate the variation in $(DLF)_m$, and Fig. 26 the $(DLF)_d$ for the behavior of the total superstructure. Similarly, Figs. 27 - 38 portray similar variation in the $(DLF)_m$ and the $(DLF)_d$ for the individual beams. The impact factors $(IF)_m$ for the 10 mph impact runs are listed in Table 9.

5. DISCUSSION OF RESULTS

5.1 Symmetry of Cross-Section and Applicability of Superposition

In Fritz Engineering Laboratory Report No. 315.2[4], the test results from a fully-gaged section were compared with those from a section in which only the beams on one side of the roadway center-line were gaged. The agreement verified the use of superposition for the subsequent tests of similar bridges, and therefore, in the Bartonsville Bridge, only three of the five girders were fully gaged.

At Section Q, gages 47 and 50 were used to check the strains of gages 30 and 40. For instance, the strains of gage 30 with the load vehicle in Lane 1 should be equal to the strains of gage 47 with the vehicle in Lane 7. The differences in strains were very small. Therefore, the idealization of symmetry of the cross-section was reasonable.

All of the measured strains were small, with a maximum of approximately 1.20×10^{-4} in/in. In addition, the bridge deflections were very small, and the material stresses were within the elastic ranges of the materials. Therefore, the validity of the use of superposition was established[3,4,5,6,7].

5.2 Experimental Strains, Neutral Axes, and Effective Slab Widths

As mentioned in Section 3.3 three gages were theoretically sufficient to determine the location of the neutral axis. However, because of the consideration of biaxial bending and torsion with the experimental variation of the location of the neutral axis, it is suggested that in future bridge tests at least seven gages should be applied, as shown below.

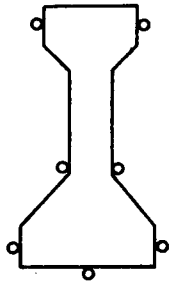

As in the previous tests of box-beam bridges[7], the neutral axes (Tables 25 - 27) were at the highest levels when the truck was directly above the girder, and at progressively lower levels as the truck moved to lanes farther away from this girder. It was also observed that there was only a small variation of neutral axis locations through the change of speed (Tables 26 - 27).

The variation of effective slab width was very great in some cases, even for identical loading conditions. This was primarily due to the sensitivity of the computed effective slab width to small changes in the experimentally determined locations of the neutral axes. When the strains were small, an accurate

determination of the neutral axis locations was very difficult.

From Tables 26, 27, 29, and 30, the variations in locations of neutral axes and in effective slab widths were larger at Section Q than at Section M because the variations of small strains at Section Q would affect the computed neutral axis locations and effective slab widths to a much greater extent than would similar variations of larger strains at Section M. Fortunately, moment coefficients are in a good agreement for identical runs. That is, moment coefficients are relatively insensitive to the changes of effective slab widths and small variations in locations of neutral axes.

5.3 Moment Coefficients and Distribution Coefficients

Comparisons of moment coefficients developed for Sections M and Q are shown in Figs. 39 - 44. In these figures, the curve representing the speed run of the load vehicle indicates the maximum speed-run response for the vehicle in the load lane indicated. For the interior girders, the crawl-run values amplified by the factor $(1 + \frac{50}{125 + L})$ are usually greater than the values from the speed runs, while for exterior girders, the amplified crawl-run values were less than speed-run values, indicating a more uniform distribution of load to the individual girders.

Under single-vehicle loading (Figs. 45 - 50), the distribution coefficients were more uniform at Section M than at

Section Q, due in part to the effect of midspan diaphragms. This effect extends from crawl runs to speed runs (Figs. 49 - 50). A similar phenomenon is shown in Fig. 17, where the influence lines for distribution coefficients at Section M have a smaller range from maximum to minimum than those developed for Section Q.

The distribution coefficients were also more uniform in the impact runs (Figs. 45 - 48) than in the crawl runs, because the increases in the moment coefficients for the girders (Figs. 41 - 44), due to impact, were not uniformly proportional to the static values.

5.4 Distribution Factors

As shown in Tables 15 and 16, Figs. 20 and 21, the experimental distribution factors at Sections M and Q are quite close. This phenomenon resulted from the compensating effect when the effects from placement of the vehicle in the design lanes were superimposed to produce maximum loading in each of the girders[7]. Therefore, it appears that the use of diaphragms is not significant, as related to effects on the live load distribution factors.

For two design traffic lanes, results similar to those presented in previous reports[3,4,5,6,7,8] show that the experimental distribution factors for exterior girders are greater than the design value. Conversely, the experimental distribution factors for interior girders are less than the design value. For

three design traffic lanes, the experimental distribution factors for the exterior beam A are again greater than the design value. For beam B, the experimental values are less than the design value, but significantly greater than for the two-lane loading case. For beam C, the experimental values are slightly greater than the design value. Although some of the experimental values are greater than the design values, there is actually no overstressing in either beam A or beam C. Beam A is substantially stiffened by the composite action with the curb and parapet sections, and beam C is not subjected to three-lane loading conditions.

In comparing the experimental factors for the Drehersville Bridge[3,4,8] with those for the Bartonsville Bridge (Table 32), the factors for interior girders were greater in the I-beam bridge. Factors for the exterior girders were greater in the box-beam bridge. (Note: The Drehersville Bridge was a spread box-beam type bridge having dimensions of length, width, beam spacing, etc., similar to those of the Bartonsville Bridge.) This indicates that the distribution factor analytically developed for interior girders of box-beam bridges[12] is not appropriate for use in I-beam bridges. Therefore a revision of the analysis is necessary for the development of distribution factors of similar form for I-beam bridges.

The experimental distribution factors for interior girders of I-beam bridges (Table 32) are near the AASHO design value[3]. Therefore, this design value, $\frac{S}{5.5}$, could be reasonably used in the design of I-beam bridges with dimensions similar to those of the

Bartonsville Bridge, until a more accurate method is developed.

5.5 Dynamic Load Factors and Impact Factors

The terms "dynamic load factor" and "impact factor" are defined in Section 3.7.

5.5.1 Dynamic Load Factors (DLF)

From the response indicated in Figs. 23 - 38, the dynamic load factors are sensitive to location and speed of the truck. In general, the $(DLF)_m$ is more uniform at Section M than at Section Q, under the single vehicle load conditions, (Figs. 33 - 38) because at Section M, the $(DLF)_m$ is less sensitive to the small variation of measured strains.

For the total bridge behavior, the peak values of the (DLF), (Figs. 23 - 26), are summarized in Table 33. For the load in Lane 2, at Section M, the highest peak value of the $(DLF)_m$ is 1.25, and occurs at a speed of 63.2 mph. Similarly, the peak value of the $(DLF)_d$ also occurs at 63.2 mph. But at Section Q, the maximum peak value of the $(DLF)_m$, 1.32, occurs at a speed of 35.8 mph. For the load in Lane 4, the highest values of the $(DLF)_m$ at Section M are 1.24 at a speed of 63.8 mph, and 1.23 at a speed of 55.9 mph, while the maximum values of the $(DLF)_d$ are 1.27 at a speed of 63.8 mph, and 1.28 at a speed of 55.9 mph. At Section Q, the highest peak value of the $(DLF)_m$ is 1.27, at a speed of 55.9 mph.

The values of the $(DLF)_m$ at Section M (Table 33) are all less than the design value $(1 + \frac{50}{125 + L}) = 1.258$. At Section Q,

the peak values of the $(DLF)_m$ for loading in Lanes 2 and 4 are 5% and 1% greater than the design value, respectively. The results at Section M are more reliable, because the measured strains are less sensitive to the small variation in the measured strains.

In general, for the individual beam responses (Tables 3 - 6 and Figs. 27 - 32), the girder located farthest away from the load has the largest (DLF), while the girder directly under the load has the smallest (DLF). This is because the static strains in the girder located farthest away from the load are small, and the increase in strains due to the dynamic load effect is only slightly less than the increases in the other girders. Generally, the (DLF) values for the exterior girders exceed the AASHO design value of 1.258 at both Sections M and Q, while in most cases, the (DLF) values for the interior girders are less than 1.258.

5.5.2 Impact Factors $(IF)_m$

It was observed (Table 9) that the impact factor $(IF)_m$ for individual beam response is smaller in the girder directly under the load than values for the other girders. Again, the reason is that the static moment coefficients for girders located farther away from the load are small, and the increases in moment coefficients resulting from the impact loading are more uniform than are the basic static coefficients. Therefore, the reason for the larger values of $(IF)_m$ for Beams A and E (Table 9) is because the moment coefficients at crawl speed for these beams are

comparatively small, while the moment coefficients from the impact runs are more uniformly large, for all beams, resulting in larger values of $(IF)_m$ for the exterior beams.

In the impact runs, the bridge sustained more deformation than that in the dynamic speed runs. Therefore, the impact factors $(IF)_m$ calculated are greater than dynamic load factors $(DLF)_m$ for the identical loading lanes. For the total bridge behavior at Section Q, the impact factors range from 1.59 to 1.95. At Section M, the impact factors based on information from three girders ranged from 1.61 to 1.95. In all cases, the impact factors for the total bridge behavior were greater than $(1 + \frac{50}{L + 125})$.

5.6 Vibration Frequency

The experimental unloaded natural frequency of this bridge was measured (see Section 3.8) as 6.09 cycles per second. The theoretical natural frequency is obtained from the equation[4,9,13,19]

$$f = \frac{\pi}{2L^2}\sqrt{\frac{EI}{m}}$$

where L = span of the bridge, center to center of bearings

E = modulus of elasticity of the concrete

I = composite moment of inertia of the total bridge cross-section

m = mass per unit length of the bridge

This equation yields the natural frequency of the first mode of vibration of a simply supported beam of uniform cross-section.

Because the full contribution of the parapets to the moment of inertia of the bridge is not certain[19], two cases are discussed as follows. If the parapets are taken into account, the theoretical natural frequency is 7.14 cps. If the contribution of the parapets is neglected, then the theoretical natural frequency is 6.36 cps. In calculating the theoretical values of the natural frequency, a value of $E = 5.97 \times 10^6$ psi was used (Table 2). The primary reason for the difference between the theoretical values of natural frequency and the experimental value is centered in the value of E used in the computation of the theoretical values. A previous study of a spread box-beam bridge[21] indicate that the occurrence of end-support restraint serves to reduce the experimentally determined moment coefficients, resulting in the relatively large value of E (determined as describe in Section 4.1). If a more realistic value of $E = 4.5 \times 10^6$ psi had been used in the computations, the theoretical values would have been 6.20 cps and 5.53 cps, as compared to the measured value of 6.09 cps. This would again serve to strengthen the observation that the curb-parapet section is effective in acting compositely with the beam-slab system.

For low vehicle speeds, the loaded frequencies were difficult to measure from the oscillograph traces due to the irregularity of the vibration pattern. But, at faster speeds, the measurement was more clearly defined. At speeds from 55.9 mph to 63.8 mph, the loaded frequency of the bridge was observed to approach the experimental natural frequency 6.09 cps.

6. SUMMARY AND CONCLUSIONS

6.1 Summary

The main objectives of this pilot I-beam bridge test on lateral distribution of live load were: (1) to obtain the information on lateral distribution of design vehicle loading at crawl speed, (2) to establish the amplification characteristics of crawl run response under dynamic and controlled impact loading, (3) to develop the information on stresses on the surface of the slab and in the slab reinforcement, and (4) to compare the structural behavior of I-beam bridges with that of box-beam bridges previously tested. This report covers items 1, 2, and 4.

The test structure was an existing ten-span bridge located near Bartonsville, Pennsylvania. The sixth span of the bridge was selected as the test span, and consisted of five identical precast prestressed concrete I-beams, with composite cast-in-place reinforced concrete slab, curbs, and parapets. This bridge was designed essentially in accordance with the PennDOT Bridge Division Standards[1], except that AASHO Type III beams were used.

The maximum moment section (Section M), located 3.55 feet east of midspan, and another section, located near the quarter point of the span (Section Q), were selected as the test sections and instrumentated with strain gages. At both sections, three of the five girders were fully gaged with SR-4 electrical strain gages (Fig. 7). At Section Q, the fourth and fifth girders were

partially gaged to check the symmetrical behavior of the bridge.

A total of 136 runs, consisting of crawl, speed, and controlled impact runs, were conducted in this bridge test. The test speed of the truck ranged from 2.0 mph to 63.8 mph. The truck was loaded with crushed stone to approximate the HS 20-44 design loading. The seven test lanes were approximately equally spaced across the roadway width of the bridge. Strain and deflection measurements were collected with continuously recording equipment.

The data reduction and evaluation was accomplished with computer programs developed for use with the CDC 6400 digital computer. From the strains, determinations were made of moment coefficients, distribution coefficients, distribution factors, modulus of elasticity, dynamic load factors, and impact factors. The effect of midspan diaphragms on the distribution coefficients was determined. Distribution factors evaluated in this bridge were compared with those of the Drehersville Bridge (box-beam), which had similar beam spacing, roadway width, and span. The peak experimental values of the dynamic load factors and impact factors were developed and compared with the AASHO impact factor. The unloaded natural frequency was measured experimentally, and compared with a theoretical value.

6.2 Conclusions

The following conclusions were made, based on the test results of the field study of the Bartonsville Bridge.

1. The actual distribution of vehicular loads to the longitudinal beams in the I-beam bridge superstructure resulted in experimental distribution factors which (1) were very close to the design value for interior beams, and (2) were greater than the design value for the exterior beams. This overall result differs substantially from the results from previous studies of spread box-beam bridges, indicating that the increased torsional stiffness of the box-beams results in a more uniform distribution of vehicular loads in bridges of the spread box-beam type.

   In view of the results from test of the Bartonsville Bridge, as well as those from tests of the spread box-beam type, the need for specification revision is apparent. Since a revision to cover spread box-beam bridges has been proposed[12], it is felt that a similar revision should be developed to cover I-beam bridges. Even though the experimental distribution factors for interior beams in the Bartonsville Bridge are close to design values, the earlier analysis of spread box-beam bridges indicated that factors other than beam spacing, such as span length, number of beams and number of traffic lanes, should be included in an appropriate design procedure. More generally, it is apparent that attention should be directed to revision of provisions for live-load distribution for

live load distribution for other types of beams, such as steel I-beams and reinforced concrete beams.

2. In the gaging of two cross-sections (M, near midspan, and Q, near quarterspan), it was felt that the results would give some insight into the effect of the midspan diaphragms. Although the distribution of a single vehicle load was found to be a little more uniform at Section M, it is felt that the influence of the diaphragm is only partly responsible. As reflected in the analytical study of box-beam bridges[1a], the span length has a substantial influence on distribution of load. Therefore, it might be postulated that even if no midspan diaphragm had been present, the distribution at Section M would still have been more uniform since Section M is at a greater distance from the end-support. However, there is no doubt whatsoever that the diaphragm does influence the distribution of a <u>single</u> vehicle load at Section M.

   In the development of experimental distribution factors, the very close agreement between values developed for Sections M and Q indicates that the midspan diaphragms have a negligible effect on the distribution factors.

3. The dynamic load factors developed from the test results vary with the speed of the vehicle, with peaks or maximum

values occurring at approximately 36 and 55 - 63 mph. In considering the overall superstructure, the factors did not exceed the design value $(1 + \frac{50}{L + 125})$, except by negligible amounts at the peak values. For the individual beams, the factors for beam A exceeded the design value at a numer of speeds. However, it is emphasized that the experimental factors for beam A reflect amplification of small crawl-run moment coefficients. The factors for beams B and C were all less than the design value. From the results of single vehicle loading, it is apparent again, as indicated by the results from earlier research, that there is a strong need for an effective analytical study of dynamic load effects which can be simplified effectively to form a usable design specification.

In this study, there was a reasonable correlation between the measured unloaded natural frequency of the superstructure and the theoretical value based on a simple beam analogy. In addition, it was found that the loaded natural frequencies at the peak values of the dynamic load factors were very close to the unloaded natural frequency. Likewise, the loaded natural frequencies at the lower values of the dynamic load factors were not as close to the unloaded natural frequency. This result was to be expected. However, the problem in a theoretical analysis

is to effectively isolate the most important factors into a form which will enable the designer to determine the speeds of the load vehicle(s) at which the loaded frequency will be essentially equal to the unloaded natural frequency, and then to determine the maximum amplification of the static load effects.

4. The controlled impact tests yielded large impact factors, primarily illustrating the critical effects of obstructions on the roadway in amplifying the static load effects. Similar effects might also be caused by pot holes in the slab surface and possibly surface roughness of the slab.

5. Finally, it is again demonstrated that the curb and parapet sections substantially stiffen the exterior beams, significantly affecting the load distribution characteristics. This effect would be lessened as roadway width is increased, and with smaller curb-parapet sections. However, it is recommended that recognition and consideration of the effect be given in future revision of design and construction procedures.

6. The test results and description of structural behavior contained in this report are not sufficient to form the basis for definite implementation in the form of changes in specifications or design procedures. As intended, the

value of the work is primarily (1) in providing the experimental evaluation of live load distribution factors in a typical prestressed concrete I-beam superstructure, (2) in verifying the existence of critical speeds (or ranges of speeds) of a design load vehicle at which maximum amplification of crawl run response is achieved, and (3) in showing that controlled impact tests can yield sizeable amplifications of crawl run response. It is intended that the results will form a data base for future analytical studies which will lead to the development of new specification provisions (1) for live load distribution in prestressed concrete I-beam bridges, and (2) for the assessment of dynamic load behavior in beam-slab superstructures.

7. ACKNOWLEDGMENTS

This study was conducted in the Department of Civil Engineering and Fritz Engineering Laboratory, under the auspices of the Lehigh University Office of Research, as a part of a research investigation sponsored by the Pennsylvania Department of Transportation; the U. S. Department of Transportantion, Federal Highway Administration; and the Reinforced Concrete Research Council.

The field test equipment was made available through Mr. C. F. Scheffey, now Director, Office of Research, Federal Highway Administration. The instrumentation of the test structure, and operation of the test equipment, were supervised by Messrs. R. F. Varney and H. Laatz, both from the Federal Highway Administration.

The basic research planning and administrative coordination in this investigation were in cooperation with the following individuals representing the Pennsylvania Department of Transportation: Mr. B. F. Kotalik, Bridge Engineer; Mr. H. P. Koretzky, and Mr. Hans Streibel, all from the Bridge Engineering Division; and Messrs. Leo D. Sandvig, Director; Wade L. Gramling, Research Engineer; and Foster C. Sankey and Kenneth L. Heilman, Research Coordinators; all from the Bureau of Materials, Testing and Research.

The following members of the faculty and staff at

Lehigh University made major contributions in the conduct of the field tests and in the reduction and processing of the test data: Dr. C. N. Kostem, Prof. J. O. Liebig, Jr., Felix Barda, Cheng-Shung Lin, Yan-Liang Chen, Gerardo Cordoba-Chen, Anton Wegmuller, Daryoush Motarjemi, and Donald Frederickson. The manuscript was typed by Mrs. Ruth Grimes, and the figures were prepared by John M. Gera and Mrs. Sharon Balogh.

8. TABLES

TABLE 1 LIST OF TEST RUNS

Description		Nominal Speed (mph)	Lanes	No.	Remarks
Series 1	Crawl	2.0	1,2,3,4,5,6,7	23	4 runs: Lanes 1 and 6 3 runs: Lanes 2,3,4,5 and 7
	Speed	5.0	2,4,6	3	
		7.0	2,4,6	3	
		10.0	2,4,6	3	
		12.0	2,4,6	3	
		15.0	2,4,6	3	
		17.5	2,4,6	3	
		20.0	2,4,6	3	
		22.5	2,4,6	3	Damping run in Lane 6
		25.0	2,4,6	3	Damping run in Lane 2
		27.5	2,4,6	3	
		30.0	2,4,6	3	
		32.5	2,4,6	3	
		35.0	2,4,6	3	
		37.5	2,4,6	3	Damping run in Lane 4
		40.0	2,4,6	3	Damping run in Lane 2
		42.5	2,4,6	3	
		45.0	2,4,6	3	
		47.5	2,4,6	3	
		50.0	2,4,6	3	
		52.5	2,4,6	3	
		55.0	2,4,6	3	
		57.5	2,3,4,6	4	Damping run in Lane 4
		60.0	2,4,6	3	
	Impact	10.0	4,5,6,7	4	Ramp at Section M
		10.0	1,2,3,4	4	Ramp at Section Q
	Sum			101	
Series 2	Crawl	2.0	1,2,3,4,5,6,7	14	Two runs in each Lane
	Speed	15.0	2,6	3	Two runs in Lane 6
		20.0	2,6	2	
		25.0	2,6	2	
		30.0	2,6	2	
		35.0	2,6	2	
	Impact	10.0	1,2,3,4,5,6,7	7	Ramp at Section Q
		10.0	5,6,7	3	Ramp at Section M
	Sum			35	
	Total			136	

TABLE 2 MOMENT COEFFICIENTS FOR CRAWL RUNS

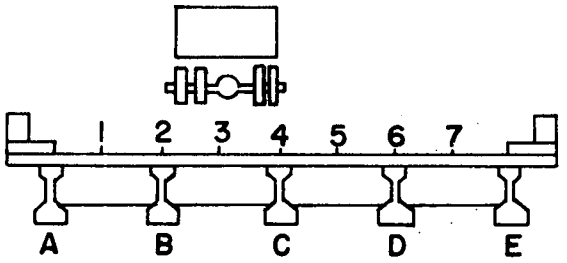

T.M.* = 897.74 k-ft

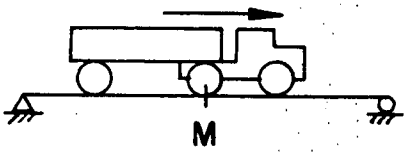

	Moment Coefficients at Section M (Fig. 3) (10^{-3} ft-in^2)					Modulus of Elasticity 10^6 psi
	A	B	C	D	E	
Truck in Lane 1	66.9	50.8	24.4	7.9	0.5	5.97
2	41.4	56.0	35.8	14.2	1.0	6.06
3	21.1	51.0	51.2	23.8	3.2	5.98
4	10.0	36.7	59.1	36.7	10.0	5.89
				Average		5.97

T.M.* = 683.65 k-ft

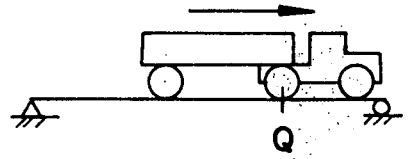

	Moment Coefficients at Section Q (Fig. 3) (10^{-3} ft-in^2)					Modulus of Elasticity 10^6 psi
	A	B	C	D	E	
Truck in Lane 1	49.8	42.2	15.9	3.9	1.4	6.04
2	30.5	45.7	27.0	6.8	1.1	6.16
3	15.2	29.2	41.3	13.4	2.2	6.34
4	6.8	25.4	47.6	25.4	6.8	6.31
				Average		6.21

* T.M. = Total Moment due to Load Vehicle

TABLE 3 MOMENT COEFFICIENTS AND DYNAMIC LOAD FACTORS AT SECTION M

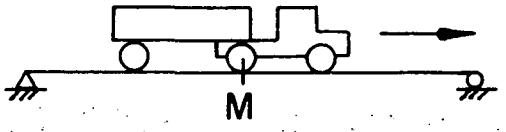

Truck in Lane 2

M.C. = Moment Coefficient (10^{-3} ft-in^2)

$(DLF)_m$ = Dynamic Load Factor = $\frac{\text{M.C. at Speed}}{\text{M.C. at Crawl}}$

SPEED (mph)	BEAM A		BEAM B		BEAM C		BEAM D		BEAM E		TOTAL	
	M.C.	$(DLF)_m$	M.C.	$(DLF)_m$	M.C.	$(DLF)_m$	M.C.	$(DLF)_m$	M.C.	$(DLF)_m$	M.C.	$(DLF)_m$
2.0	41.4	1.00	56.0	1.00	35.8	1.00	14.2	1.00	1.0	1.00	148.2	1.00
5.0	41.3	1.00	54.5	0.97	38.6	1.08	14.9	1.05	3.2	3.31	152.5	1.03
8.8	46.6	1.13	61.5	1.09	39.6	1.11	15.7	1.11	4.1	4.23	167.4	1.13
10.4	45.2	1.09	58.2	1.04	36.4	1.02	16.1	1.14	3.9	4.07	159.8	1.08
12.3	43.7	1.06	58.5	1.04	39.7	1.11	16.8	1.19	2.9	3.04	161.6	1.09
13.7	46.0	1.12	54.8	0.98	36.7	1.03	17.0	1.20	4.1	4.23	158.6	1.07
17.1	43.8	1.06	54.9	0.98	39.3	1.10	16.0	1.13	3.6	3.74	157.5	1.06
20.0	46.8	1.13	60.3	1.07	38.6	1.08	16.3	1.16	3.3	3.43	165.3	1.12
21.4	48.2	1.17	59.9	1.07	40.6	1.14	15.5	1.09	1.1	1.10	165.2	1.12
23.9	46.7	1.13	57.5	1.02	40.3	1.13	14.7	1.04	1.0	1.04	160.2	1.08
26.4	42.1	1.02	58.4	1.04	38.9	1.09	16.7	1.18	3.6	3.72	159.7	1.08
31.7	45.6	1.10	58.6	1.04	40.7	1.14	18.2	1.28	3.6	3.72	166.7	1.12
32.4	45.4	1.10	62.7	1.12	42.7	1.19	16.8	1.19	3.7	3.86	171.3	1.16
35.4	50.8	1.23	65.6	1.17	43.0	1.20	17.0	1.20	3.3	3.42	179.7	1.21
37.2	49.4	1.19	64.2	1.14	41.4	1.16	16.5	1.17	3.6	3.80	175.1	1.18
40.6	49.5	1.20	64.4	1.15	41.1	1.15	17.1	1.21	4.4	4.53	176.6	1.19
44.8	50.3	1.22	63.0	1.12	38.6	1.08	15.6	1.10	3.6	3.76	171.1	1.15
47.5	41.4	1.00	60.6	1.08	39.3	1.10	16.9	1.20	3.9	4.04	162.0	1.09
51.1	51.3	1.24	64.5	1.15	44.7	1.25	16.0	1.13	3.9	4.04	180.3	1.22
53.2	52.1	1.28	64.4	1.15	44.0	1.23	15.8	1.12	3.3	3.40	179.5	1.21
55.8	50.4	1.22	63.7	1.13	44.7	1.25	15.4	1.09	3.4	3.53	177.5	1.20
56.0	54.0	1.31	66.0	1.17	44.4	1.24	15.5	1.10	3.9	4.03	183.8	1.24
63.2	55.3	1.34	65.8	1.17	42.2	1.18	17.8	1.26	3.9	4.03	184.9	1.25

TABLE 4 MOMENT COEFFICIENTS AND DYNAMIC LOAD FACTORS AT SECTION M

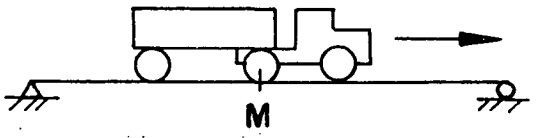

Truck in Lane 4

M.C. = Moment Coefficient (10^{-3} ft-in^2)

$(DLF)_m$ = Dynamic Load Factor = $\frac{\text{M.C. at Speed}}{\text{M.C. at Crawl}}$

SPEED (mph)	BEAM A		BEAM B		BEAM C		BEAM D		BEAM E		TOTAL	
	M.C.	$(DLF)_m$	M.C.	$(DLF)_m$	M.C.	$(DLF)_m$	M.C.	$(DLF)_m$	M.C.	$(DLF)_m$	M.C.	$(DLF)_m$
2.0	10.0	1.00	36.7	1.00	59.1	1.00	36.7	1.00	10.0	1.00	152.5	1.00
5.0	11.3	1.13	39.0	1.06	61.3	1.04	39.0	1.06	11.3	1.13	161.9	1.06
8.6	13.4	1.34	37.8	1.03	57.7	0.98	37.8	1.03	13.4	1.34	160.0	1.05
10.4	12.5	1.25	37.5	1.02	57.3	0.97	37.5	1.02	12.5	1.25	157.3	1.03
12.3	11.3	1.13	37.4	1.02	59.0	1.00	37.4	1.02	11.3	1.13	156.4	1.03
14.3	12.4	1.24	37.4	1.02	60.0	1.01	37.4	1.02	12.4	1.24	159.5	1.05
16.8	14.8	1.48	40.7	1.11	64.4	1.09	40.7	1.11	14.8	1.48	175.3	1.15
20.1	11.6	1.16	39.4	1.07	63.5	1.07	39.4	1.07	11.6	1.16	165.4	1.08
21.4	11.0	1.10	39.0	1.06	62.5	1.05	39.0	1.06	11.0	1.10	162.6	1.07
23.9	14.6	1.46	40.2	1.10	64.0	1.08	40.2	1.10	14.6	1.46	173.5	1.14
27.0	13.9	1.39	40.3	1.10	63.5	1.07	40.3	1.10	13.9	1.39	171.8	1.13
30.1	9.0	0.90	37.3	1.02	57.2	0.97	37.3	1.02	9.0	0.90	149.8	0.98
30.8	10.5	1.05	38.2	1.04	60.0	1.01	38.2	1.04	10.5	1.05	157.0	1.03
34.8	15.7	1.57	44.8	1.22	66.1	1.12	44.8	1.22	15.7	1.57	187.0	1.23
37.0	15.0	1.50	42.1	1.15	65.0	1.10	42.1	1.15	15.0	1.50	179.2	1.18
39.8	13.2	1.32	40.9	1.11	64.6	1.09	40.9	1.11	13.2	1.32	172.8	1.13
41.8	14.2	1.42	42.1	1.15	65.5	1.11	42.1	1.15	14.2	1.42	178.1	1.17
46.5	12.0	1.20	39.6	1.08	61.7	1.04	39.6	1.08	12.0	1.20	164.8	1.08
49.5	14.1	1.41	41.2	1.12	63.2	1.07	41.2	1.12	14.1	1.41	173.7	1.14
52.0	15.9	1.59	43.2	1.18	65.5	1.11	43.2	1.18	15.9	1.59	183.8	1.21
55.9	18.6	1.86	42.7	1.16	65.2	1.10	42.7	1.16	18.6	1.86	187.9	1.23
56.8	17.1	1.71	42.7	1.16	65.1	1.10	42.7	1.16	17.1	1.71	184.7	1.21
63.8	16.4	1.64	43.5	1.18	68.4	1.15	43.5	1.18	16.4	1.64	188.3	1.24

TABLE 5 MOMENT COEFFICIENTS AND DYNAMIC LOAD FACTORS AT SECTION Q

Truck in Lane 2

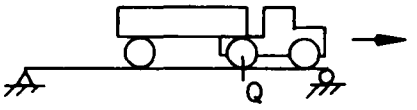

M.C. = Moment Coefficient (10^{-3} ft-in^2)

$(DLF)_m$ = Dynamic Load Factor = $\frac{\text{M.C. at Speed}}{\text{M.C. at Crawl}}$

SPEED (mph)	BEAM A		BEAM B		BEAM C		BEAM D		BEAM E		TOTAL	
	M.C.	$(DLF)_m$	M.C.	$(DLF)_m$	M.C.	$(DLF)_m$	M.C.	$(DLF)_m$	M.C.	$(DLF)_m$	M.C.	$(DLF)_m$
2.0	30.5	1.00	45.7	1.00	27.0	1.00	6.8	1.00	1.1	1.00	111.0	1.00
5.0	30.5	1.00	45.0	0.99	28.4	1.05	6.8	1.00	1.4	1.30	112.0	1.01
8.8	31.8	1.09	50.3	1.10	30.0	1.11	8.0	1.18	4.5	4.13	124.6	1.12
10.4	30.3	1.00	45.6	1.00	28.9	1.07	9.5	1.41	3.2	2.97	117.6	1.06
12.3	38.3	1.26	49.2	1.08	30.1	1.11	9.3	1.38	3.7	3.44	130.7	1.18
13.6	39.4	1.29	48.4	1.06	27.7	1.03	10.4	1.55	3.7	3.45	129.7	1.17
13.7	36.1	1.19	45.0	0.99	27.0	1.00	10.4	1.55	3.7	3.42	122.3	1.10
17.1	36.0	1.18	47.0	1.03	27.7	1.02	9.5	1.41	4.4	4.11	124.6	1.12
20.0	37.0	1.21	45.2	0.99	33.1	1.22	8.8	1.30	3.4	3.12	127.4	1.15
20.4	36.6	1.20	48.0	1.05	28.3	1.05	9.3	1.37	3.2	2.96	125.4	1.13
21.4	33.8	1.11	45.9	1.01	31.8	1.18	8.5	1.26	1.9	1.73	121.9	1.10
23.9	37.2	1.22	47.6	1.04	31.8	1.18	8.6	1.27	3.7	3.42	128.8	1.16
26.0	42.0	1.38	50.3	1.10	28.1	1.04	9.2	1.37	4.7	4.31	134.3	1.21
26.4	37.2	1.22	46.1	1.01	34.2	1.26	9.5	1.41	4.0	3.72	131.0	1.18
31.7	38.6	1.27	51.2	1.12	31.7	1.17	9.2	1.36	3.4	3.18	134.2	1.21
32.4	40.4	1.33	53.2	1.16	33.0	1.22	9.7	1.43	2.6	2.40	138.8	1.25
35.4	40.2	1.32	52.4	1.15	33.0	1.22	9.9	1.46	3.4	3.12	138.8	1.25
35.8	41.8	1.37	58.4	1.28	32.7	1.21	11.0	1.62	2.8	2.60	146.7	1.32
37.2	38.9	1.28	55.7	1.22	32.6	1.20	9.3	1.38	3.1	2.78	139.6	1.26
40.6	44.2	1.45	56.2	1.23	28.6	1.06	8.8	1.30	5.2	4.78	143.0	1.28
44.8	40.3	1.32	52.9	1.16	30.0	1.11	9.5	1.40	3.6	3.32	136.3	1.23
47.5	39.4	1.29	52.3	1.15	31.6	1.17	10.4	1.54	2.9	2.66	136.6	1.23
51.1	36.4	1.20	50.0	1.10	31.3	1.16	11.8	1.75	4.5	4.15	134.1	1.21
53.2	38.2	1.25	52.4	1.15	30.1	1.11	11.6	1.71	4.9	4.51	137.1	1.23
55.8	37.5	1.23	54.0	1.18	30.3	1.12	11.4	1.69	4.3	3.96	137.5	1.24
56.0	38.7	1.27	52.8	1.16	30.9	1.14	12.7	1.87	6.6	6.10	141.7	1.28
63.2	40.0	1.31	47.6	1.04	30.5	1.13	10.3	1.53	5.1	4.69	133.5	1.20

TABLE 6 MOMENT COEFFICIENTS AND DYNAMIC LOAD FACTORS AT SECTION Q

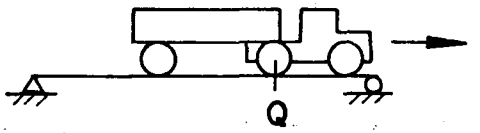

Truck in Lane 4

M.C. = Moment Coefficient (10^{-3} ft-in^2)

$(DLF)_m$ = Dynamic Load Factor = $\frac{\text{M.C. at Speed}}{\text{M.C. at Crawl}}$

SPEED (mph)	BEAM A		BEAM B		BEAM C		BEAM D		BEAM E		TOTAL	
	M.C.	$(DLF)_m$	M.C.	$(DLF)_m$	M.C.	$(DLF)_m$	M.C.	$(DLF)_m$	M.C.	$(DLF)_m$	M.C.	$(DLF)_m$
2.0	6.8	1.00	25.4	1.00	47.6	1.00	25.4	1.00	6.8	1.00	112.0	1.00
5.0	6.4	0.94	24.9	0.98	45.7	0.96	24.9	0.98	6.4	0.94	108.4	0.97
8.6	9.6	1.41	28.1	1.11	50.1	1.05	28.1	1.11	9.6	1.41	125.6	1.12
10.4	9.3	1.37	26.2	1.03	48.0	1.01	26.2	1.03	9.3	1.37	119.0	1.06
12.3	10.0	1.47	27.4	1.08	48.9	1.03	27.4	1.08	10.0	1.47	123.8	1.10
14.3	10.0	1.47	28.3	1.11	49.6	1.04	28.3	1.11	10.0	1.47	126.2	1.13
16.8	9.8	1.44	27.4	1.08	51.9	1.09	27.4	1.08	9.8	1.44	126.2	1.13
20.1	10.0	1.47	28.3	1.11	47.5	1.00	28.3	1.11	10.0	1.47	124.1	1.11
21.4	8.6	1.26	26.5	1.04	48.8	1.03	26.5	1.04	8.6	1.26	119.0	1.06
23.9	9.8	1.44	28.5	1.12	48.5	1.02	28.5	1.12	9.8	1.44	125.0	1.12
27.0	9.4	1.38	30.9	1.22	54.6	1.15	30.9	1.22	9.4	1.38	135.2	1.21
30.1	9.8	1.44	26.9	1.06	52.7	1.11	26.9	1.06	9.8	1.44	126.1	1.13
30.8	7.9	1.16	27.5	1.08	51.1	1.07	27.5	1.08	7.9	1.16	121.9	1.09
34.6	9.8	1.44	29.5	1.16	55.7	1.17	29.5	1.16	6.8	1.44	134.3	1.20
37.0	11.8	1.59	28.7	1.13	56.5	1.19	28.7	1.13	11.8	1.59	137.6	1.23
39.8	11.4	1.68	29.9	1.18	53.6	1.13	29.9	1.18	11.4	1.68	136.4	1.22
41.8	8.7	1.28	32.1	1.26	52.8	1.11	32.1	1.26	8.7	1.28	134.4	1.20
46.5	10.6	1.56	28.3	1.11	52.8	1.11	28.3	1.11	10.6	1.56	130.6	1.17
49.5	12.5	1.84	27.1	1.07	51.3	1.08	27.1	1.07	12.5	1.84	130.5	1.16
52.0	12.6	1.85	27.9	1.10	50.2	1.05	27.9	1.10	12.6	1.85	131.2	1.17
55.9	14.1	2.08	29.9	1.18	53.9	1.13	29.9	1.18	14.1	2.08	141.9	1.27
56.8	13.5	1.98	30.6	1.20	54.3	1.14	30.6	1.20	13.5	1.98	142.5	1.27
63.8	14.3	2.10	29.9	1.18	50.6	1.06	29.9	1.18	14.3	2.10	139.0	1.24

TABLE 7 MOMENT COEFFICIENTS FOR IMPACT RUNS

Section M

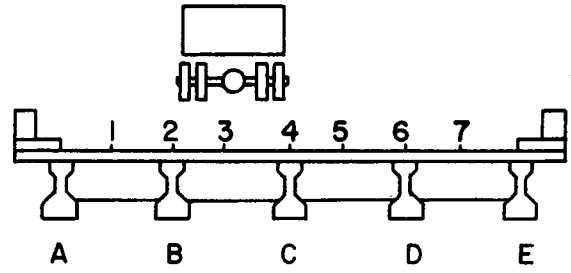

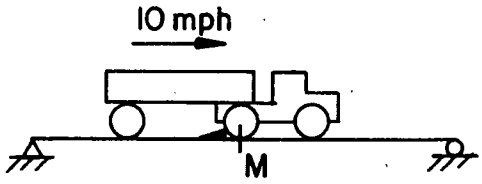

Moment Coefficients at Section M (10^{-3} ft-in^2)					
	A	B	C	D	E
Truck in Lane 1	106.6	77.8	43.8	---	---
2	61.4	80.3	82.9	---	---
3	46.6	85.4	90.1	---	---
4	41.7	57.9	98.5	---	---

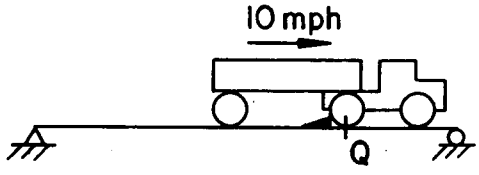

Moment Coefficients at Section M (10^{-3} ft-in^2)					
	A	B	C	D	E
Truck in Lane 4	39.1	54.0	88.1	---	---
5	21.6	33.3	71.8	---	---
6	12.6	25.6	42.1	---	---
7	12.1	13.2	31.7	---	---

TABLE 8 MOMENT COEFFICIENTS FOR IMPACT RUNS

Section Q

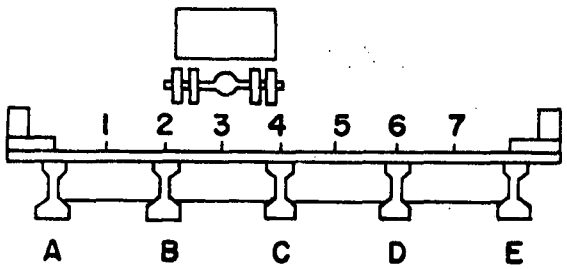

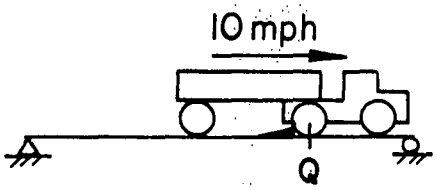

Moment Coefficients at Section Q (10^{-3} ft-in^2)				
A	B	C	D	E
74.9	59.2	21.4	11.5	12.8
53.2	63.9	41.4	13.3	14.2
37.1	56.9	65.0	17.2	21.1
26.0	28.6	71.6	28.6	26.0

Truck in Lane 1
2
3
4

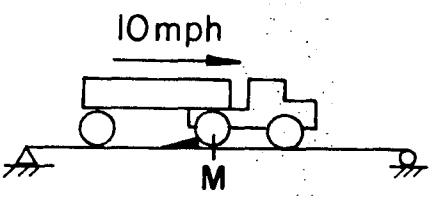

Moment Coefficients at Section Q (10^{-3} ft-in^2)				
A	B	C	D	E
28.9	36.0	74.5	----	----
22.4	23.9	64.0	----	----
13.4	11.9	51.5	----	----
10.7	8.5	27.4	----	----

Truck in Lane 4
5
6
7

TABLE 9 IMPACT FACTORS FOR IMPACT RUNS

Sections M and Q

$$\text{Impact Factor} = (IF)_m = \frac{\text{M.C. (impact)}}{\text{M.C. (crawl)}}$$

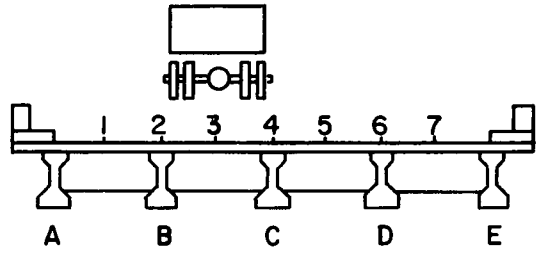

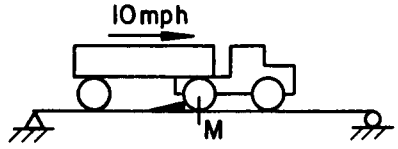

	$(IF)_m$ at Section M					Full Bridge Behavior
	A	B	C	D	E	
Truck in Lane 1	1.59	1.53	1.79	---	---	1.61*
2	1.48	1.61	2.32	---	---	1.76*
3	2.20	1.68	1.76	---	---	1.80*
4	4.22	1.59	1.67	---	---	1.95

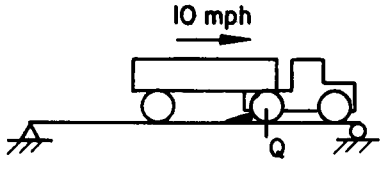

	$(IF)_m$ at Section Q					Full Bridge Behavior
	A	B	C	D	E	
Truck in Lane 1	1.50	1.35	1.35	2.93	8.91	1.59
2	1.74	1.40	1.53	1.98	13.20	1.68
3	2.45	1.95	1.57	1.28	9.60	1.95
4	3.82	1.13	1.51	1.13	3.82	1.61

* Based on three girders

TABLE 10 DISTRIBUTION COEFFICIENTS FOR CRAWL RUNS

$$\text{Distribution Coefficient} = \frac{\text{Moment Coefficient}}{\Sigma \text{ Moment Coefficients}} \quad (100)$$

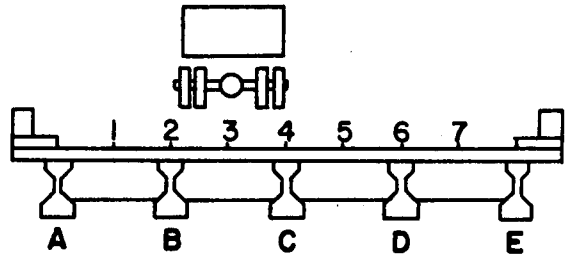

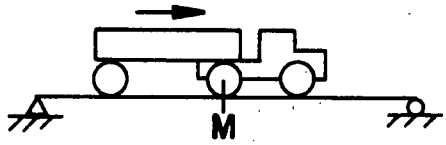

Truck in Lane	Distribution Coefficients at Section M				
	A	B	C	D	E
1	44.5	33.8	16.2	5.2	0.3
2	27.9	37.8	24.1	9.5	0.7
3	14.1	33.9	34.1	15.8	2.1
4	6.6	24.0	38.8	24.0	6.6

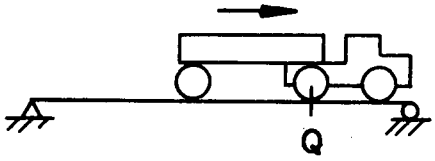

Truck in Lane	Distribution Coefficients at Section Q				
	A	B	C	D	E
1	44.0	37.3	14.0	3.5	1.2
2	27.4	41.2	24.3	6.1	1.0
3	13.6	35.2	37.1	12.0	2.1
4	6.1	22.7	42.4	22.7	6.1

TABLE 11 DISTRIBUTION COEFFICIENTS --- SPEED RUNS IN LANE 2

$$\text{Distribution Coefficient} = \frac{\text{Moment Coefficient}}{\Sigma \text{ Moment Coefficients}} (100)$$

SPEED	SECTION M					SECTION Q				
(mph)	A	B	C	D	E	A	B	C	D	E
Crawl	27.8	37.8	24.0	9.4	1.0	27.4	41.2	24.3	6.1	1.0
5.0	27.1	35.7	25.3	9.8	2.1	27.2	40.3	25.3	6.0	1.2
8.8	27.8	36.7	23.6	9.4	2.5	25.6	40.4	24.0	6.4	3.6
10.4	28.3	36.5	22.8	10.0	2.4	25.7	38.9	24.6	8.1	2.7
12.3	27.1	36.1	24.6	10.4	1.8	29.3	37.7	23.1	7.1	2.8
13.6	----	----	----	----	---	30.6	37.7	21.6	7.8	2.3
13.7	29.0	34.6	23.1	10.7	2.6	29.5	36.9	22.1	8.5	3.0
17.1	27.8	34.8	24.9	10.2	2.3	28.9	37.7	22.2	7.6	3.6
20.0	28.3	36.5	23.3	9.9	2.0	29.0	35.5	26.0	6.9	2.6
20.4	----	----	----	----	---	29.2	38.3	22.6	7.4	2.5
21.4	29.1	36.2	24.5	9.3	0.9	27.8	37.6	26.1	7.0	1.5
23.9	29.1	35.8	25.1	9.1	0.9	28.9	36.9	24.7	6.6	2.9
26.0	----	----	----	----	---	31.3	37.4	20.9	6.9	3.5
26.4	26.4	36.6	24.3	10.5	2.2	28.4	35.2	26.1	7.2	3.1
31.7	27.4	35.1	24.4	10.9	2.1	28.8	38.2	23.6	6.8	2.6
32.4	26.5	36.6	24.9	9.8	2.2	29.1	38.3	23.8	6.9	1.9
35.4	28.3	36.6	23.9	9.4	1.8	29.0	37.8	23.7	7.1	2.4
35.8	----	----	----	----	---	28.5	39.8	22.3	7.5	1.9
37.2	28.2	36.7	23.6	9.4	2.1	27.8	39.8	23.3	6.9	2.2
40.6	28.0	36.5	23.3	9.7	2.5	30.9	39.4	20.0	6.1	3.6
44.8	29.4	36.8	22.6	9.1	2.1	29.6	38.9	22.0	6.9	2.6
47.5	25.5	37.4	24.2	10.5	2.4	28.9	38.3	23.1	7.6	2.1
51.1	28.5	35.7	24.8	8.9	2.1	27.2	37.4	23.3	8.8	3.3
53.2	29.0	35.9	24.5	8.8	1.8	27.9	38.2	21.9	8.4	3.6
55.8	28.4	35.9	25.2	8.6	1.9	27.3	39.3	22.0	8.3	3.1
56.0	29.4	35.9	24.2	8.4	2.1	27.3	37.4	21.8	8.9	4.6
63.2	29.9	35.6	22.8	9.6	2.1	30.0	35.7	22.8	7.7	3.8

TABLE 12 DISTRIBUTION COEFFICIENTS --- SPEED RUNS IN LANE 4

$$\text{Distribution Coefficient} = \frac{\text{Moment Coefficient}}{\Sigma \text{ Moment Coefficients}} (100)$$

SPEED	SECTION M					SECTION Q				
(mph)	A	B	C	D	E	A	B	C	D	E
Crawl	6.5	24.0	39.0	24.0	6.5	6.0	22.7	42.6	22.7	6.0
5.0	7.0	24.1	37.8	24.1	7.0	5.9	23.0	42.2	23.0	5.9
8.6	8.4	23.6	36.0	23.6	8.4	7.7	22.4	39.8	22.4	7.7
10.4	8.0	23.8	36.4	23.8	8.0	7.8	22.0	40.4	22.0	7.8
12.3	7.2	23.9	37.8	23.9	7.2	8.1	22.1	39.6	22.1	8.1
14.3	7.8	23.4	37.6	23.4	7.8	7.9	22.4	39.4	22.4	7.9
16.8	8.4	23.2	36.8	23.2	8.4	7.7	21.7	41.2	21.7	7.7
20.1	7.0	23.8	38.4	23.8	7.0	8.0	22.8	38.4	22.8	8.0
21.4	6.8	24.0	38.4	24.0	6.8	7.2	22.2	41.2	22.2	7.2
23.9	8.4	23.1	37.0	23.1	8.4	7.8	22.8	38.8	22.8	7.8
27.0	8.1	23.4	37.0	23.4	8.1	7.0	22.9	40.2	22.9	7.0
30.1	6.0	24.9	38.2	24.9	6.0	7.7	21.4	41.8	21.4	7.7
30.8	6.7	24.3	38.0	24.3	6.7	6.5	22.6	41.8	22.6	6.5
34.6	8.4	23.9	35.4	23.9	8.4	7.3	22.0	41.4	22.0	7.3
37.0	8.4	23.5	36.2	23.5	8.4	8.6	20.9	41.0	20.9	8.6
39.8	7.6	23.7	37.4	23.7	7.6	8.4	22.0	39.2	22.0	8.4
41.8	8.0	23.6	36.8	23.6	8.0	6.5	23.9	39.2	23.9	6.5
46.5	7.3	24.0	37.4	24.0	7.3	8.1	21.7	40.4	21.7	8.1
49.5	8.1	23.7	36.4	23.7	8.1	9.6	20.8	39.2	20.8	9.6
52.0	8.7	23.5	35.6	23.5	8.7	9.6	21.3	38.2	21.3	9.6
55.9	9.9	22.7	34.8	22.7	9.9	9.9	21.1	38.0	21.1	9.9
56.8	9.3	23.1	35.2	23.1	9.3	9.5	21.5	38.0	21.5	9.5
63.8	8.7	23.1	36.4	23.1	8.7	10.3	21.5	36.4	21.5	10.3

TABLE 13 DISTRIBUTION COEFFICIENTS FOR IMPACT RUNS

Section Q

$$\text{Distribution Coefficient} = \frac{\text{Moment Coefficient}}{\Sigma \text{ Moment Coefficients}} \ (100)$$

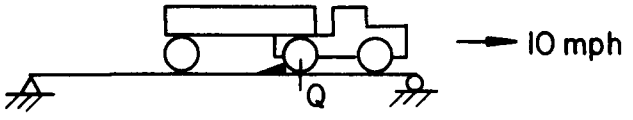

LANE	BEAM A	BEAM B	BEAM C	BEAM D	BEAM E
1	41.7	32.9	11.9	6.4	7.1
2	28.6	34.3	22.3	7.2	7.6
3	18.8	28.8	32.9	8.7	10.7
4	14.4	15.8	39.6	15.8	14.4

TABLE 14 DISTRIBUTION COEFFICIENTS BASED ON DEFLECTIONS

$$\text{Distribution Coefficient} = \frac{\text{Girder Deflection}}{\Sigma \text{ Girder Deflections}} \quad (100)$$

$$\Sigma \text{ Girder Deflections} = 1.25\ (\delta_A + \delta_E) + \delta_B + \delta_C + \delta_D$$

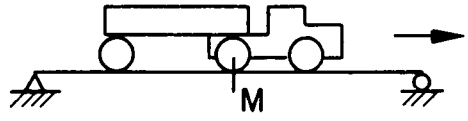

LANE	BEAM A	BEAM B	BEAM C	BEAM D	BEAM E
1	47.0	27.2	15.7	5.6	4.5
2	33.6	30.1	20.4	9.8	6.1
3	18.2	29.1	30.2	15.7	6.8
4	11.4	22.0	33.1	22.0	11.4

TABLE 15 DISTRIBUTION COEFFICIENTS MEASURED FROM INFLUENCE LINES

3 Traffic Lanes

Section	Beam	Lanes			Σ	Distribution Factor	
		Left	Center	Right			
M	A	40.7	6.8	0.5	48.0	0.960	
	B	36.3	24.9	6.8	68.0	1.360	S*/5.88
	C	19.0	38.4	19.2	76.6	1.532	S/5.21
Q	A	40.1	6.5	1.1	47.7	0.954	
	B	40.0	23.5	4.3	67.8	1.356	S/5.90
	C	17.3	42.1	17.5	76.9	1.538	S/5.20

2 Traffic Lanes

Section	Beam	Lanes		Σ	Distribution Factor	
		Left	Right			
M	A	40.7	1.6	42.3	0.846	
	B	37.7	14.3	52.0	1.040	S/7.70
	C	31.3	32.0	63.3	1.266	S/6.32
Q	A	40.1	1.6	41.7	0.834	
	B	41.2	10.3	51.5	1.030	S/7.76
	C	33.5	34.5	68.0	1.360	S/5.88

* S = 8 feet

TABLE 16 DISTRIBUTION FACTORS BASED ON MOMENT COEFFICIENTS

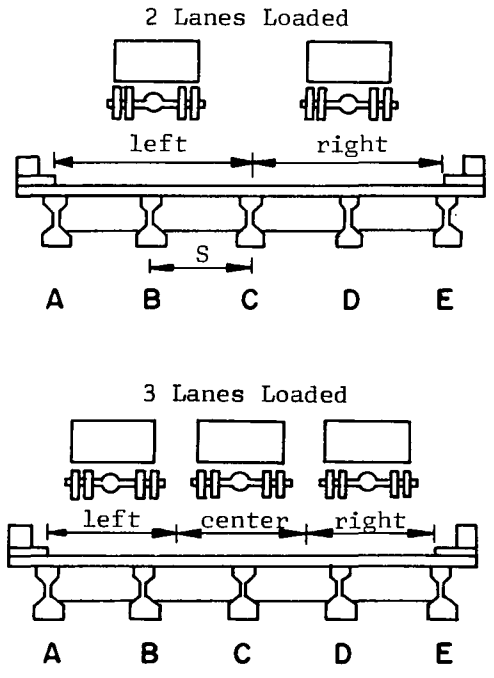

Case	Girder	Experimental Distr. Factor at Section M	Experimental Distr. Factor at Section Q	PennDOT Design Value	Experimental/Design at Section M	Experimental/Design at Section Q
2 Lanes Loaded	A	0.846	0.834	0.750	1.128	1.112
	B	$1.040 = \frac{S}{7.70}$	$1.030 = \frac{S}{7.76}$	$1.455 = \frac{S}{5.5}$	0.715	0.708
	C	$1.266 = \frac{S}{6.32}$	$1.360 = \frac{S}{5.88}$	$1.455 = \frac{S}{5.5}$	0.870	0.935
3 Lanes Loaded	A	0.960	0.954	0.750	1.280	1.272
	B	$1.360 = \frac{S}{5.88}$	$1.356 = \frac{S}{5.90}$	$1.455 = \frac{S}{5.5}$	0.935	0.932
	C	$1.532 = \frac{S}{5.21}$	$1.538 = \frac{S}{5.20}$	$1.455 = \frac{S}{5.5}$	1.053	1.057

TABLE 17 GIRDER DEFLECTIONS AT SECTION M FOR CRAWL RUNS

Units are inches

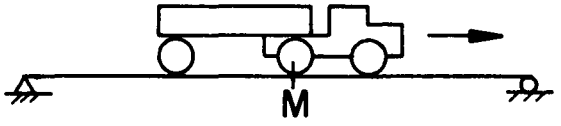

LANE	BEAM A	BEAM B	BEAM C	BEAM D	BEAM E
1	0.156	0.113	0.065	0.024	0.015
2	0.110	0.123	0.089	0.040	0.020
3	0.066	0.112	0.116	0.060	0.025
4	0.035	0.086	0.129	0.086	0.035

TABLE 18 GIRDER DEFLECTIONS AT SECTION M -- SPEED RUNS IN LANE 2

Beam Deflection (δ) - Units are inches

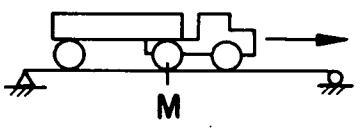

$(DLF)_d$ = Dynamic Load Factor = $\frac{\text{Deflection at Speed}}{\text{Deflection at Crawl}}$

Total Bridge Behavior; $(DLF)_d = \frac{\Sigma^* \text{ at Speed}}{\Sigma^* \text{ at Crawl}}$

$$\Sigma^* = 1.25\ (\delta_A + \delta_E) + \delta_B + \delta_C + \delta_D$$

SPEED (mph)	BEAM A		BEAM B		BEAM C		BEAM D		BEAM E		TOTAL	
	Defl.	$(DLF)_d$	Defl.	$(DLF)_d$	Defl.	$(DLF)_d$	Defl.	$(DLF)_d$	Defl.	$(DLF)_d$	Σ^*	$(DLF)_d$
2.0	0.110	1.00	0.123	1.00	0.089	1.00	0.040	1.00	0.020	1.00	0.414	1.00
5.0	0.113	1.03	0.124	1.01	0.090	1.01	0.039	0.98	0.020	1.00	0.419	1.01
8.8	0.118	1.07	0.132	1.07	0.092	1.03	0.042	1.05	0.024	1.20	0.467	1.13
10.4	0.116	1.05	0.130	1.06	0.096	1.08	0.043	1.08	0.027	1.35	0.448	1.08
12.3	0.115	1.05	0.130	1.06	0.097	1.09	0.045	1.12	0.026	1.30	0.449	1.08
13.6	0.121	1.10	0.129	1.05	0.092	1.03	0.041	1.02	0.025	1.25	0.444	1.07
13.7	0.119	1.08	0.129	1.05	0.096	1.08	0.043	1.07	0.031	1.55	0.456	1.10
17.1	0.113	1.03	0.125	1.02	0.100	1.12	0.043	1.07	0.025	1.25	0.440	1.06
20.0	0.123	1.12	0.150	1.22	0.111	1.25	0.043	1.07	0.026	1.30	0.491	1.19
21.4	0.121	1.10	0.145	1.18	0.104	1.17	0.043	1.07	0.022	1.10	0.470	1.13
23.9	0.125	1.14	0.144	1.17	0.104	1.17	0.042	1.05	0.024	1.20	0.476	1.15
26.0	0.129	1.17	0.138	1.12	0.101	1.13	0.044	1.10	0.028	1.40	0.479	1.16
26.4	0.114	1.04	0.137	1.11	0.106	1.19	0.043	1.07	0.025	1.25	0.459	1.11
31.7	0.127	1.15	0.137	1.11	0.101	1.13	0.045	1.12	0.024	1.20	0.472	1.14
32.4	0.115	1.05	0.138	1.12	0.104	1.17	0.044	1.10	0.023	1.15	0.459	1.11
35.4	0.128	1.16	0.140	1.14	0.104	1.17	0.044	1.10	0.022	1.10	0.475	1.15
35.8	0.126	1.15	0.136	1.11	0.103	1.16	0.044	1.10	0.024	1.20	0.470	1.13
37.2	0.125	1.14	0.138	1.12	0.104	1.17	0.042	1.05	0.022	1.10	0.468	1.13
40.6	0.126	1.15	0.135	1.10	0.098	1.10	0.043	1.07	0.026	1.30	0.466	1.12
44.8	0.121	1.10	0.132	1.07	0.098	1.10	0.043	1.07	0.023	1.15	0.453	1.10
47.5	0.113	1.03	0.132	1.07	0.102	1.15	0.044	1.10	0.024	1.20	0.449	1.18
51.1	0.134	1.22	0.148	1.20	0.109	1.23	0.045	1.12	0.027	1.35	0.503	1.22
53.2	0.139	1.26	0.146	1.19	0.110	1.24	0.044	1.10	0.026	1.30	0.507	1.22
55.8	0.136	1.24	0.138	1.12	0.094	1.06	0.042	1.05	0.027	1.35	0.478	1.15
56.0	0.141	1.28	0.148	1.20	0.094	1.06	0.042	1.05	0.026	1.30	0.493	1.19
63.2	0.141	1.28	0.146	1.19	0.105	1.18	0.047	1.17	0.027	1.35	0.508	1.23

TABLE 19 GIRDER DEFLECTIONS AT SECTION M -- SPEED RUNS IN LANE 4

Beam Deflection (δ) - Units are inches

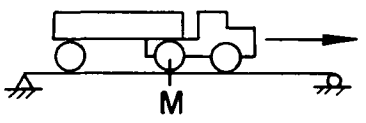

$(DLF)_d$ = Dynamic Load Factor = $\frac{\text{Deflection at Speed}}{\text{Deflection at Crawl}}$

Total Bridge Behavior; $(DLF)_d = \frac{\Sigma^* \text{ at Speed}}{\Sigma^* \text{ at Crawl}}$

$$\Sigma^* = 1.25\ (\delta_A + \delta_E) + \delta_B + \delta_C + \delta_D$$

SPEED (mph)	BEAM A		BEAM B		BEAM C		BEAM D		BEAM E		TOTAL	
	Defl.	$(DLF)_d$	Defl.	$(DLF)_d$	Defl.	$(DLF)_d$	Defl.	$(DLF)_d$	Defl.	$(DLF)_d$	Σ^*	$(DLF)_d$
2.0	0.035*	1.00	0.086	1.00	0.129	1.00	0.086	1.00	0.035	1.00	0.389	1.00
5.0	0.041	1.17	0.092	1.07	0.137	1.06	0.092	1.07	0.041	1.17	0.423	1.09
8.6	0.041	1.17	0.091	1.06	0.134	1.04	0.091	1.06	0.041	1.17	0.418	1.08
10.4	0.041	1.17	0.091	1.06	0.133	1.03	0.091	1.06	0.041	1.17	0.417	1.07
12.3	0.043	1.23	0.092	1.07	0.137	1.06	0.092	1.07	0.043	1.23	0.429	1.10
14.3	0.039	1.11	0.087	1.01	0.129	1.00	0.087	1.01	0.039	1.11	0.401	1.03
16.8	0.049	1.40	0.098	1.14	0.147	1.14	0.098	1.14	0.049	1.40	0.465	1.20
20.1	0.043	1.23	0.099	1.15	0.147	1.14	0.099	1.15	0.043	1.23	0.453	1.17
21.4	0.041	1.17	0.098	1.14	0.144	1.12	0.098	1.14	0.041	1.17	0.442	1.14
23.9	0.048	1.37	0.102	1.19	0.152	1.18	0.102	1.19	0.048	1.37	0.476	1.22
27.0	0.044	1.26	0.100	1.16	0.150	1.16	0.100	1.16	0.044	1.26	0.460	1.18
30.1	0.040	1.14	0.093	1.08	0.135	1.05	0.093	1.08	0.040	1.14	0.421	1.08
30.8	0.039	1.11	0.090	1.05	0.136	1.05	0.090	1.05	0.039	1.11	0.414	1.06
34.6	0.047	1.34	0.106	1.23	0.156	1.21	0.106	1.23	0.047	1.34	0.486	1.25
37.0	0.048	1.37	0.101	1.17	0.150	1.16	0.101	1.17	0.048	1.37	0.472	1.21
39.8	0.044	1.26	0.092	1.07	0.141	1.09	0.092	1.07	0.044	1.26	0.435	1.12
41.8	0.042	1.20	0.097	1.13	0.141	1.09	0.097	1.13	0.042	1.20	0.441	1.13
46.5	0.043	1.23	0.096	1.12	0.141	1.09	0.096	1.12	0.043	1.23	0.441	1.13
49.5	0.049	1.40	0.101	1.17	0.143	1.11	0.101	1.17	0.049	1.40	0.467	1.20
52.0	0.048	1.37	0.104	1.21	0.150	1.16	0.104	1.21	0.048	1.37	0.478	1.23
55.9	0.057	1.63	0.104	1.21	0.149	1.16	0.104	1.21	0.057	1.63	0.499	1.28
63.8	0.054	1.54	0.103	1.20	0.153	1.19	0.103	1.20	0.054	1.54	0.495	1.27

TABLE 20 GIRDER DEFLECTIONS AT SECTION M FOR IMPACT RUNS

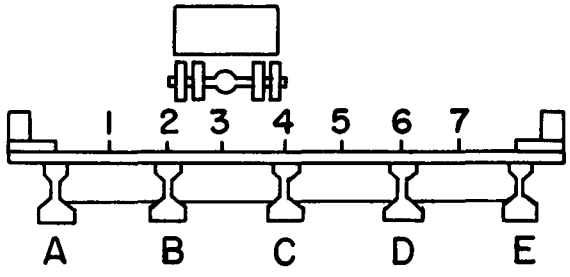

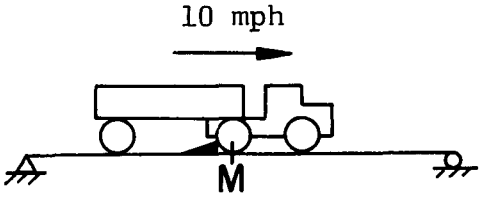

	Deflection (inches)				
	A	B	C	D	E
Truck in Lane 1	0.262	0.183	0.117	---	---
2	0.219	0.212	0.172	---	---
3	0.156	0.203	0.226	---	---
4	0.115	0.167	0.244	---	---

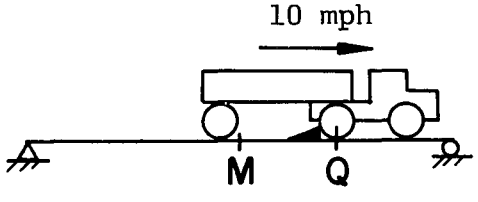

	Deflection (inches)				
	A	B	C	D	E
Truck in Lane 4	0.094	0.128	0.190	---	---
5	0.069	0.109	0.179	---	---
6	0.043	0.060	0.126	---	---
7	0.036	0.044	0.090	---	---

TABLE 21 GIRDER ROTATIONS AT SECTION M FOR CRAWL RUNS

Units are 10^{-6} radians

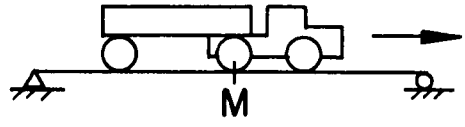

LANE	BEAM A	BEAM B	BEAM C	BEAM D	BEAM E
1	-216*	-485	-455	-295	82
2	292	-92	-501	-365	-79
3	501	373	-423	-456	-287
4	530	520	80	-520	-530

* For sign convention, see Figure 22

TABLE 22 GIRDER ROTATIONS AT SECTION M -- SPEED RUNS IN LANE 2

Units are 10^{-6} radians

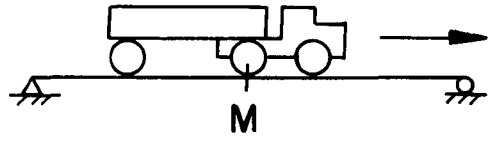

SPEED (mph)	BEAM				
	A	B	C	D	E
2.0	292*	-92	-501	-365	-79
5.0	289	-68	-481	-370	-71
8.8	280	-98	-475	-357	-64
10.4	299	-82	-522	-339	-53
12.3	304	-69	-507	-372	-90
13.6	230	-108	-507	-329	-48
13.7	239	-103	-436	-353	-169
17.1	218	-3	-578	-411	20
20.0	348	-26	-615	-383	-8
20.4	234	-91	-554	-407	-53
21.4	315	-78	-601	-422	-45
23.9	313	-89	-574	-384	-21
26.0	190	-88	-570	-356	32
26.4	281	14	-579	-408	-15
31.7	238	-47	-540	-410	-39
32.4	371	-26	-536	-443	-23
35.4	284	-49	-546	-414	-49
35.8	184	-65	-545	-419	-44
37.2	302	-71	-570	-416	-39
40.6	223	-89	-588	-404	58
44.8	278	-54	-522	-383	-19
47.5	307	-47	-524	-396	-64
51.1	255	-101	-573	-388	-36
53.2	209	-86	-531	-420	-58
55.8	198	7	-508	-363	-9
56.0	139	-101	-493	-379	0
63.2	150	-144	-551	-420	-28

* For sign convention, see Figure 22

TABLE 23 GIRDER ROTATIONS AT SECTION M -- SPEED RUNS IN LANE 4

Units are 10^{-6} radians

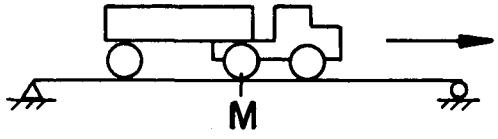

SPEED (mph)	BEAM				
	A	B	C	D	E
2.0	530	520	80	-520	-530
5.0	554	546	83	-546	-554
8.6	534	516	136	-516	-534
10.4	539	505	78	-505	-539
12.3	500	511	73	-511	-500
14.3	503	508	86	-508	-503
16.8	504	533	81	-533	-504
20.1	504	600	70	-600	-504
21.4	500	609	72	-609	-500
23.9	466	615	31	-615	-466
27.0	508	617	28	-617	-508
30.1	446	552	64	-552	-446
30.8	435	605	44	-605	-435
34.6	468	712	43	-712	-468
37.0	426	604	46	-604	-426
39.8	382	585	27	-585	-382
41.8	434	594	99	-594	-434
46.5	536	529	88	-529	-536
49.5	515	517	26	-517	-515
52.0	627	524	52	-524	-627
55.9	427	562	127	-562	-427
63.8	441	579	37	-579	-441

* For sign convention, see Figure 22

TABLE 24 GIRDER ROTATIONS AT SECTION M --- IMPACT RUNS

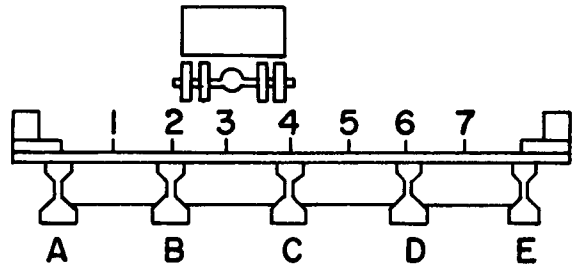

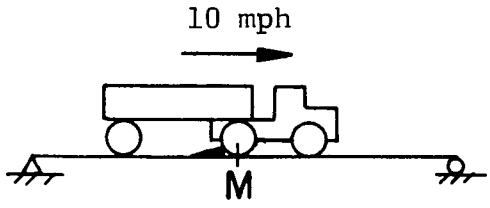

	Rotation (10^{-6} radians)				
	A	B	C	D	E
Truck in Lane 1	-407*	-759	-677	---	---
2	-164	125	-1015	---	---
3	85	762	-603	---	---
4	110	947	-173	---	---

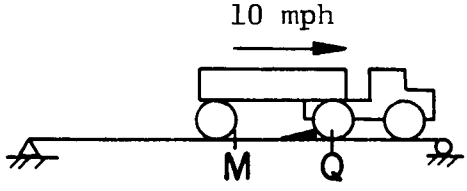

	Rotation (10^{-6} radians)				
	A	B	C	D	E
Truck in Lane 4	-39	765	-235	---	---
5	-115	982	280	---	---
6	-98	498	612	---	---
7	-55	235	571	---	---

* For sign convention, see Figure 22

TABLE 25 LOCATION OF NEUTRAL AXES -- CRAWL RUNS AND IMPACT RUNS

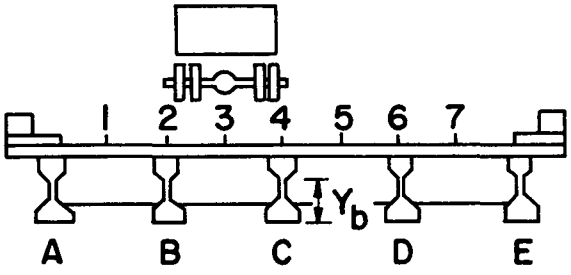

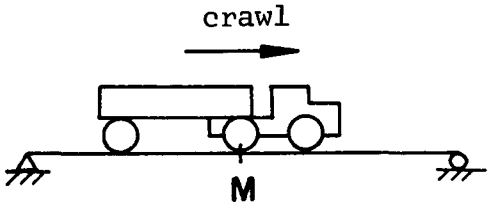

	Y_b (inches)				
	A	B	C	D	E
Truck in Lane 1	37.4	37.6	32.8	27.2	20.9
2	35.0	37.5	34.7	30.3	17.8
3	30.9	35.5	36.4	32.6	20.3
4	25.7	33.8	36.8	33.8	25.7

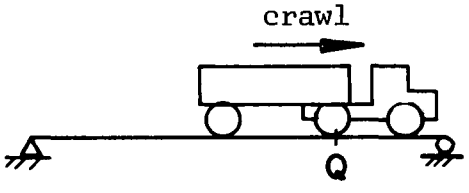

	Y_b (inches)				
	A	B	C	D	E
Truck in Lane 1	34.2	36.7	32.9	27.0	33.1
2	32.9	35.7	33.2	28.6	23.6
3	29.3	33.0	33.8	31.1	22.6
4	27.6	31.6	36.4	31.6	27.6

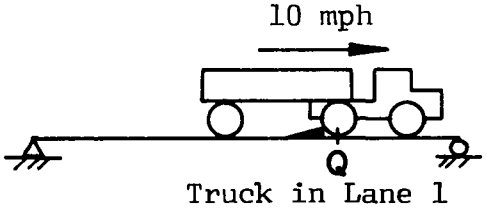

	Y_b (inches)				
	A	B	C	D	E
Truck in Lane 1	38.3	35.8	35.2	32.8	43.8
2	33.4	39.9	35.6	38.2	35.0
3	35.3	34.2	38.2	35.2	35.3
4	37.3	35.8	36.5	35.8	37.3

TABLE 26 LOCATION OF NEUTRAL AXES --- SPEED RUNS IN LANE 2

Units are inches

SPEED (mph)	SECTION M					SECTION Q				
	Beam A	Beam B	Beam C	Beam D	Beam E	Beam A	Beam B	Beam C	Beam D	Beam E
2.0	35.0*	37.5	34.7	30.3	17.8	32.9	35.7	33.2	28.6	23.6
5.0	35.3	37.0	34.3	30.8	28.7	32.4	36.0	37.6	26.6	41.0
8.8	35.2	38.4	33.5	29.9	28.0	32.2	35.5	32.9	27.3	29.4
10.4	35.7	37.8	33.6	30.3	29.1	31.7	34.3	33.4	28.7	41.1
12.3	35.0	38.1	35.2	30.9	24.2	34.7	35.2	33.5	28.6	36.8
13.6	----	----	----	----	----	36.3	34.2	37.0	30.2	28.2
13.7	35.8	37.6	33.3	32.2	28.0	34.6	35.4	38.0	31.2	32.3
17.1	35.8	37.5	36.3	29.7	25.8	33.7	35.9	37.3	29.4	29.5
20.0	35.4	38.1	34.8	30.6	28.3	34.5	35.7	41.7	27.2	32.4
20.4	----	----	----	----	----	34.6	34.4	34.2	29.1	31.7
21.4	38.4	39.4	35.9	30.2	13.1	33.1	35.6	38.0	27.8	24.6
23.9	35.3	37.6	35.3	29.8	9.1	34.8	36.3	34.1	29.4	31.2
26.0	----	----	----	----	----	36.4	34.2	31.6	28.3	36.5
26.4	34.9	37.3	34.0	30.9	32.0	35.2	36.3	34.0	28.6	32.3
31.7	35.5	38.1	36.3	31.3	30.7	34.6	38.9	32.8	29.4	31.2
32.4	34.9	38.6	35.9	30.3	30.3	34.9	36.0	32.9	29.2	27.4
35.4	35.1	37.8	35.8	30.8	33.3	35.1	36.0	34.2	31.1	33.9
35.8	----	----	----	----	----	33.8	34.2	32.9	30.0	32.7
37.2	35.2	38.8	36.1	30.5	27.6	33.3	36.7	32.7	29.4	32.5
40.6	36.0	38.0	36.1	31.5	26.9	35.3	35.8	35.1	29.8	35.7
44.8	35.4	37.8	33.7	31.5	27.7	33.7	36.4	37.6	30.9	34.2
47.5	34.4	37.8	33.7	30.6	27.3	34.6	35.9	32.8	30.8	28.8
51.1	34.4	37.5	35.4	29.6	26.7	35.1	35.7	33.0	32.5	30.9
53.2	35.8	37.5	35.7	29.6	26.5	34.5	36.7	33.1	30.9	36.5
55.8	35.7	36.8	36.0	29.6	27.1	34.4	34.7	37.9	31.1	29.0
56.0	35.2	37.5	35.6	29.6	28.0	36.2	35.5	37.9	31.6	37.1
63.2	35.6	37.7	33.9	31.2	26.6	34.1	39.0	32.7	29.5	30.0

* See Table 25

TABLE 27 LOCATION OF NEUTRAL AXES --- SPEED RUNS IN LANE 4

Units are inches

SPEED	SECTION M					SECTION Q				
(mph)	Beam A	Beam B	Beam C	Beam D	Beam E	Beam A	Beam B	Beam C	Beam D	Beam E
2.0	25.7*	33.8	36.8	33.8	25.7	27.6	31.6	36.4	31.6	27.6
5.0	26.7	35.1	36.9	35.1	26.7	24.6	31.5	34.6	31.5	24.6
8.6	29.7	34.6	36.4	34.6	29.7	30.5	32.2	36.8	32.2	30.5
10.4	28.3	34.9	37.0	34.9	28.3	30.9	32.6	36.7	32.6	30.9
12.3	26.5	35.2	37.0	35.2	26.5	31.2	32.1	35.8	32.1	31.2
14.3	27.4	34.6	36.5	34.6	27.4	31.5	31.1	36.3	31.1	31.5
16.8	29.3	35.6	37.2	35.6	29.3	29.2	31.9	36.8	31.9	29.2
20.1	28.5	35.7	37.1	35.7	28.5	29.1	32.7	36.8	32.7	29.1
21.4	27.9	35.4	37.7	35.4	27.9	28.8	33.1	37.3	33.1	28.8
23.9	29.2	35.8	37.5	35.8	29.2	29.5	33.0	37.1	33.0	29.5
27.0	28.4	35.9	37.7	35.9	28.4	29.8	32.4	37.5	32.4	29.8
30.1	26.6	34.7	37.3	34.7	26.6	30.6	31.6	36.0	31.6	30.6
30.8	27.6	35.0	36.8	35.0	27.6	28.4	31.7	37.4	31.7	28.4
34.6	29.3	37.8	38.0	37.8	29.3	30.7	31.5	36.4	31.5	30.7
37.0	29.0	34.7	37.4	34.7	29.0	31.9	32.0	36.8	32.0	31.9
39.8	28.5	33.7	37.5	33.7	28.5	32.7	33.1	36.8	33.1	32.7
41.8	29.7	34.6	37.2	34.6	29.7	27.8	33.5	36.5	33.5	27.8
46.5	26.8	34.1	36.7	34.1	26.8	31.2	32.3	36.1	32.3	31.2
49.5	28.3	34.1	36.4	34.1	28.3	31.4	32.1	37.1	32.1	31.4
52.0	29.4	34.6	36.8	34.6	29.4	31.6	33.5	36.4	33.5	31.6
55.9	30.2	34.8	37.1	34.8	30.2	33.2	31.8	36.9	31.8	33.2
56.8	29.7	34.9	36.2	34.9	29.7	31.9	31.1	36.7	31.1	31.9
63.8	29.8	34.0	36.5	34.0	29.8	32.1	32.3	36.5	32.3	32.1

* See Table 25

TABLE 28 EFFECTIVE SLAB WIDTHS FOR CRAWL RUNS AND IMPACT RUNS

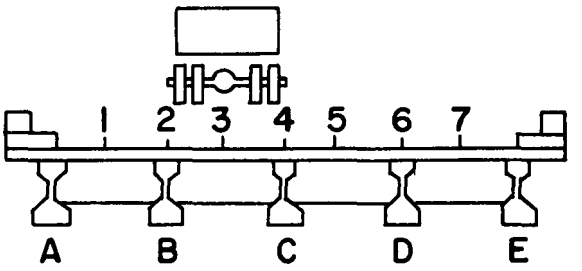

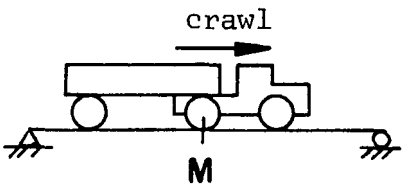

	Effective Slab Width (inches)					Total
	A	B	C	D	E	
Truck in Lane 1	94.3	161.4	89.6	34.0	6.0	385.3
2	64.3	160.3	112.1	55.6	0.5	392.8
3	37.1	119.7	146.9	77.7	0.4	381.8
4	15.2	93.5	149.7	93.5	15.2	367.1

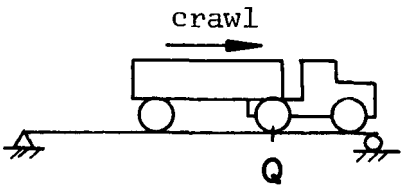

	Effective Slab Width (inches)					Total
	A	B	C	D	E	
Truck in Lane 1	51.7	151.3	77.2	30.2	47.8	358.2
2	43.4	124.4	74.7	40.6	10.6	293.7
3	29.7	90.1	85.0	58.4	4.3	267.5
4	19.0	69.8	123.1	69.8	19.0	300.7

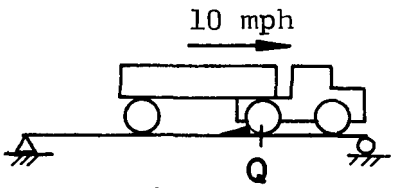

	Effective Slab Width (inches)					Total
	A	B	C	D	E	
Truck in Lane 1	93.0	133.4	102.7	76.9	352.3	758.3
2	46.1	252.6	110.0	166.3	55.6	630.6
3	59.1	104.6	159.2	107.8	57.7	488.4
4	87.0	131.0	124.4	131.0	87.0	560.4

TABLE 29 EFFECTIVE SLAB WIDTHS -- SPEED RUNS IN LANE 2

Units are inches

SPEED	SECTION M						SECTION Q					
(mph)	A	B	C	D	E	Total	A	B	C	D	E	Total
2.0	64.3	160.3	112.1	55.6	0.5	392.8	43.4	124.4	74.7	40.6	10.6	293.7
5.0	66.8	147.4	103.2	59.9	24.2	401.5	40.6	135.4	145.2	28.1	168.4	517.7
8.8	65.6	182.0	114.8	52.1	21.8	436.3	39.5	126.2	144.2	31.7	25.9	367.5
10.4	70.5	167.3	93.2	55.1	25.8	411.9	36.8	107.2	80.5	40.6	173.0	438.1
12.3	63.7	175.1	117.7	60.7	9.6	426.8	54.3	122.1	81.4	40.4	70.0	368.2
13.6	----	-----	-----	----	----	-----	67.1	104.7	134.0	52.0	21.5	379.3
13.7	70.8	163.0	89.6	73.2	21.8	418.4	53.8	124.9	155.3	60.5	39.1	433.6
17.1	70.8	159.6	96.3	50.8	14.3	391.8	47.7	133.4	139.9	46.1	26.1	393.2
20.0	67.1	176.2	111.2	57.9	22.9	435.3	53.1	130.9	288.2	31.4	39.9	543.5
20.4	----	-----	-----	----	----	-----	53.9	107.3	90.1	43.4	36.2	330.9
21.4	120.8	214.2	110.9	54.5	0.0	500.4	44.2	128.2	85.7	34.7	10.1	302.9
23.9	66.5	162.5	119.7	51.0	0.0	399.7	55.5	142.0	88.2	46.2	33.9	365.8
26.0	----	-----	-----	----	----	-----	68.3	105.4	62.3	38.0	67.8	341.8
26.4	63.7	154.2	98.9	61.2	39.3	417.3	57.8	141.9	87.4	40.4	39.4	366.9
31.7	68.7	175.3	137.2	64.9	33.1	479.2	47.9	160.5	98.9	39.6	28.1	375.0
32.4	63.3	188.2	130.6	55.4	31.2	468.7	56.0	136.0	75.1	44.2	18.6	329.9
35.4	65.3	167.6	129.4	59.7	46.9	468.9	57.1	136.1	89.8	60.1	48.2	391.3
35.8	----	-----	-----	----	----	-----	48.7	105.7	74.7	50.2	41.1	320.4
37.2	65.6	195.6	133.4	56.9	20.4	471.9	45.2	150.6	72.5	32.6	40.2	341.1
40.6	72.8	172.9	133.2	66.6	17.9	463.4	58.5	132.4	101.9	49.1	61.0	402.9
44.8	67.7	168.0	95.5	66.3	20.6	418.1	47.9	143.9	146.3	58.2	50.5	446.8
47.5	58.9	166.8	95.5	58.2	19.4	398.8	53.8	133.6	74.2	57.0	23.6	342.2
51.1	58.9	155.7	121.5	49.7	17.2	403.0	51.7	130.1	75.7	72.9	32.3	362.7
53.2	70.9	159.9	126.1	49.6	16.6	423.1	53.0	151.0	77.4	58.1	68.0	407.5
55.8	70.7	144.5	132.5	49.8	18.6	416.1	52.7	113.2	152.8	59.4	24.4	402.5
56.0	66.3	160.0	123.9	49.5	21.8	421.5	65.8	126.8	153.0	64.3	73.5	483.4
63.2	68.9	165.9	98.2	63.2	17.1	413.3	50.4	217.7	72.8	46.8	28.4	416.1

TABLE 30 EFFECTIVE SLAB WIDTHS -- SPEED RUNS IN LANE 4

Units are inches

SPEED	SECTION M						SECTION Q					
(mph)	A	B	C	D	E	Total	A	B	C	D	E	Total
2.0	15.2	93.5	149.7	93.5	15.2	367.1	19.0	69.8	123.1	69.8	19.0	300.7
5.0	18.0	111.2	151.0	111.2	18.0	409.4	10.3	66.9	95.3	66.9	10.3	249.7
8.6	29.8	104.6	139.2	104.6	29.8	407.9	30.8	74.1	129.4	74.1	30.8	339.2
10.4	23.9	109.2	154.2	109.2	23.9	420.4	32.4	79.3	128.5	79.3	32.4	351.9
12.3	17.3	113.1	153.0	113.1	17.3	413.8	34.0	73.4	112.7	73.4	34.0	327.5
14.3	20.7	104.3	141.5	104.3	20.7	391.5	35.2	63.3	120.6	63.3	35.2	317.6
16.8	28.1	121.0	157.1	121.0	28.1	455.2	25.4	71.3	129.5	71.3	25.4	322.9
20.1	24.5	121.7	155.6	121.7	24.5	448.0	24.8	80.1	130.6	80.1	24.8	340.4
21.4	22.4	117.7	168.9	117.7	22.4	449.1	23.8	84.5	140.1	84.5	23.8	356.7
23.9	27.4	124.2	164.3	124.2	27.4	467.5	26.7	83.7	135.8	83.7	26.7	356.6
27.0	24.2	126.0	168.9	126.0	24.2	469.3	27.8	76.8	145.0	76.8	27.8	354.2
30.1	17.6	106.2	159.8	106.2	17.6	407.4	31.2	68.4	116.1	68.4	31.2	315.3
30.8	21.1	111.0	149.0	111.0	21.1	413.2	22.5	68.9	141.1	68.9	22.5	324.0
34.8	28.1	165.0	178.8	165.0	28.1	565.0	31.8	66.8	122.7	66.8	31.8	319.9
37.0	26.9	105.9	163.2	105.9	26.9	428.8	37.1	72.5	130.7	72.5	37.1	349.9
39.8	24.8	91.7	164.8	91.7	24.8	397.8	31.6	84.2	129.5	84.2	31.6	361.1
41.8	30.0	103.8	157.8	103.8	30.0	425.4	20.1	89.5	123.9	89.5	20.1	343.1
46.5	18.3	97.5	145.9	97.5	18.3	377.5	33.9	75.0	117.2	75.0	33.9	335.0
49.5	24.0	96.6	139.6	96.6	24.0	380.8	35.2	73.4	134.9	73.4	35.2	351.9
52.0	28.6	103.7	147.7	103.7	28.6	412.3	36.1	90.3	123.7	90.3	36.1	376.5
55.9	32.1	106.5	155.1	106.5	32.1	432.3	44.4	70.3	132.6	70.3	44.4	362.0
56.8	29.9	108.8	136.4	108.8	29.9	413.8	37.3	63.8	128.4	63.8	37.3	330.6
63.8	30.3	96.0	141.9	96.0	30.3	394.5	38.7	75.9	124.0	75.9	38.7	353.2

TABLE 31 COMPARISON OF MAXIMUM DEFLECTIONS

Units are mph for Speed and Inches for Deflection

Load Lane	BEAM A		BEAM B		BEAM C		BEAM D		BEAM E		REMARK
	Speed	Defl.	Speed	Defl.	Speed	Defl.	Speed	Defl.	Speed	Defl.	
1	2.0	0.156	2.0	0.113	2.0	0.065	2.0	0.024	2.0	0.015	Crawl
	10.0	0.262	10.0	0.183	10.0	0.117	---	-----	---	-----	Impact
2	2.0	0.110	2.0	0.123	2.0	0.089	2.0	0.040	2.0	0.020	Crawl
	56.0	0.141	20.0	0.150	20.0	0.111	63.2	0.047	13.7	0.031	Speed
	10.0	0.219	10.0	0.212	10.0	0.172	----	-----	----	-----	Impact
3	2.0	0.066	2.0	0.112	2.0	0.116	2.0	0.060	2.0	0.025	Crawl
	10.0	0.156	10.0	0.203	10.0	0.226	---	-----	---	-----	Impact
4	2.0	0.035	2.0	0.086	2.0	0.129	2.0	0.086	2.0	0.035	Crawl
	55.9	0.057	34.6	0.106	34.6	0.156	34.6	0.106	55.9	0.057	Speed
	10.0	0.115	10.0	0.167	10.0	0.244	----	-----	----	-----	Impact

TABLE 32 COMPARISON OF DISTRIBUTION FACTORS FOR DREHERSVILLE AND BARTONSVILLE BRIDGE

Bridge		Drehersville	Bartonsville			
Type		Spread Box-Beam	I-Beam			
Skew		90°	90°			
Roadway Width(w)		30' - 0"	32' - 0"			
Beam Spacing(s)		7' - 2"	8' - 0"			
Beam Size		4' - 33"	AASHO Type III (22" x 45")			
Span		61' - 6"	68' - 6"			
Loading Lanes		2	2		3	
Test Section		M*	M	Q**	M	Q
Beam A	Experimental	1.048	0.846	0.834	0.960	0.954
	Design	0.810	0.750	0.750	0.750	0.750
	Experimental / Design	1.295	1.128	1.112	1.280	1.272
Beam B	Experimental	0.850	1.040	1.030	1.360	1.356
	Design	1.300	1.455	1.455	1.455	1.455
	Experimental / Design	0.654	0.715	0.708	0.935	0.932
Beam C	Experimental	0.800	1.266	1.360	1.532	1.538
	Design	1.300	1.455	1.455	1.455	1.455
	Experimental / Design	0.615	0.870	0.935	1.053	1.057

* At Maximum Moment Section, with Diaphragm at Midspan
** At Quarter Span Section, no Diaphragm nearby

TABLE 33 PEAK VALUES OF DYNAMIC LOAD FACTORS - TOTAL BRIDGE BEHAVIOR

M.C. = Moment Coefficient (10^{-3} ft-in^2)

δ = Beam Deflection (inch)

$$(DLF)_m = \frac{\sum_{1}^{5} \text{M.C. at Speed}}{\sum_{1}^{5} \text{M.C. at Crawl}}$$

$$(DLF)_d = \frac{[1.25\ (\delta_A + \delta_E) + \delta_B + \delta_C + \delta_D] \text{ at Speed}}{[1.25\ (\delta_A + \delta_E) + \delta_B + \delta_C + \delta_D] \text{ at Crawl}}$$

LANE	SPEED (mph)	SECTION M		SECTION Q
		$(DLF)_m$	$(DLF)_d$	$(DLF)_m$
2	20.0	1.12	1.19	----
	26.0	----	----	1.21
	35.4	1.21	1.15	----
	35.8	----	----	1.32
	40.0	----	----	1.28
	51.1	1.22	1.22	----
	53.2	----	1.22	----
	56.0	1.24	----	1.28
	63.2	1.25	1.23	----
4	16.8	----	1.20	----
	23.9	----	1.22	----
	27.0	----	----	1.21
	34.6	1.23	1.25	----
	37.0	----	----	1.23
	55.9	1.23	1.28	1.27
	63.8	1.24	1.27	----

9. FIGURES

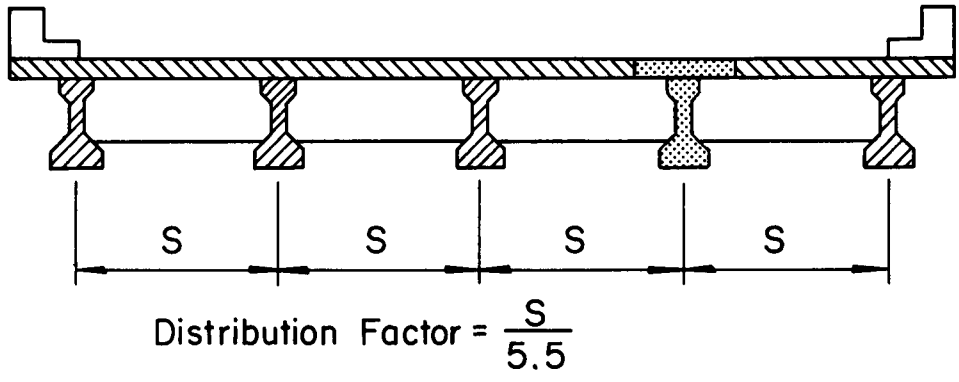

INTERIOR BEAM

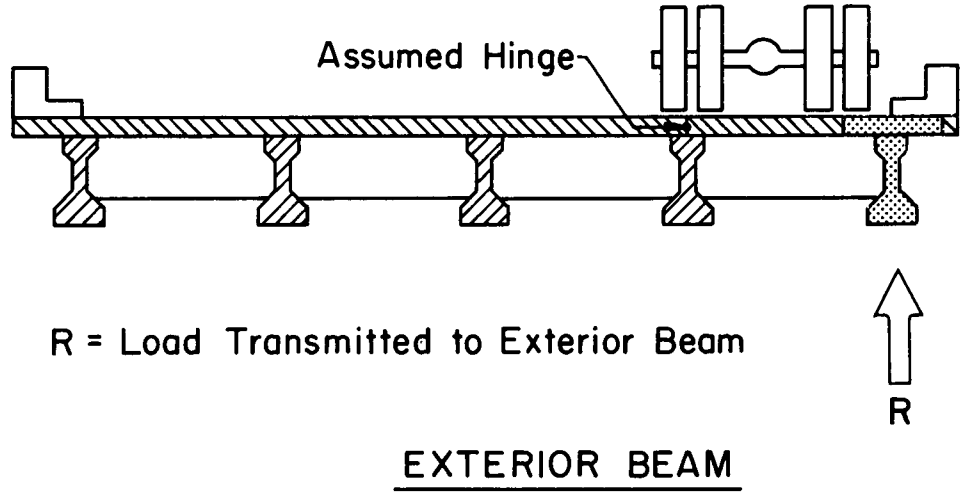

EXTERIOR BEAM

Fig. 1 Distribution of Vehicular Loads Assumed in Design of I-Beam Superstructures

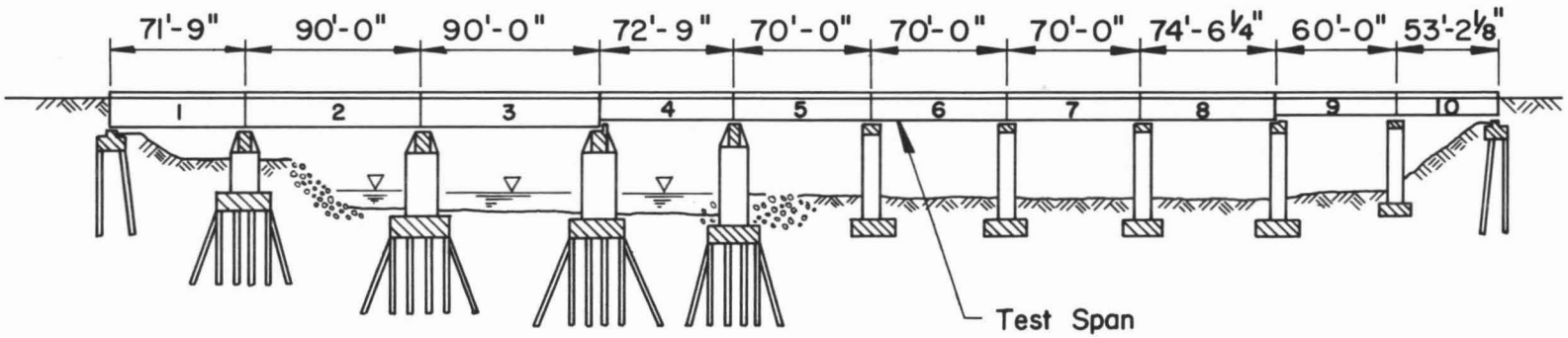

Fig. 2 Elevation of the Test Bridge

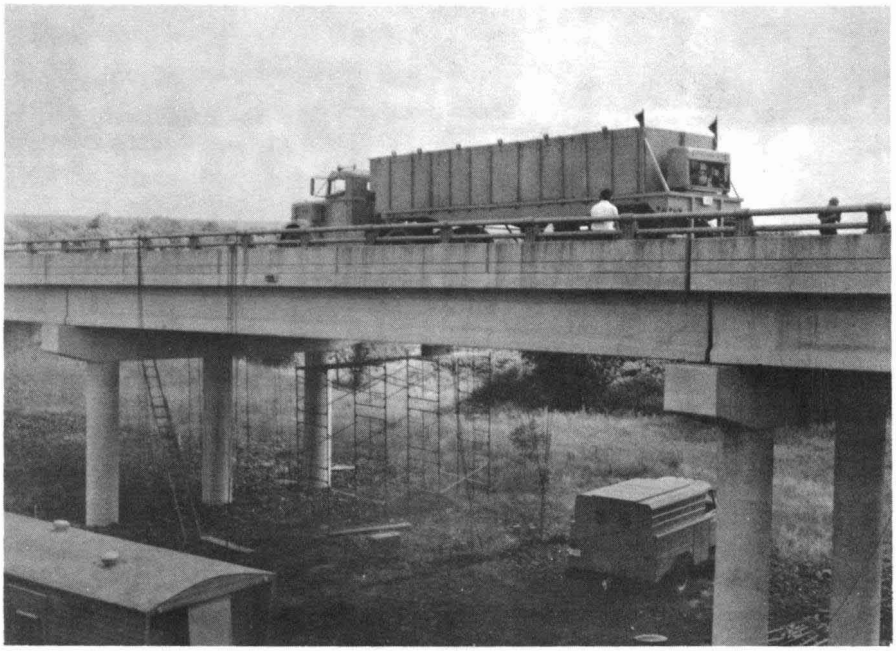

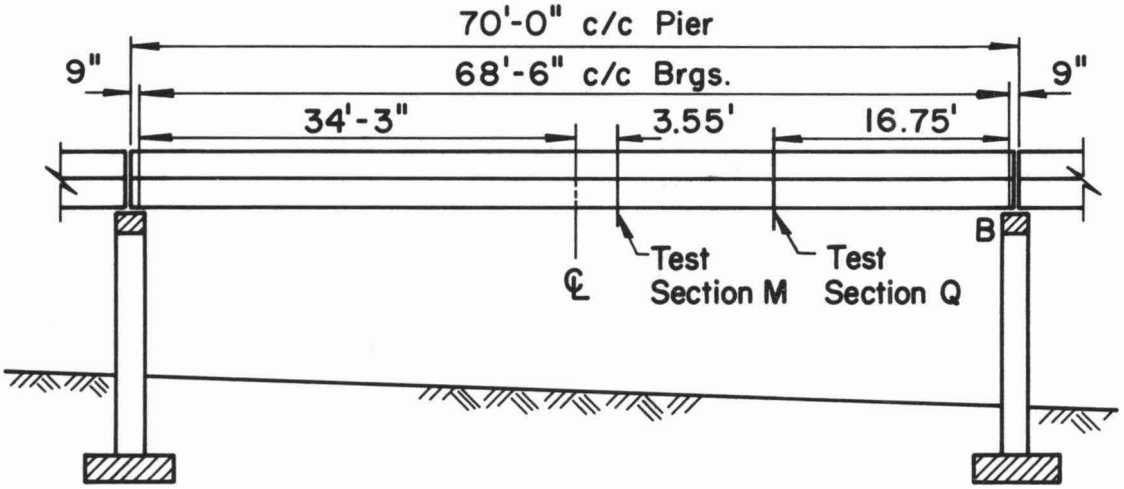

Fig. 3 Elevation of Test Span

DESIGN DIMENSIONS

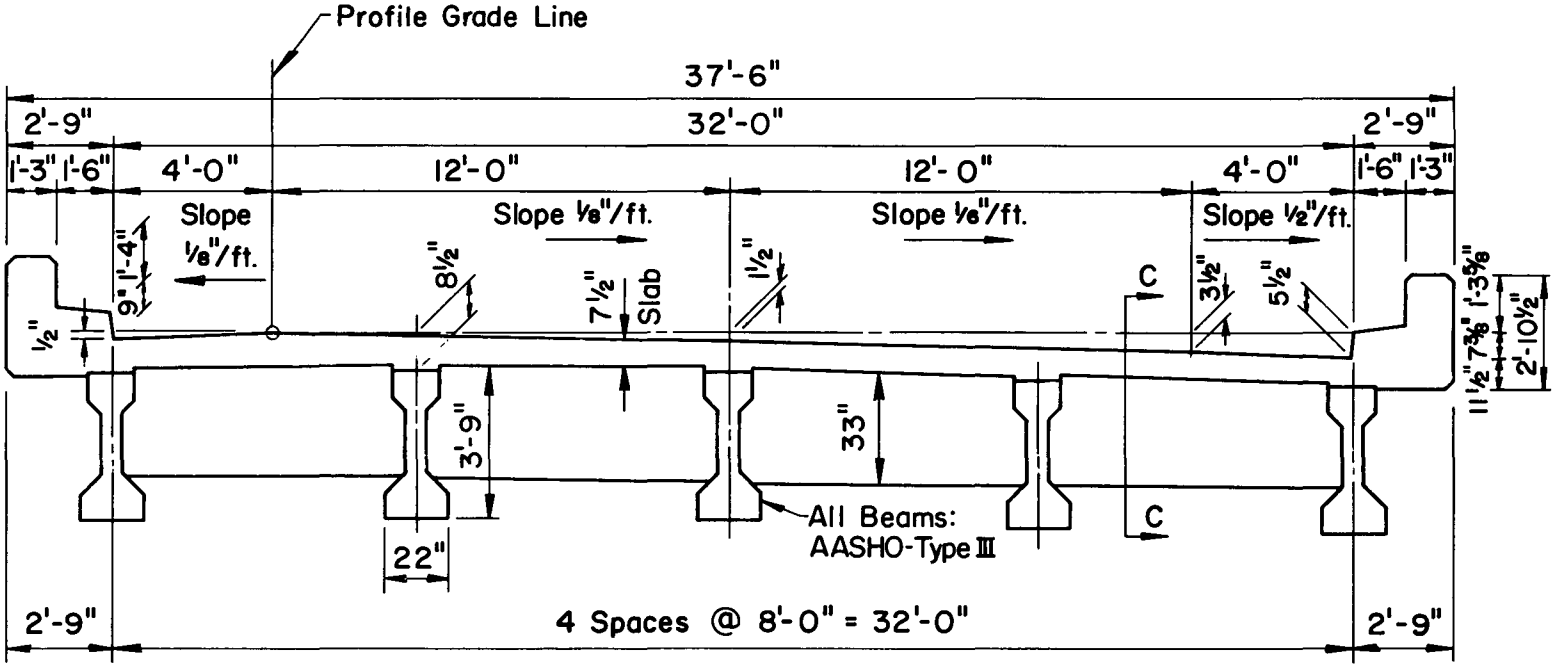

Fig. 4 Cross-Section of Test Bridge

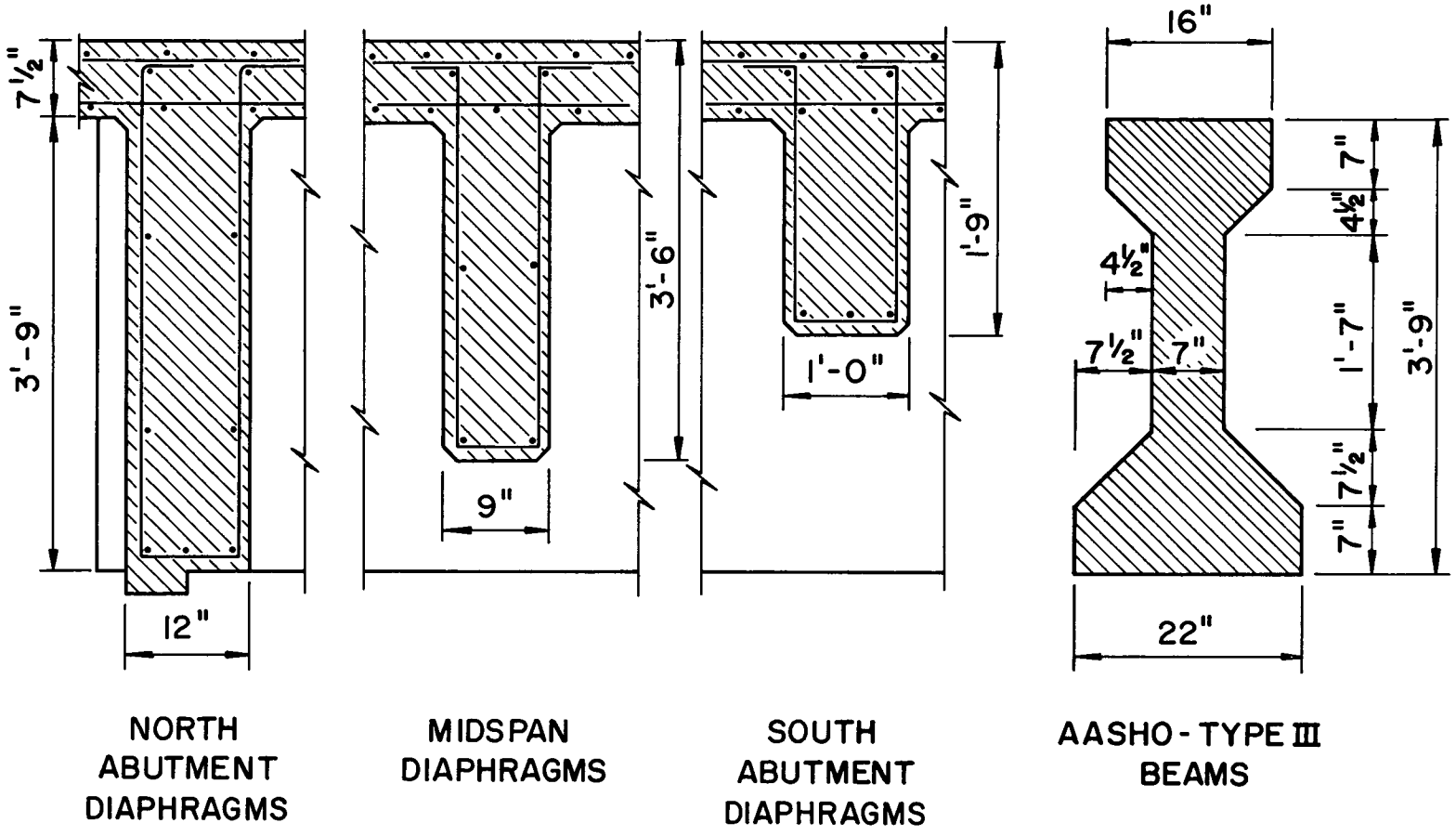

Fig. 5 Cross-Sectional Dimensions of Diaphragms and Beams

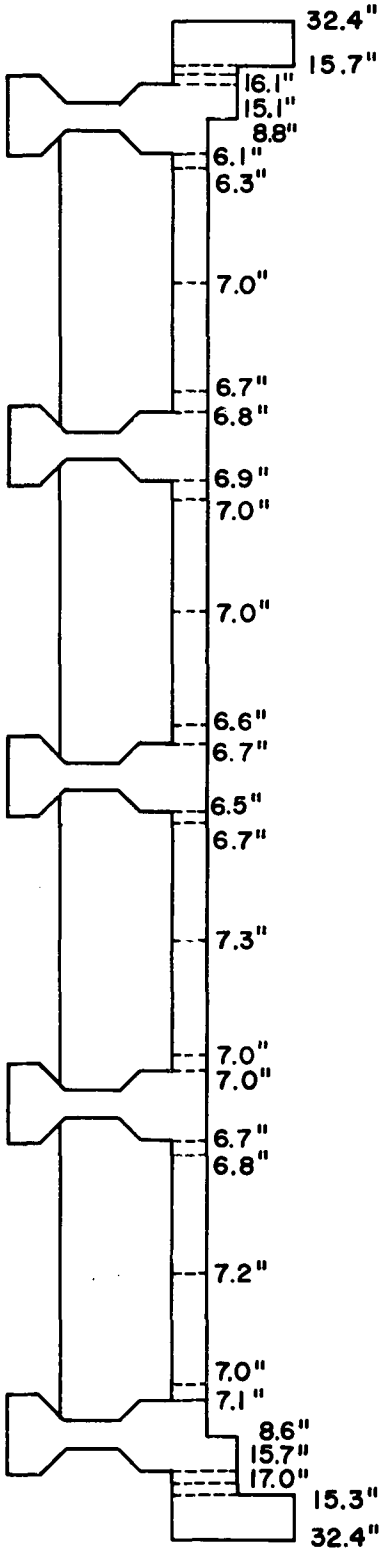

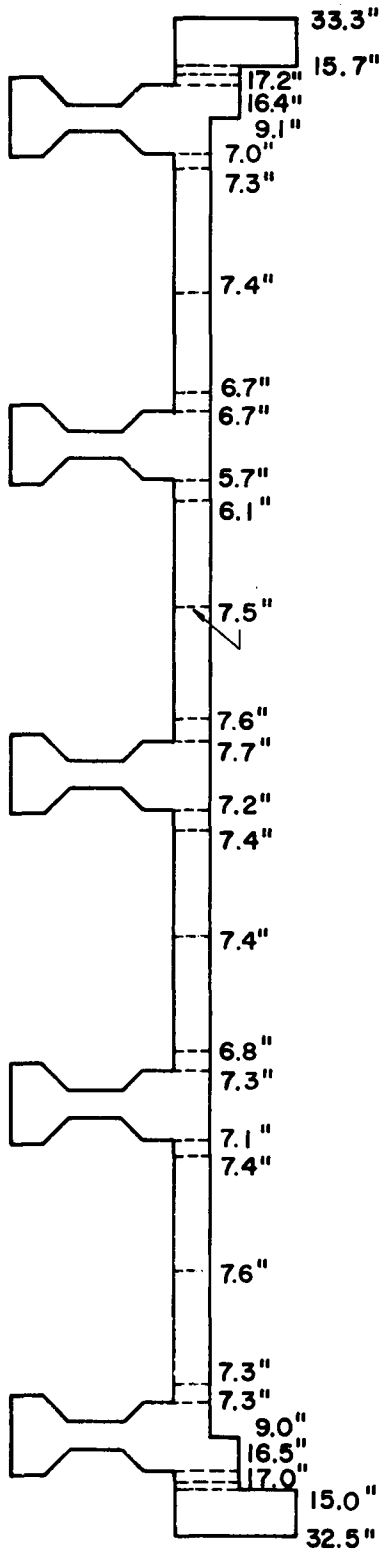

Fig. 6 Measured Thickness of Superstructures

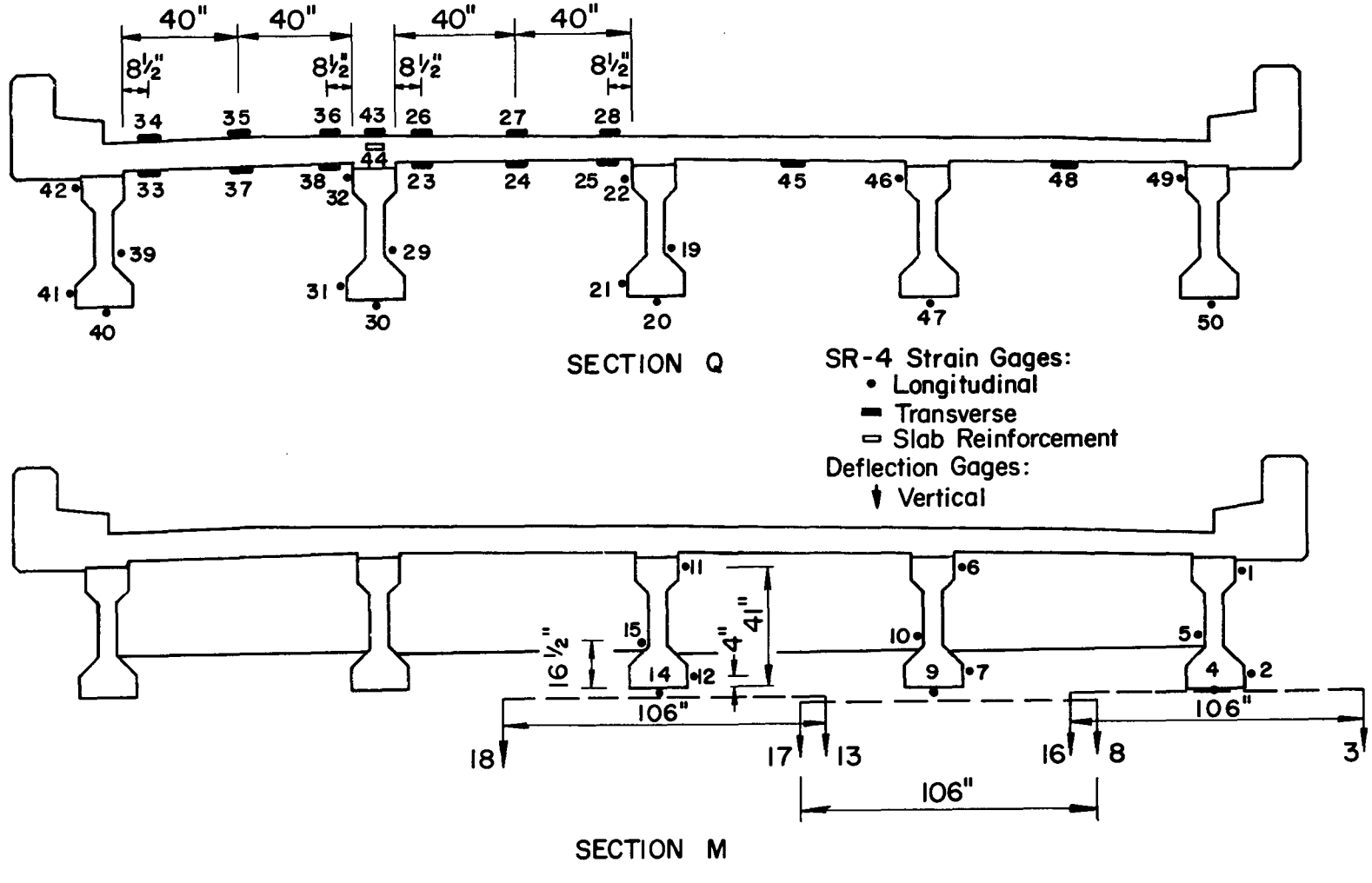

Fig. 7 Location of Gages

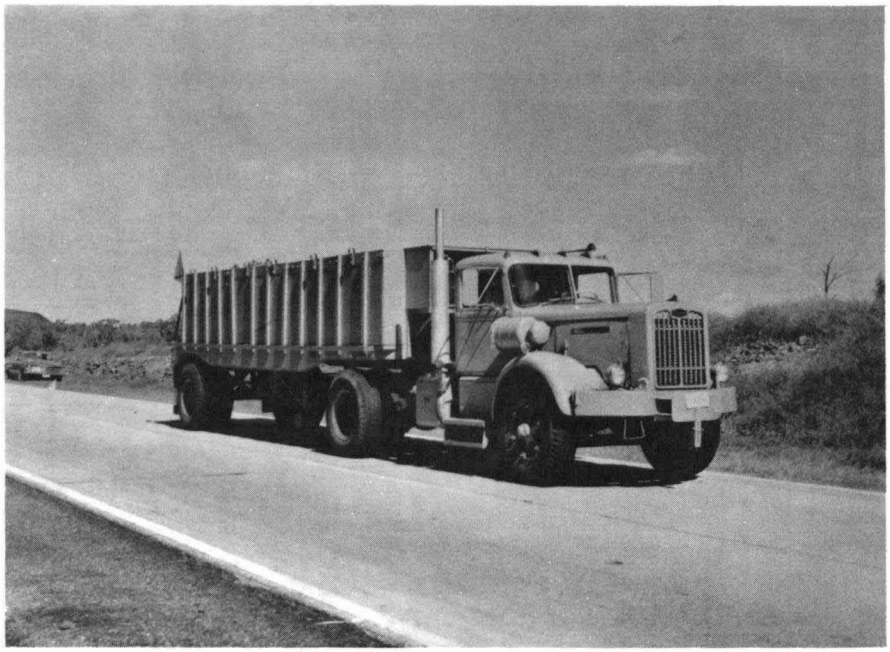

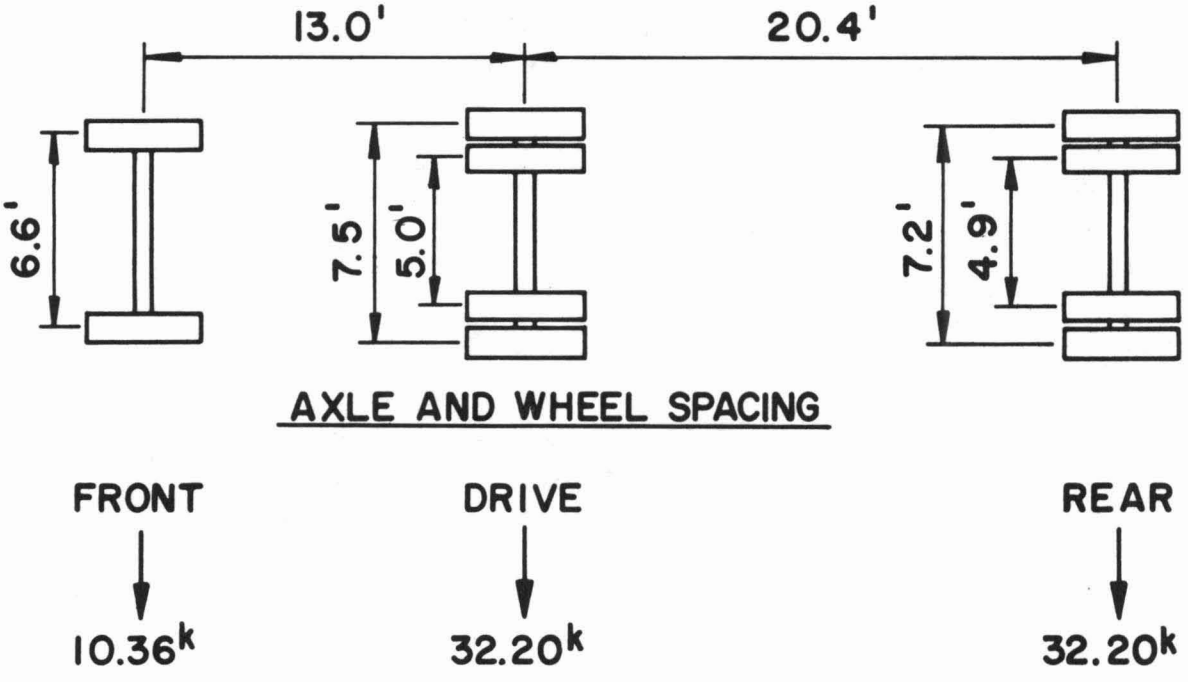

Fig. 8 Test Vehicle

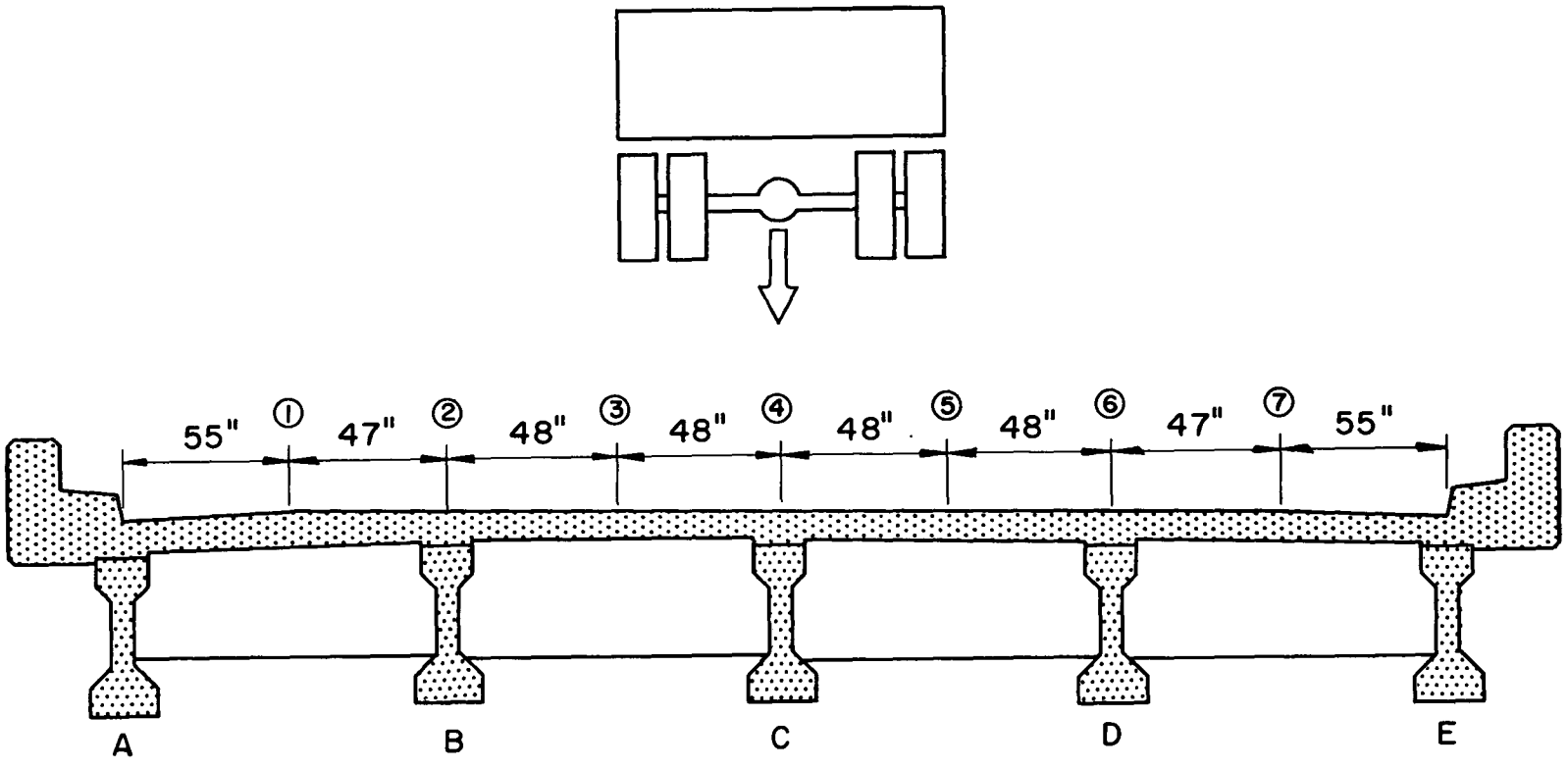

Fig. 9 Loading Lanes

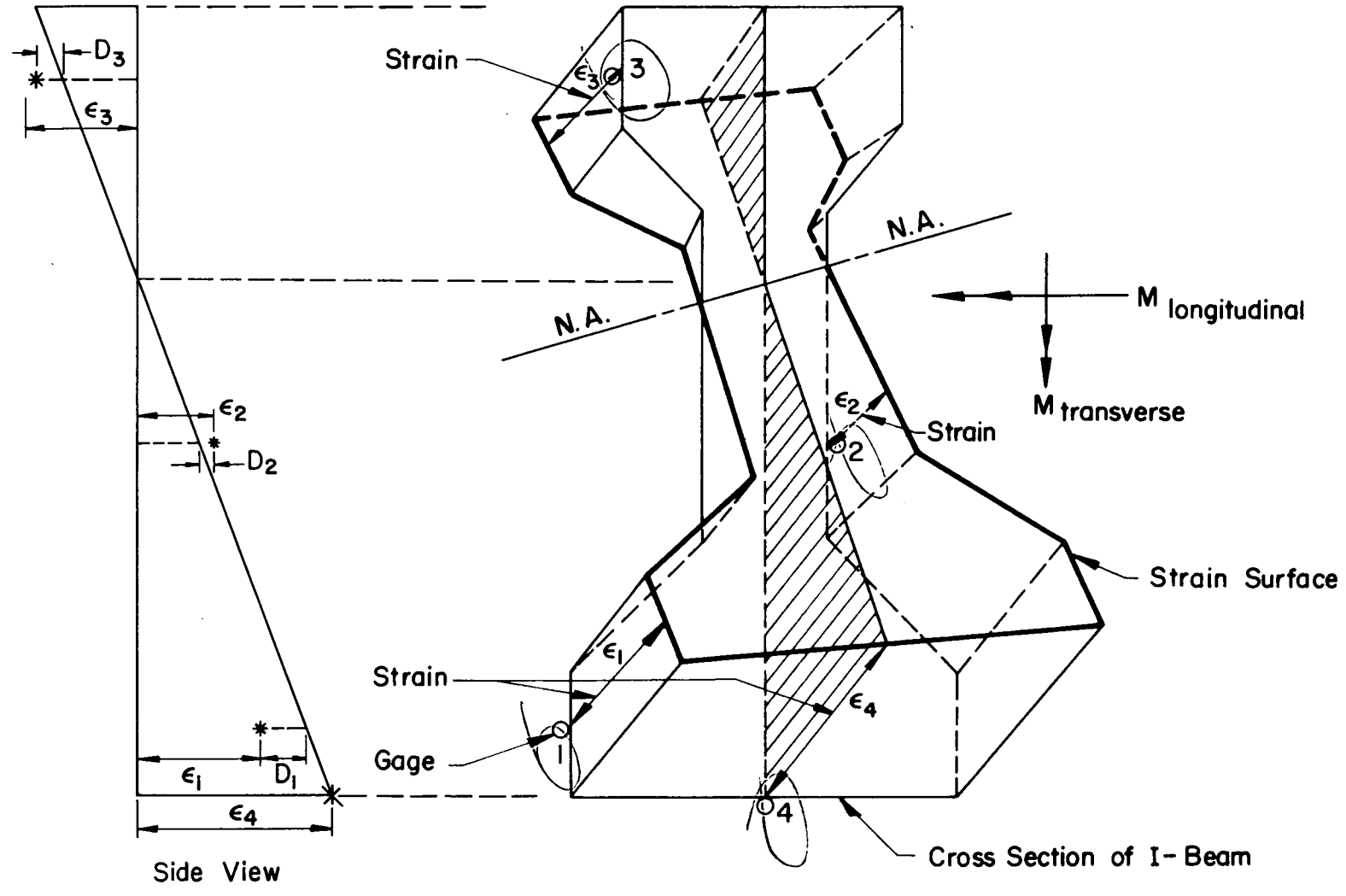

Fig. 10 Distribution of Strains

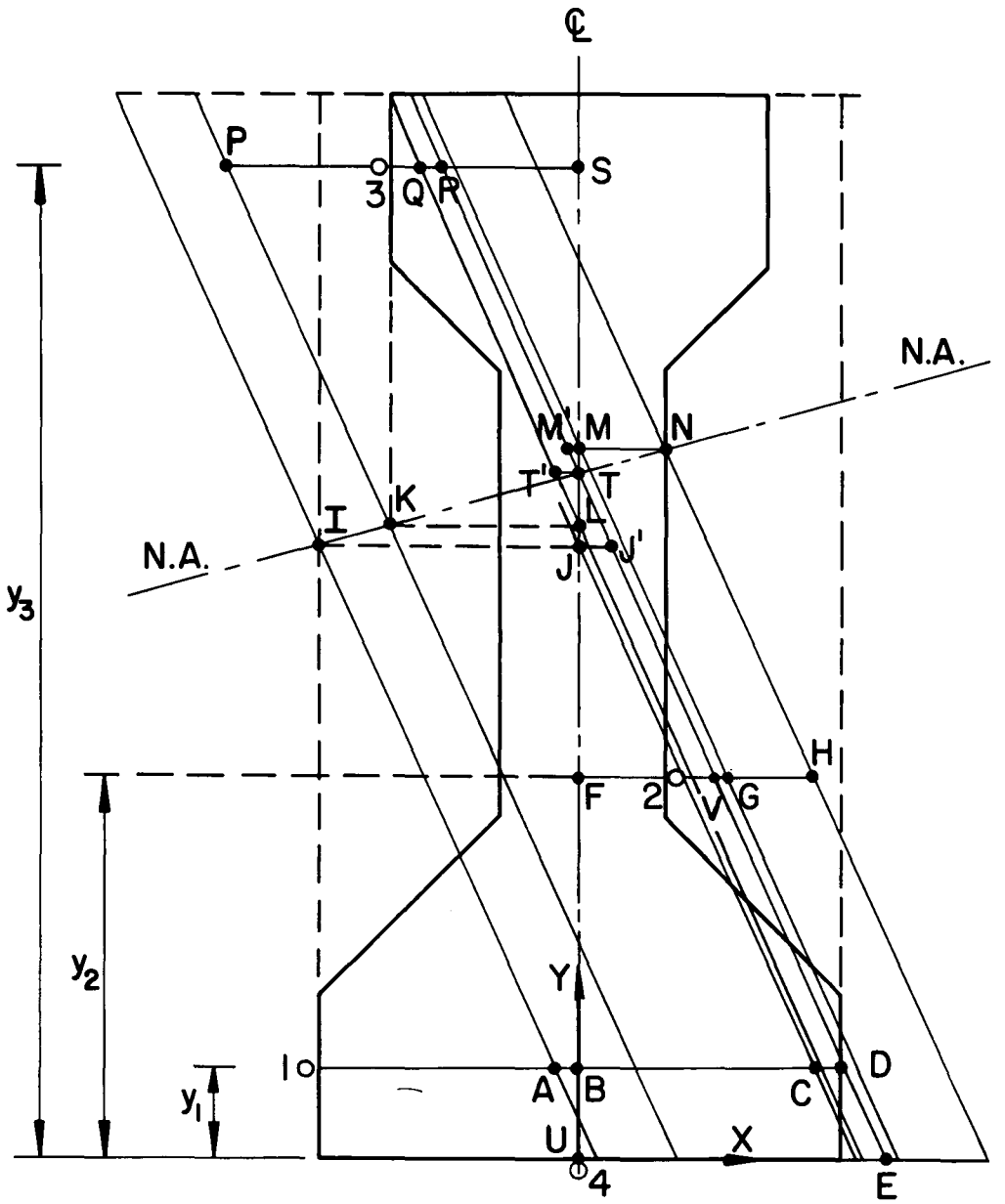

Fig. 11 Geometry of Gage Strains and Locations

Natural Frequency

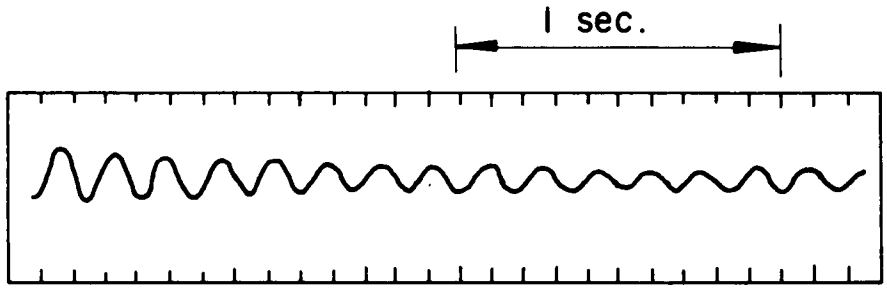

Loaded Frequency

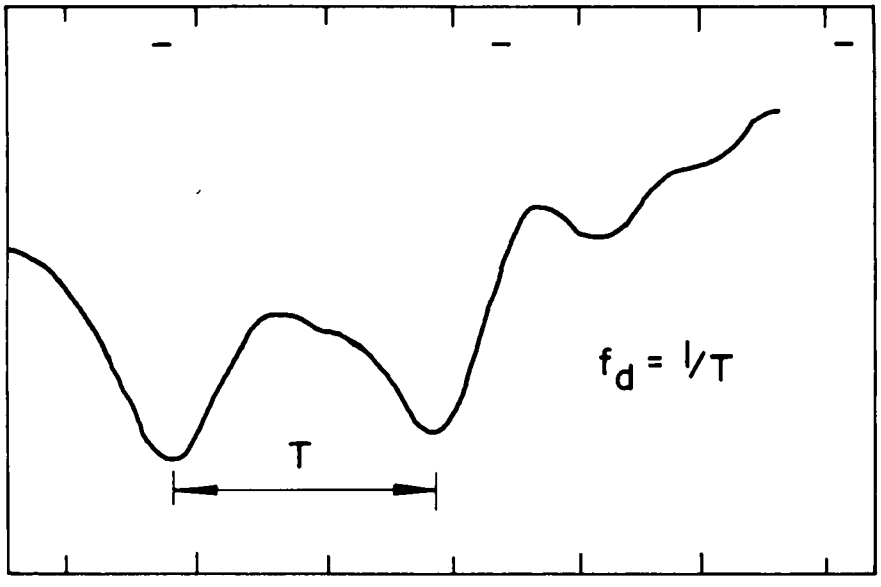

f_d: Loaded Frequency

T: Period

Fig. 12 Nature Frequency and Loaded Frequency

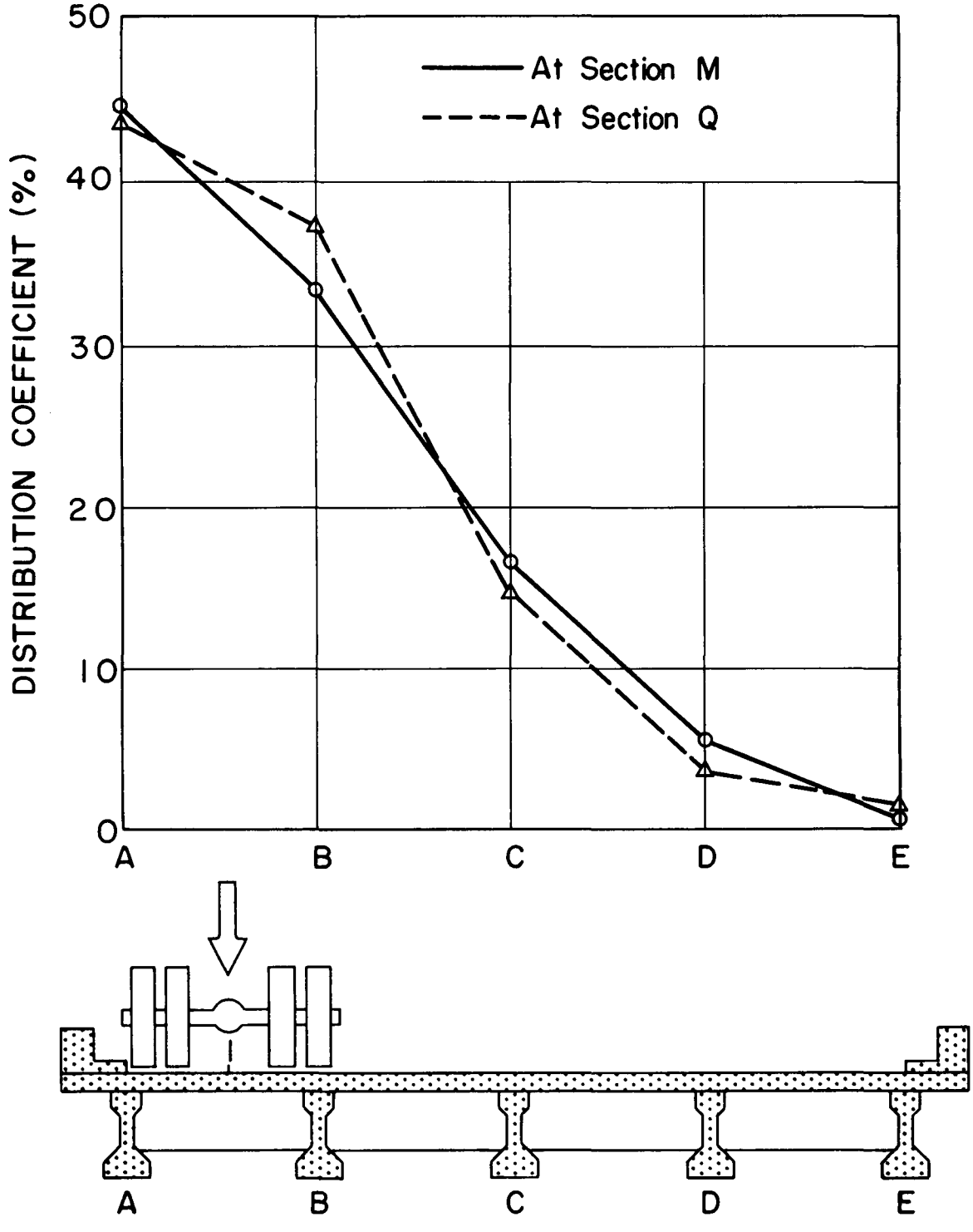

Fig. 13 Distribution Coefficients - Lane 1, Crawl Runs

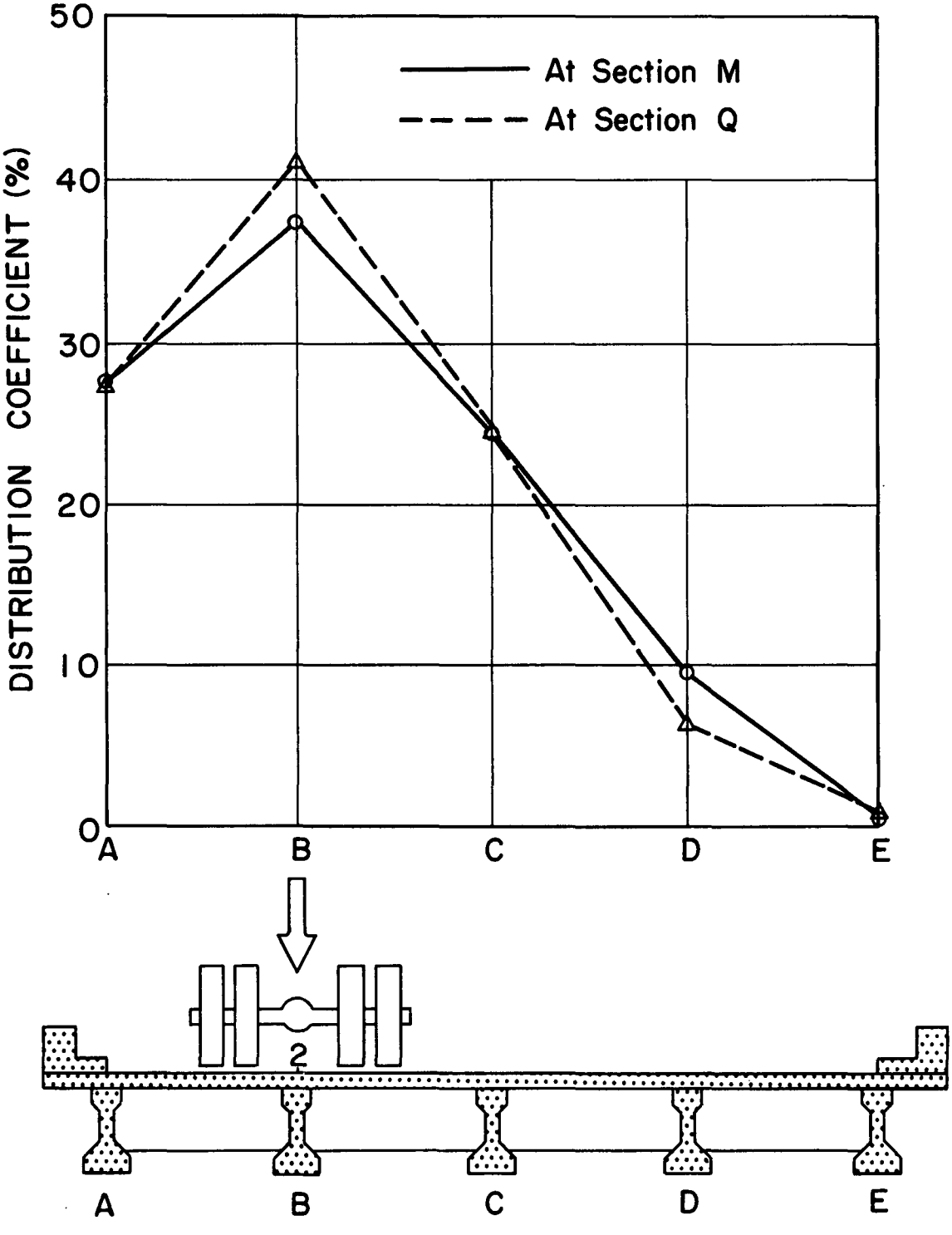

Fig. 14 Distribution Coefficients - Lane 2, Crawl Runs

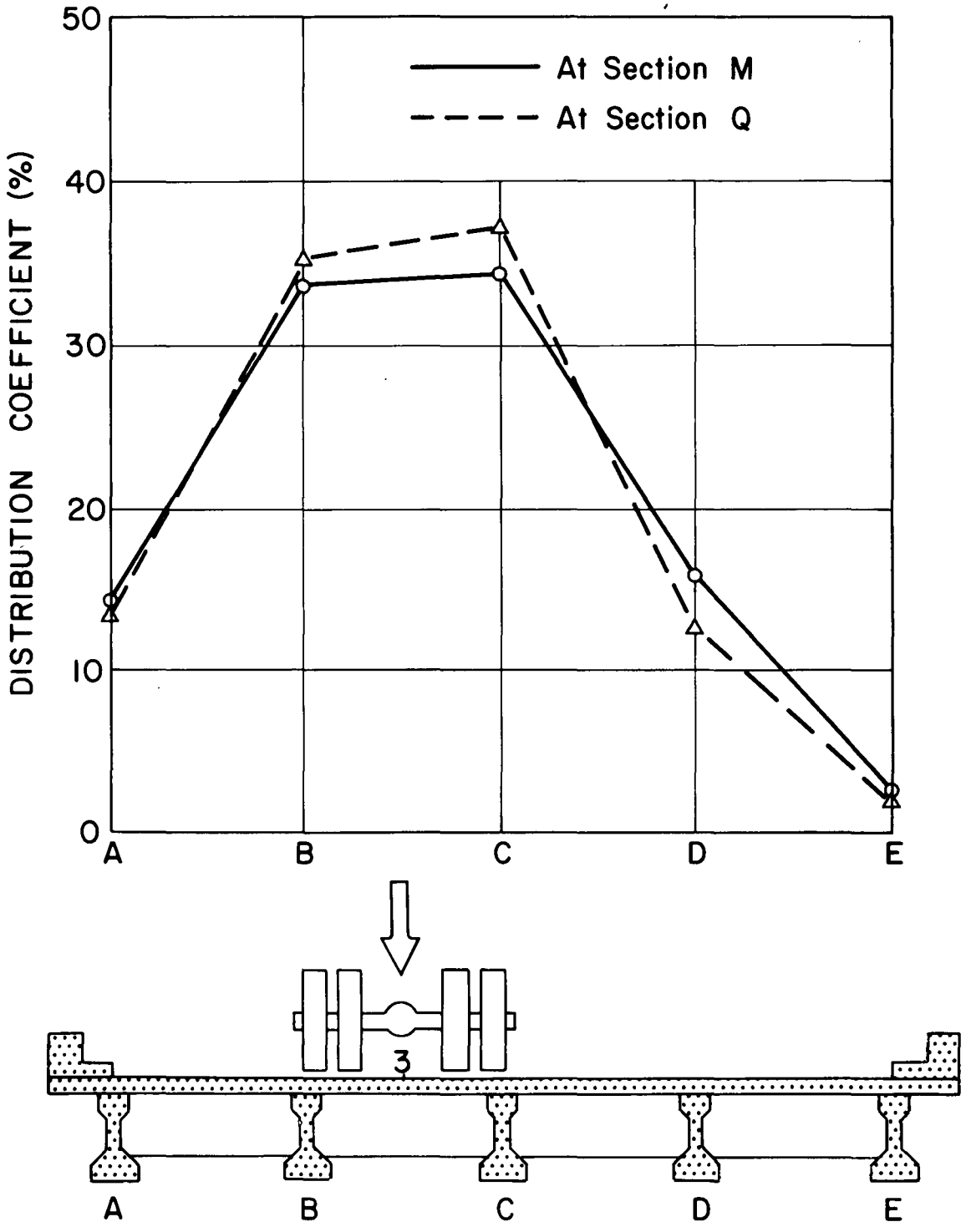

Fig. 15 Distribution Coefficients - Lane 3, Crawl Runs

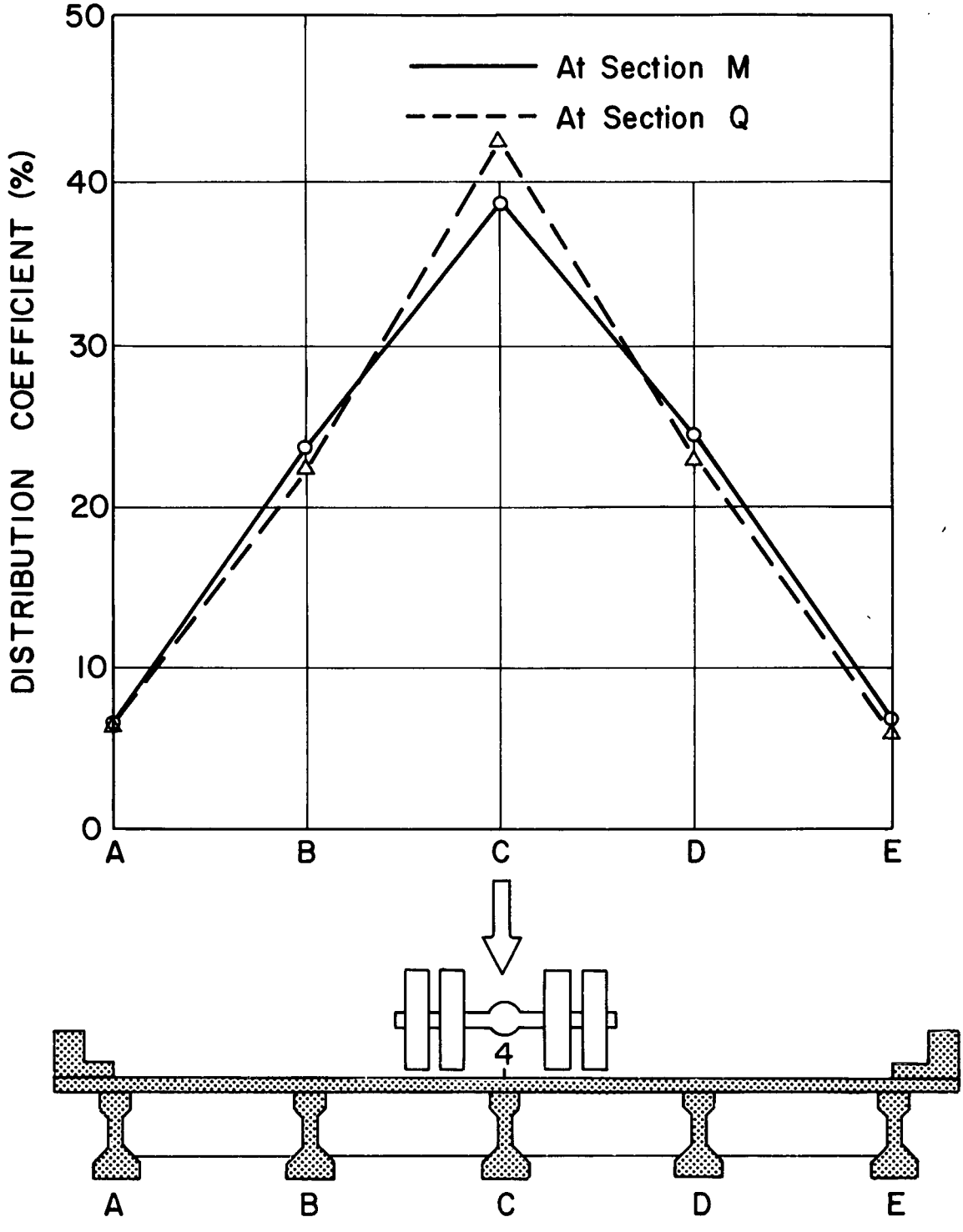

Fig. 16 Distribution Coefficients - Lane 4, Crawl Runs

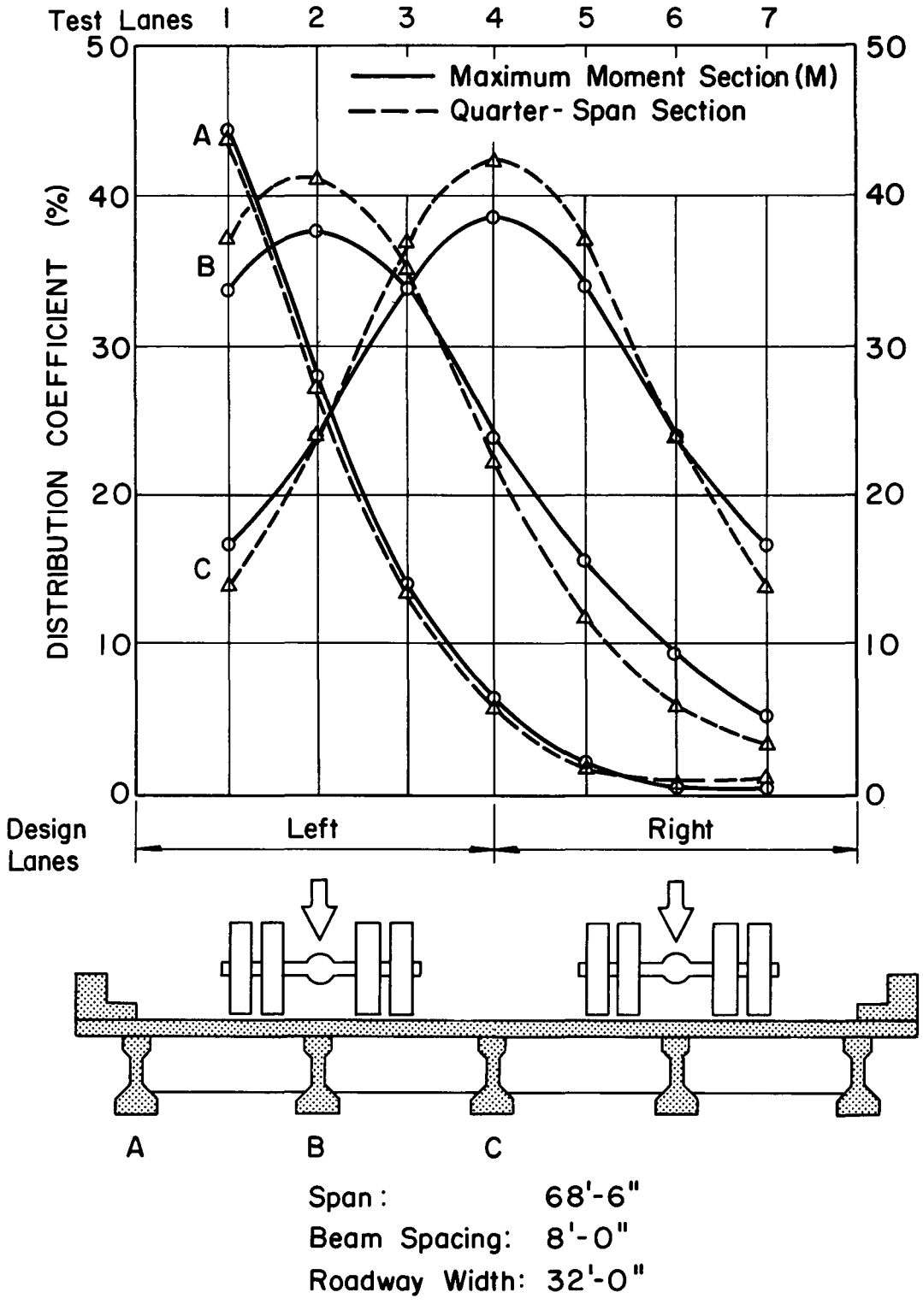

Fig. 17 Influence Lines for Bending Moments in Beams

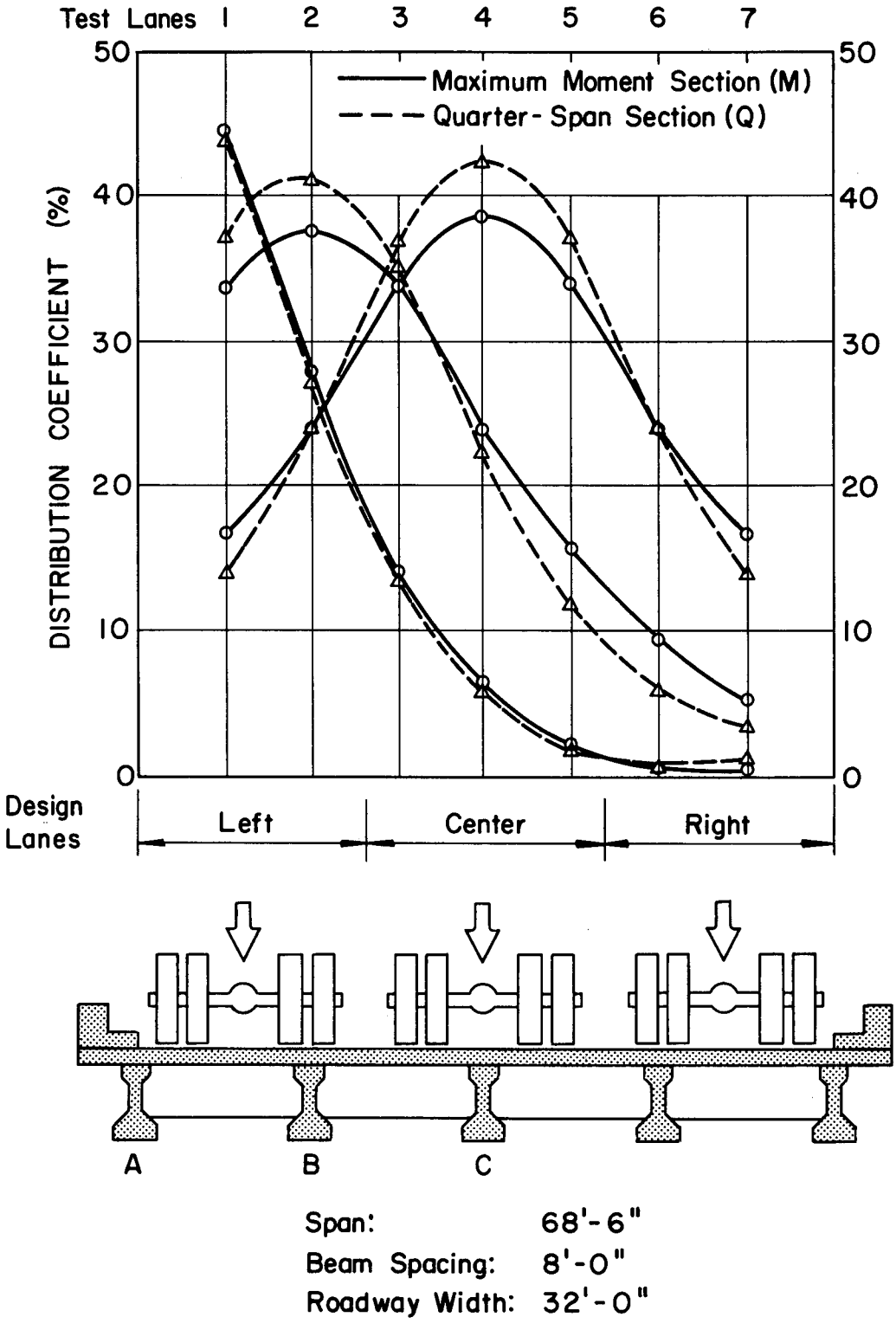

Fig. 18 Influence Lines for Bending Moments in Beams

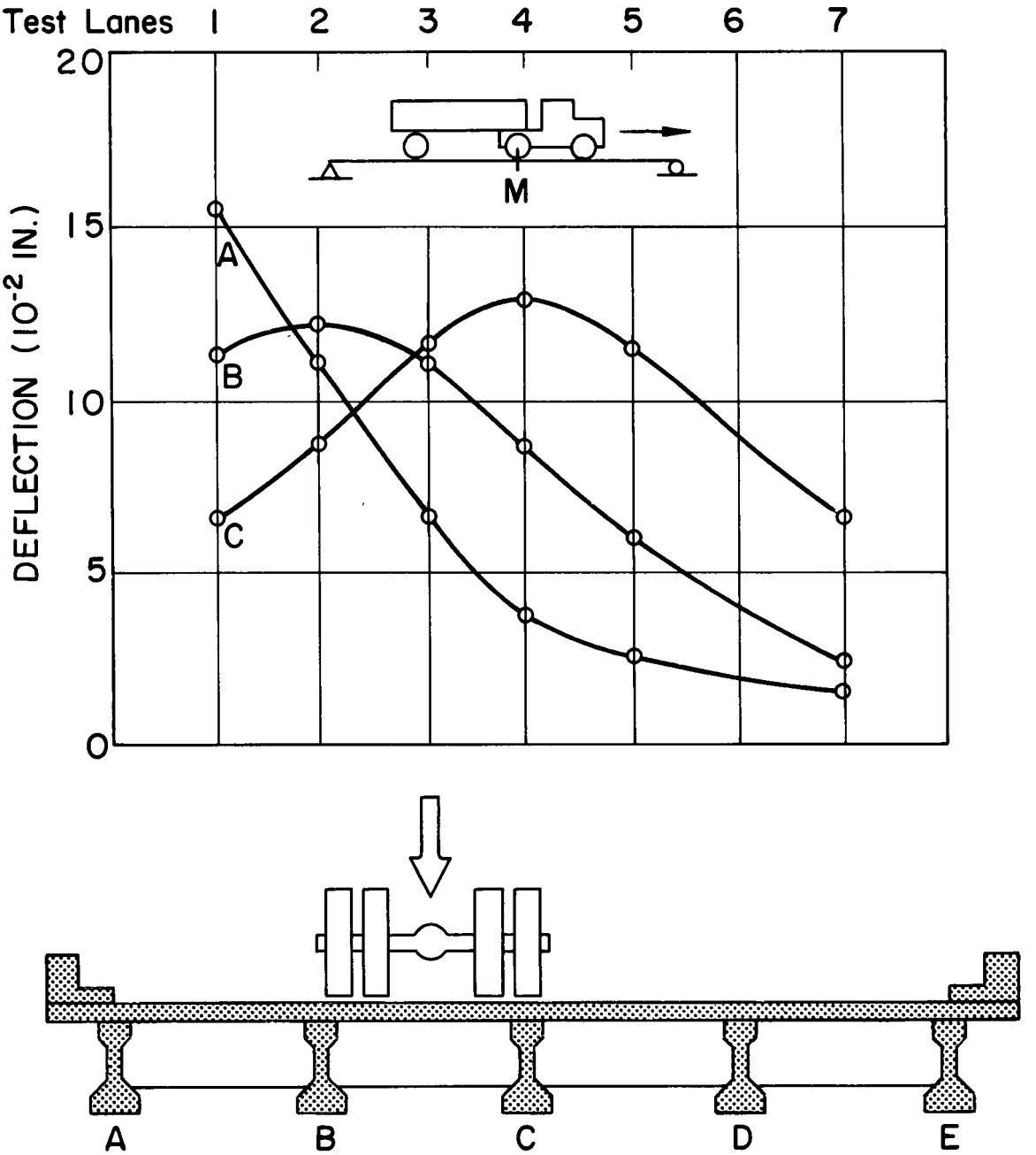

Fig. 19 Influence Lines for Deflection in Beams, Section M

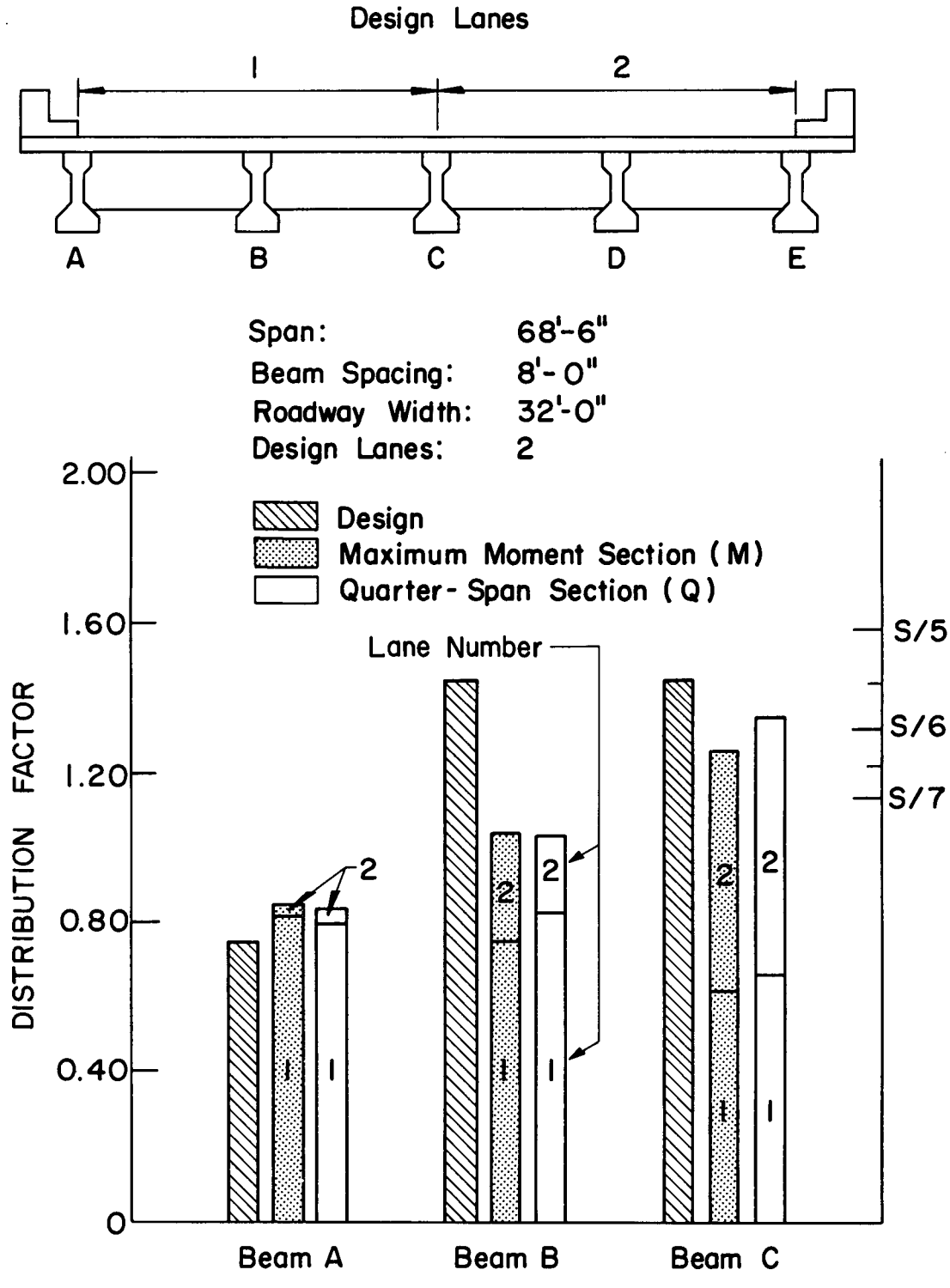

Fig. 20 Experimentally Developed Distribution Factors and Design Values

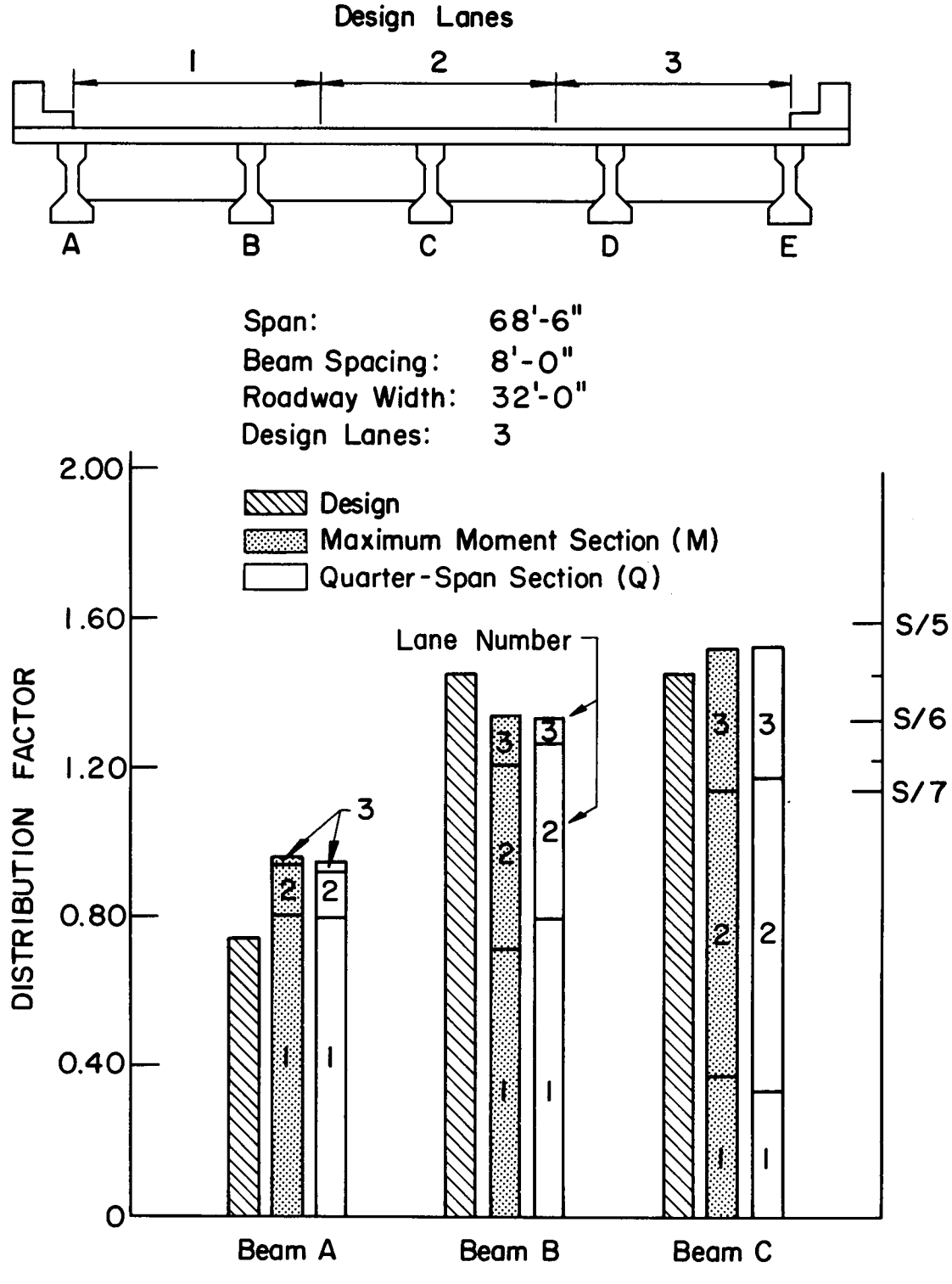

Fig. 21 Experimentally Developed Distribution Factors and Design Values

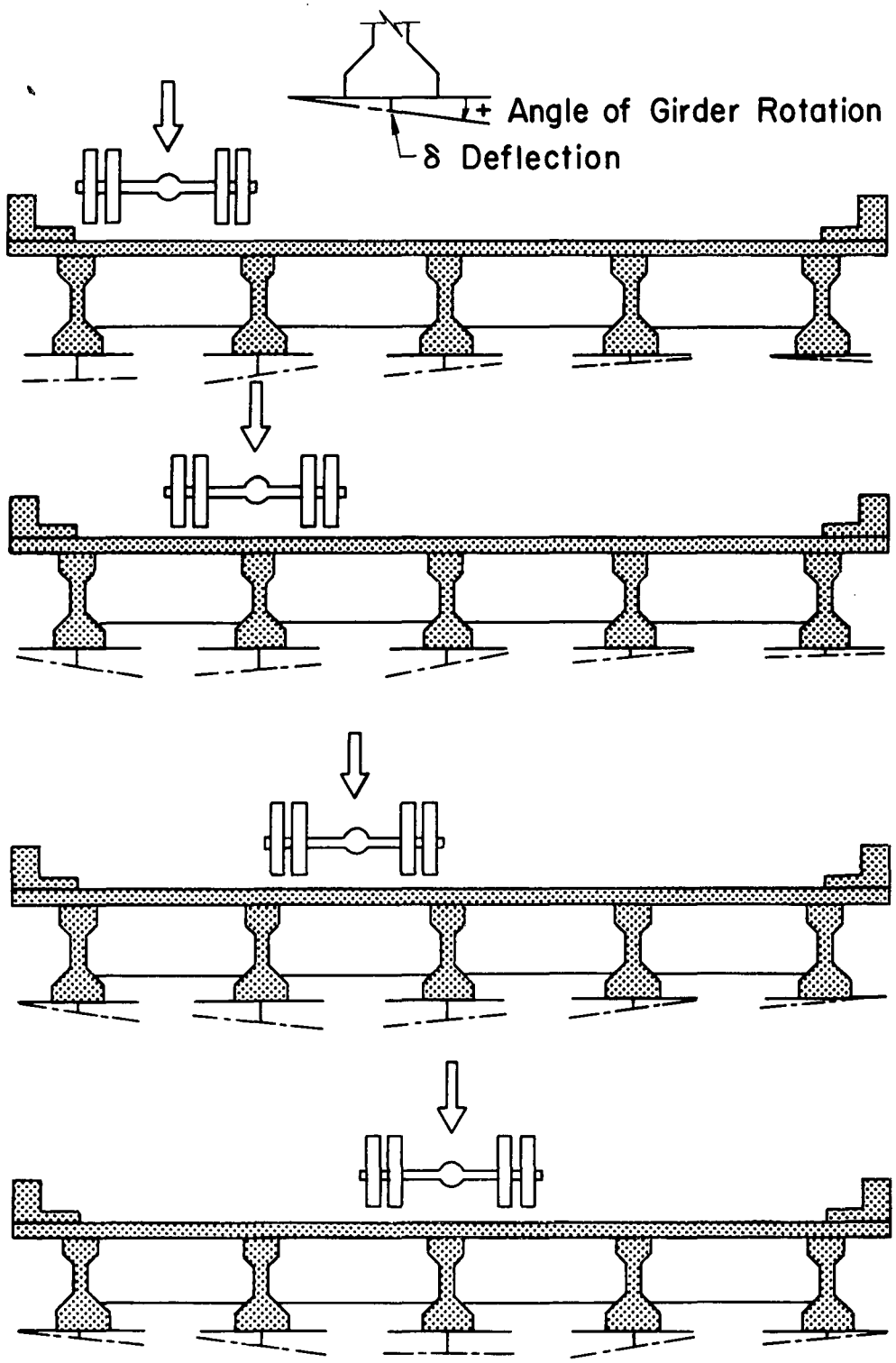

Fig. 22 Typical Examples of Girder Deflections and Rotations for Various Lane Loadings in Crawl Runs

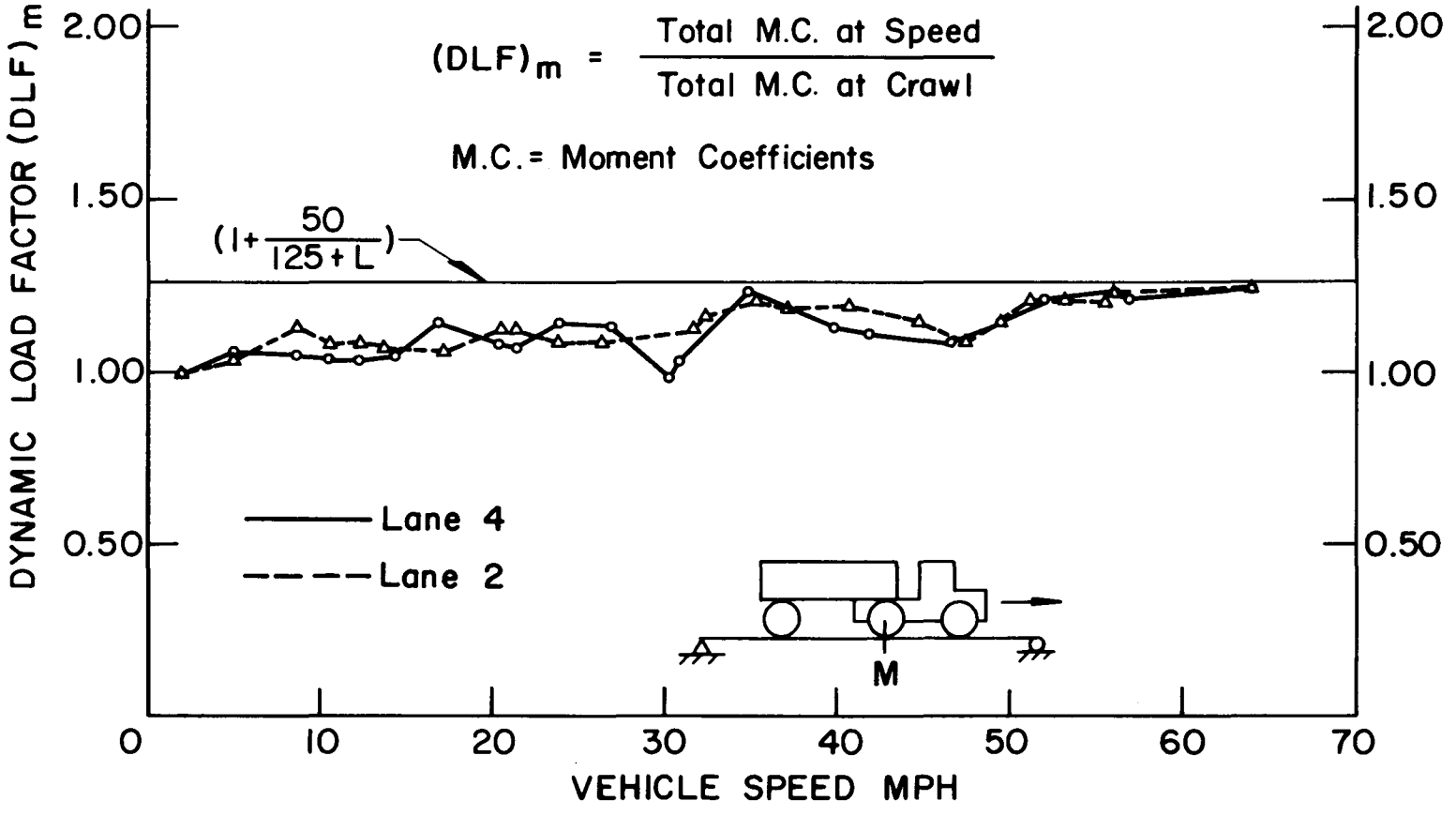

Fig. 23 Dynamic Load Factors Based on Total Bridge Moments at Section M

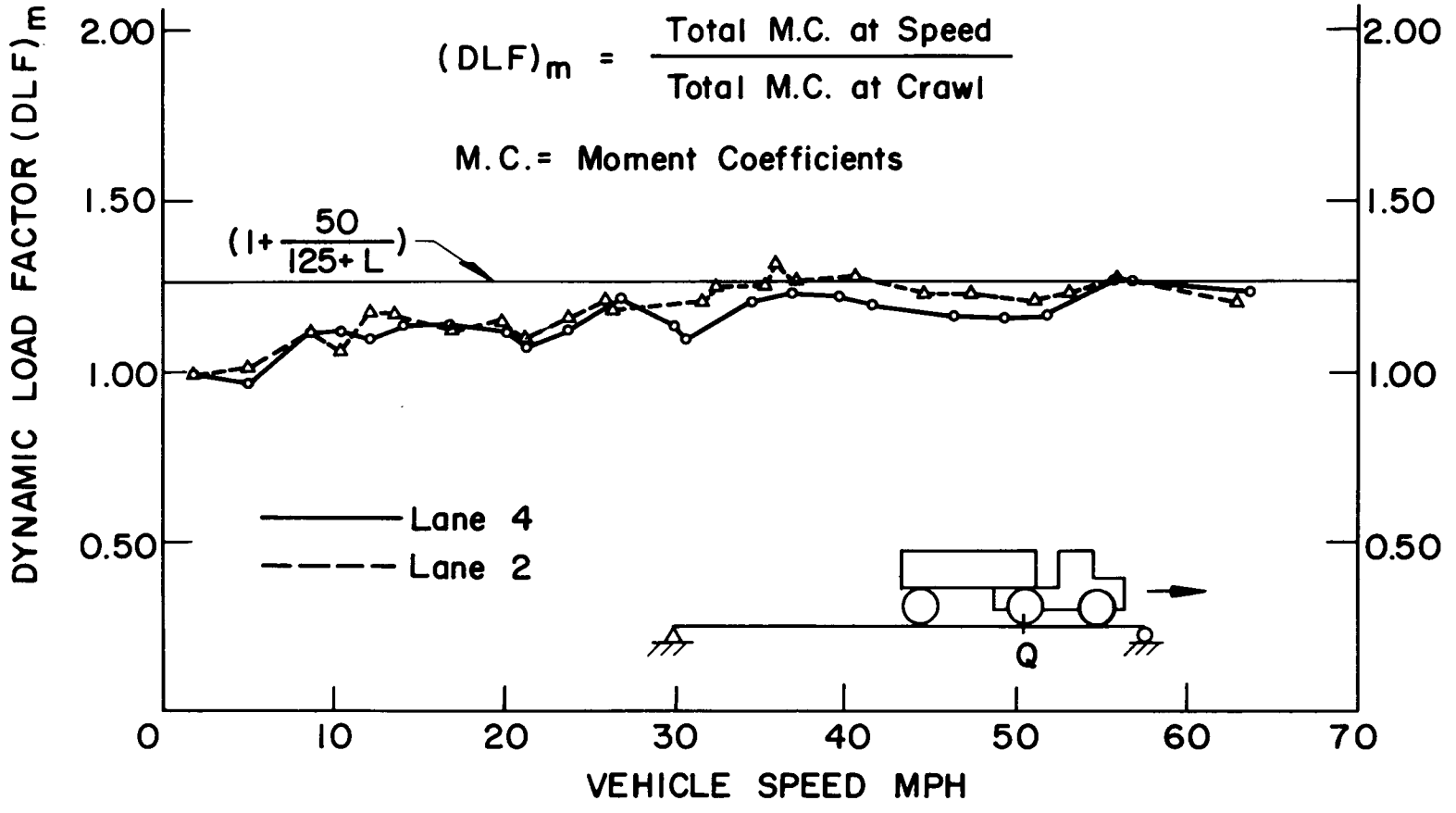

Fig. 24 Dynamic Load Factors Based on Total Bridge Moments at Section Q

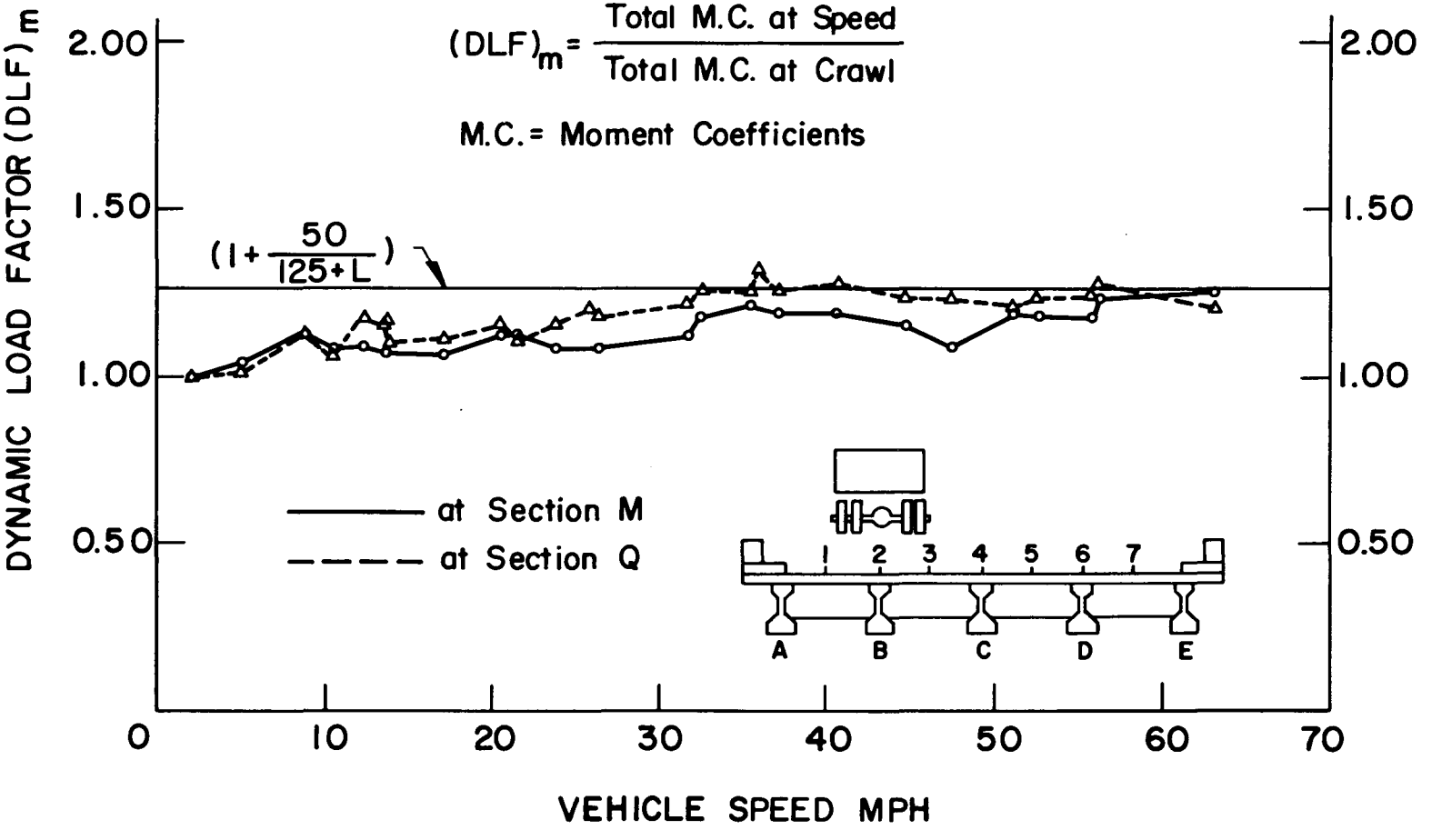

Fig. 25 Dynamic Load Factors Based on Total Bridge Moments, Truck in Lane 2

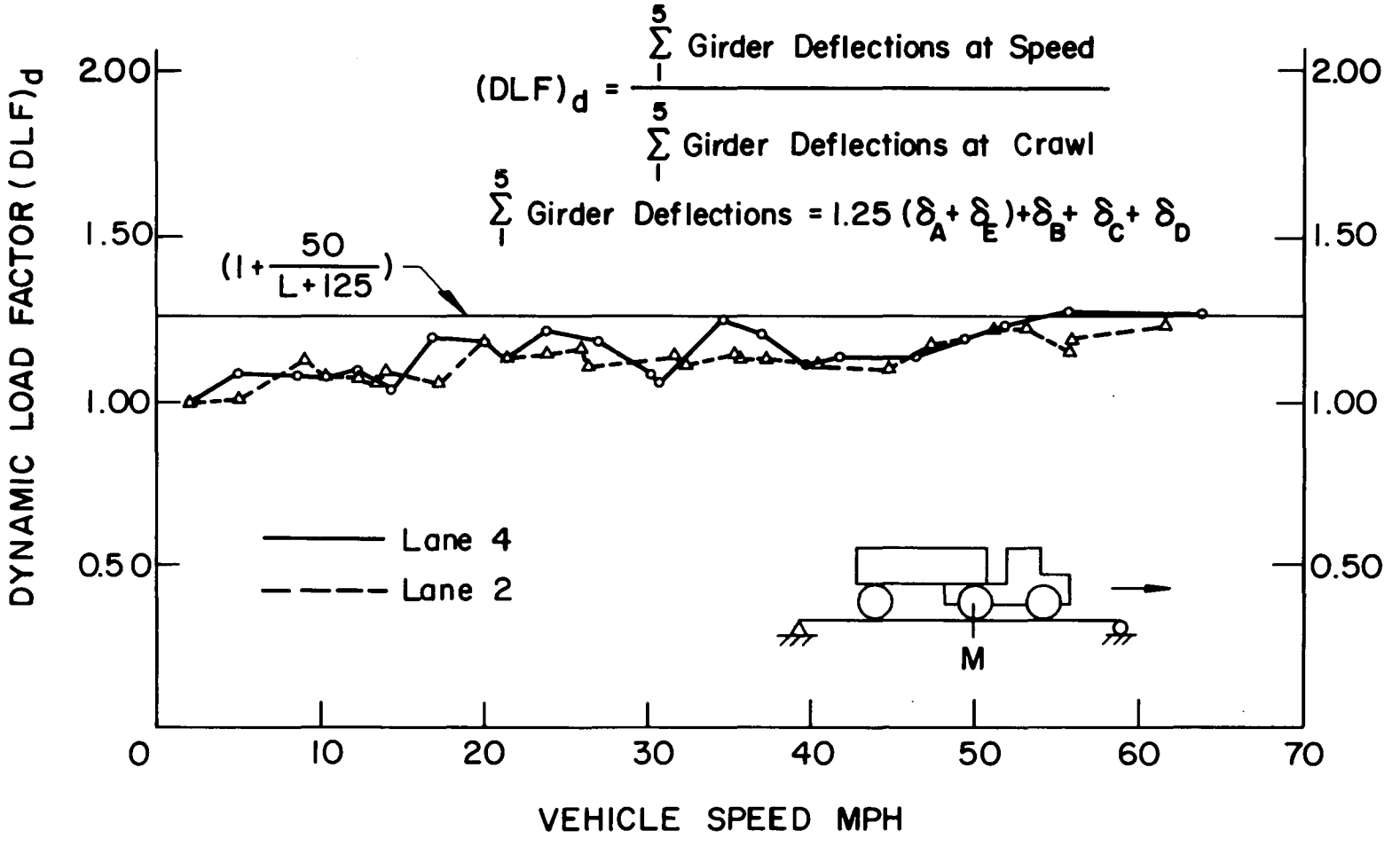

Fig. 26 Dynamic Load Factors Based on Deflections at Section M - Total Bridge Behavior

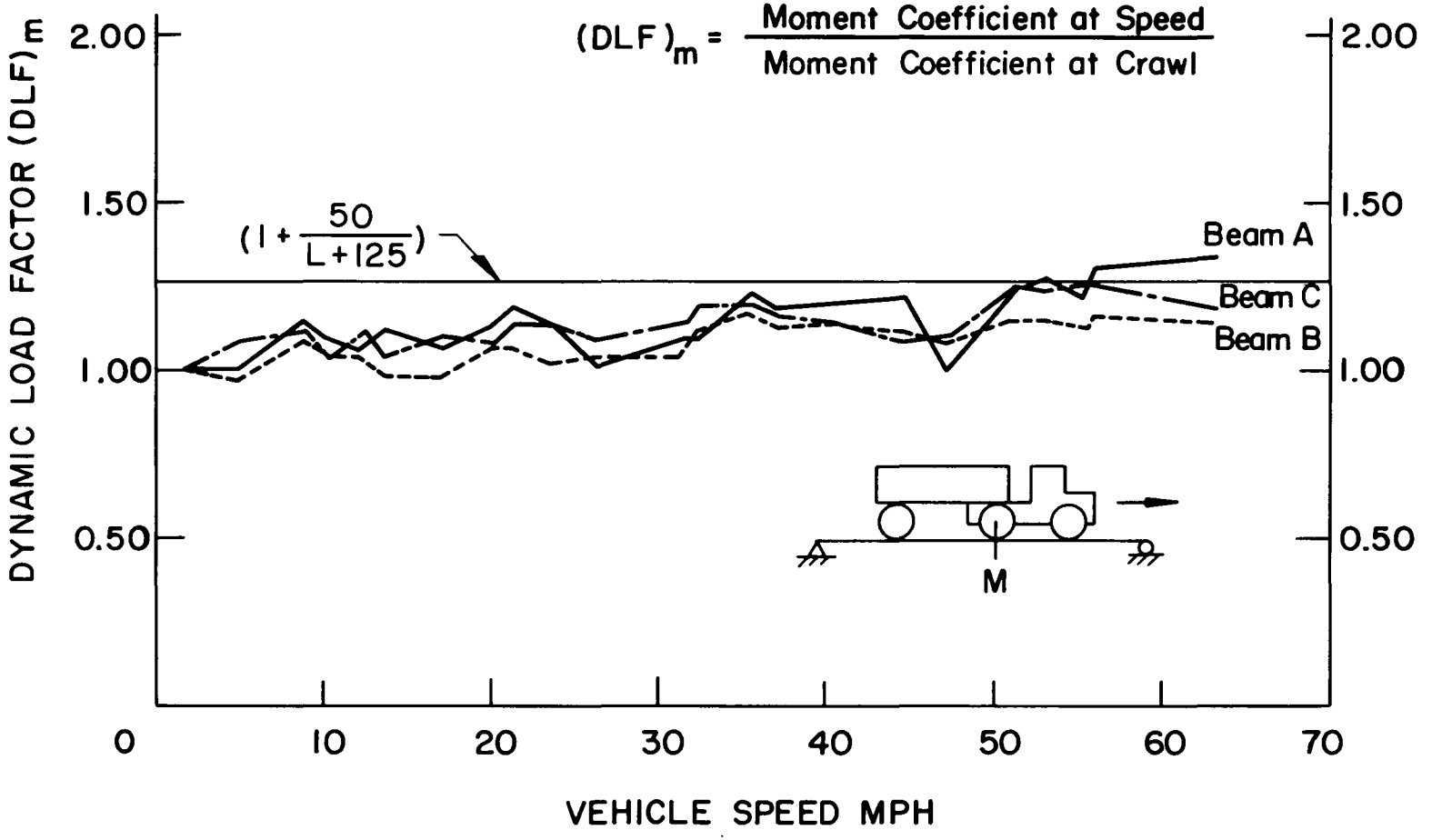

Fig. 27 Amplification of Moment Coefficient for Beams - Truck in Lane 2, Section M

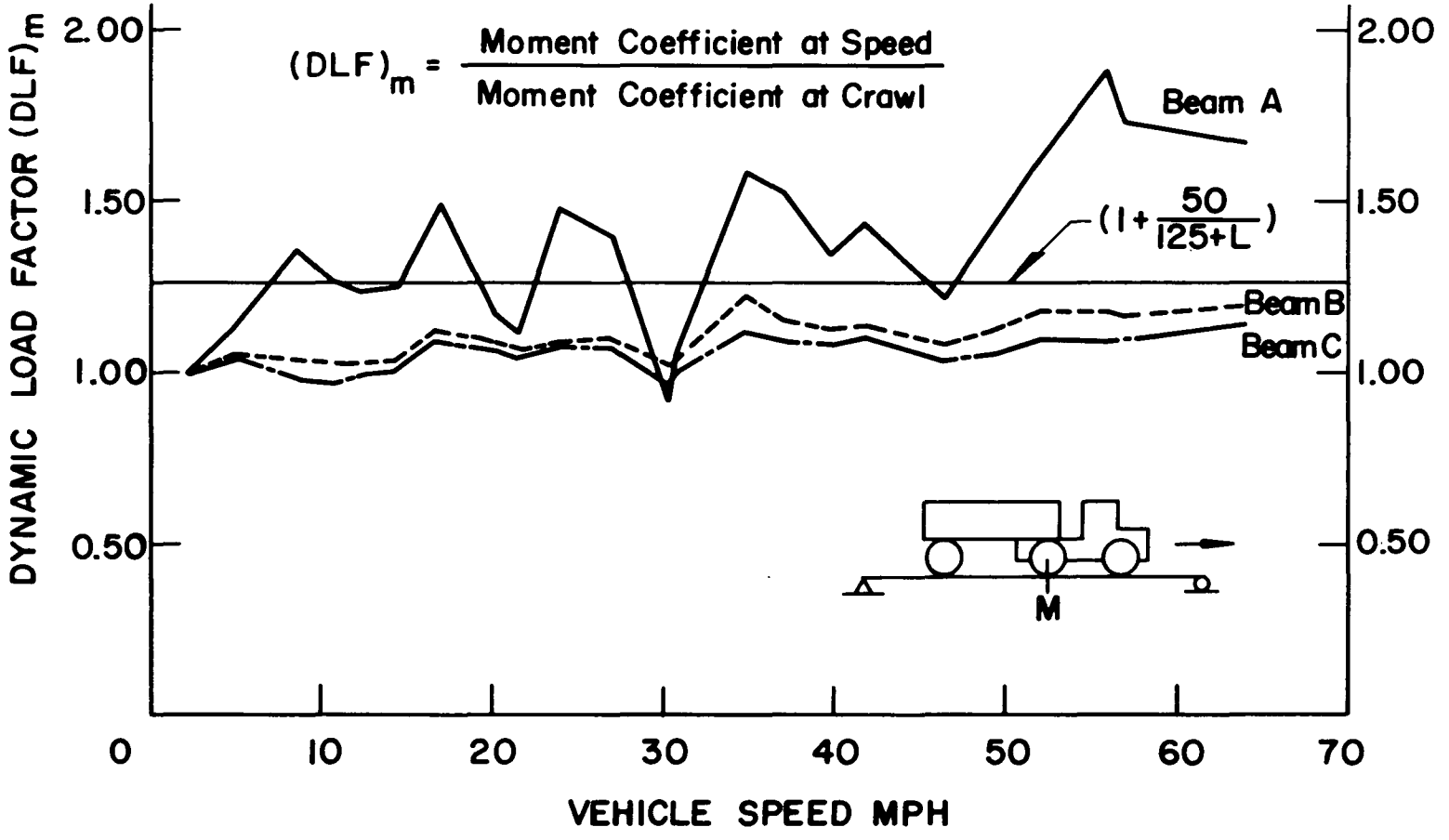

Fig. 28 Amplification of Moment Coefficient for Beams - Truck in Lane 4, Section M

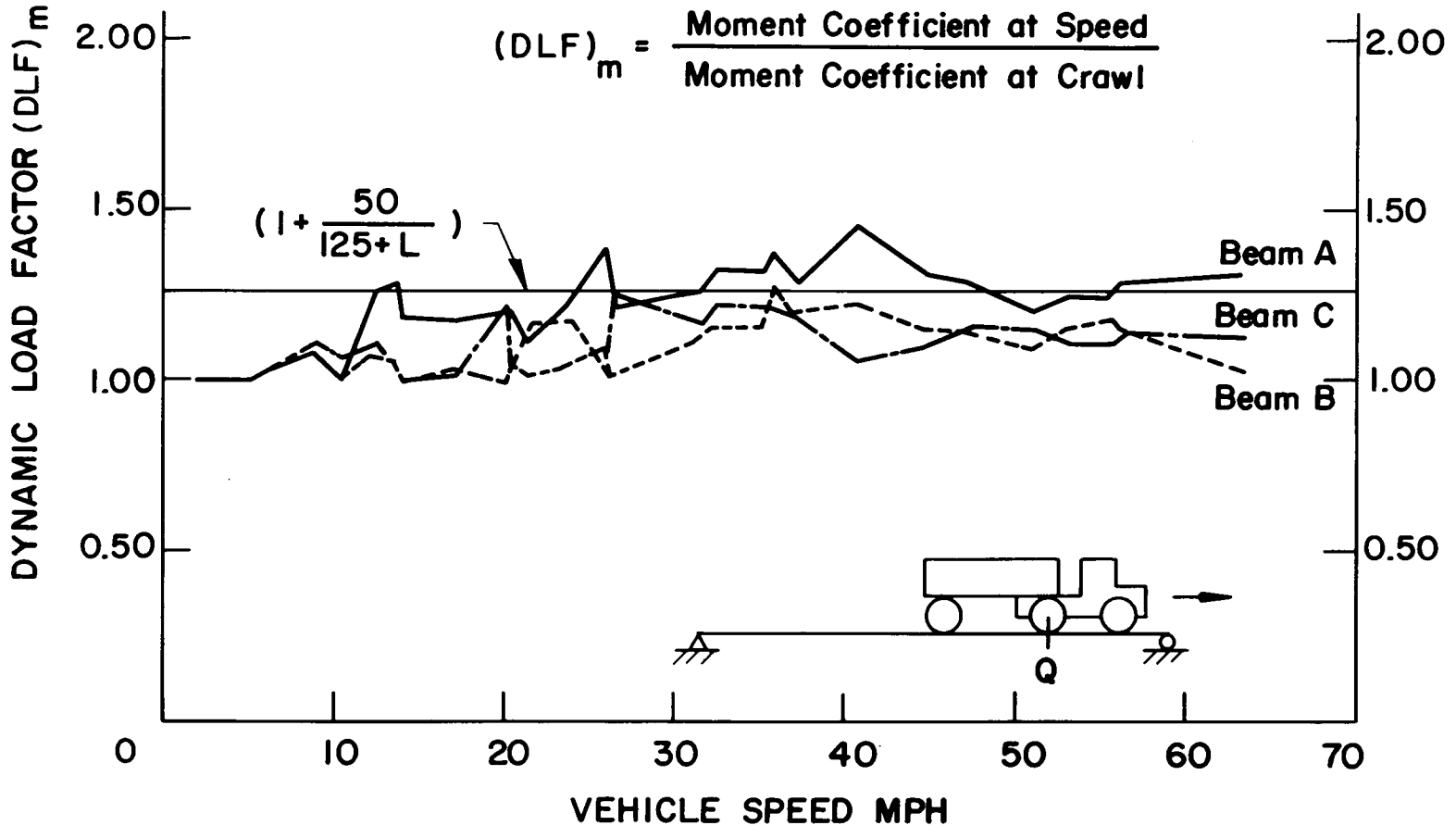

Fig. 29 Amplification of Moment Coefficient for Beams - Truck in Lane 2, Section Q

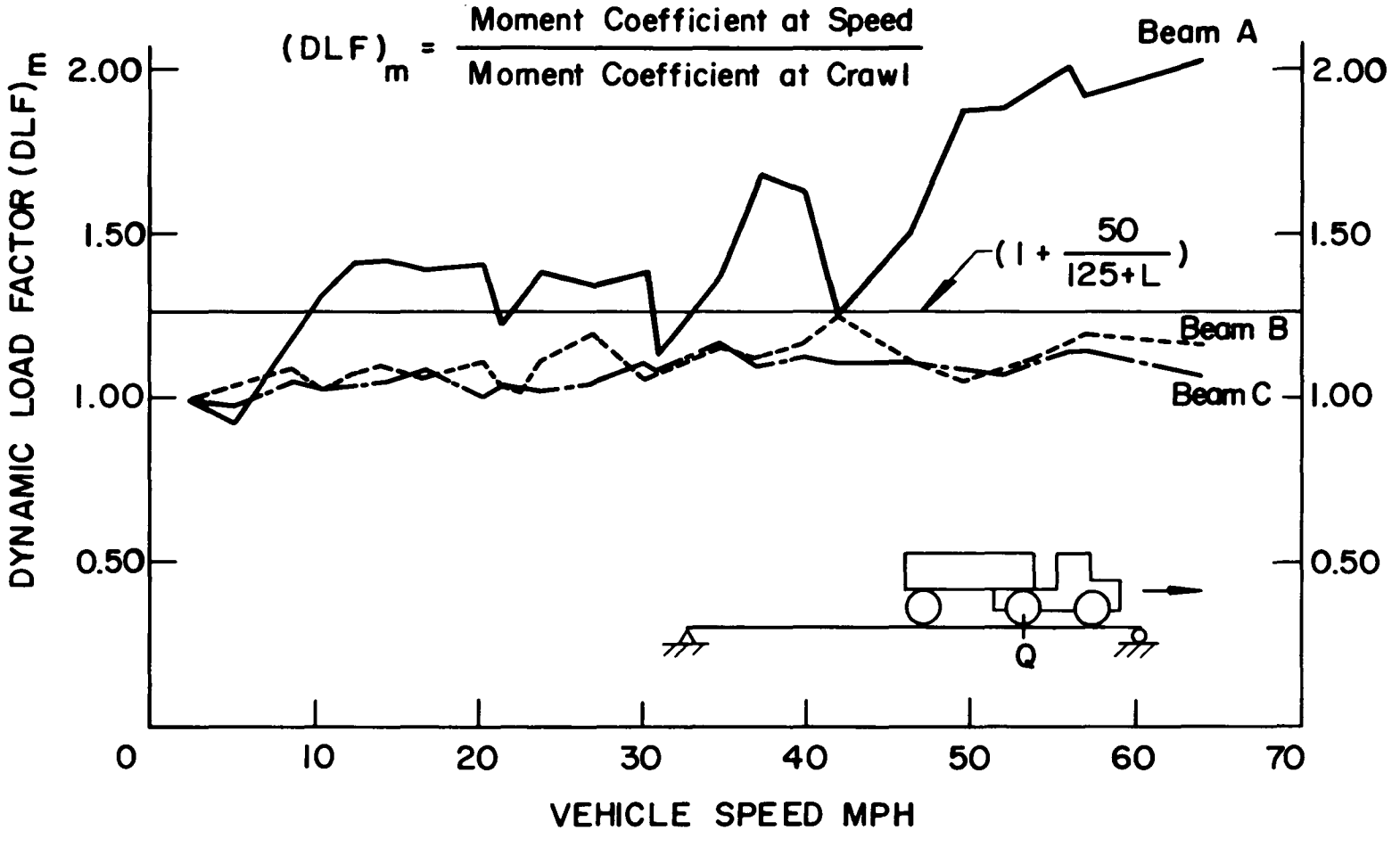

Fig. 30 Amplification of Moment Coefficient for Beams - Truck in Lane 4, Section Q

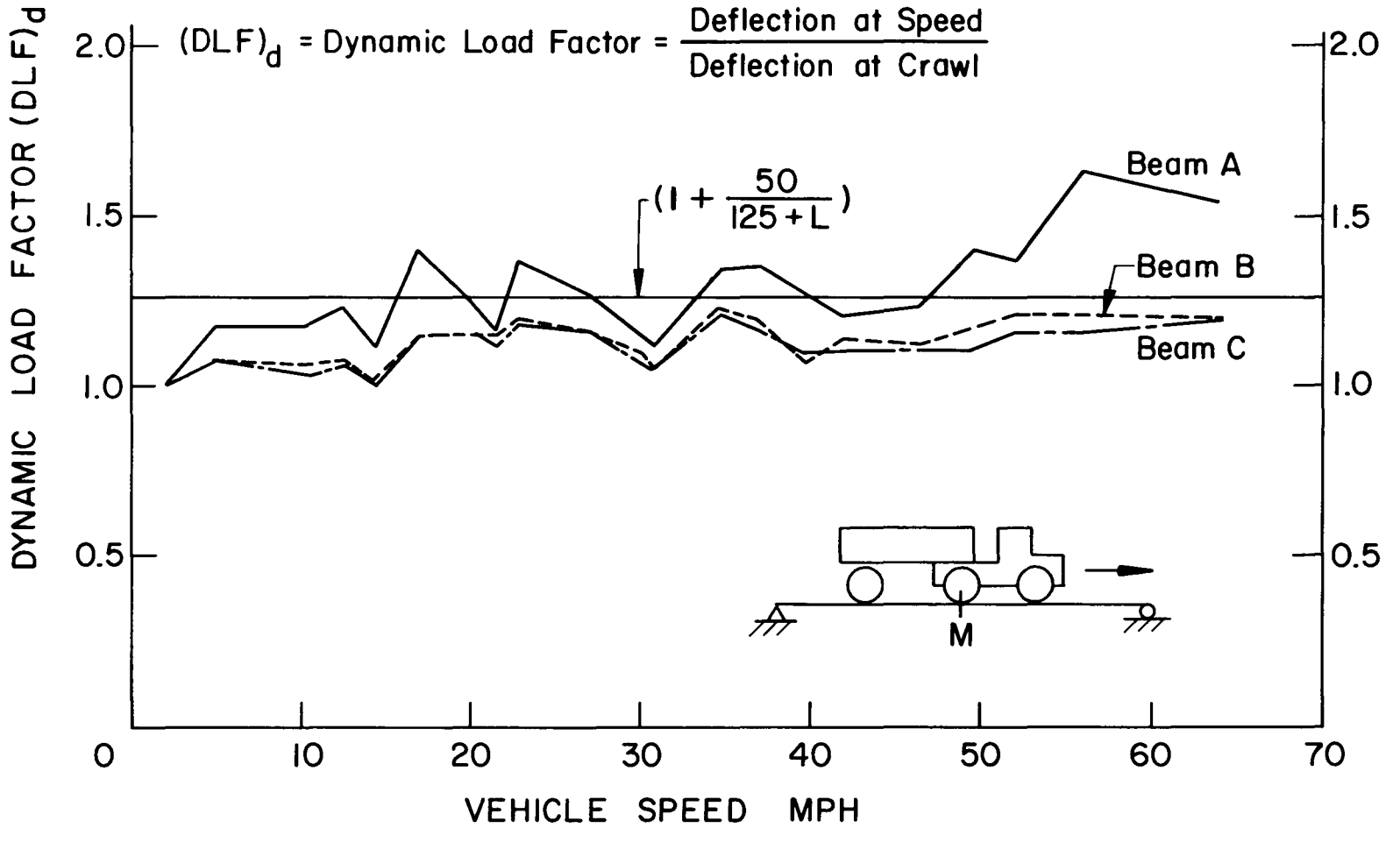

Fig. 31 Dynamic Load Factors Based on Deflections - Single Beam Effect
Truck in Lane 4, Section M

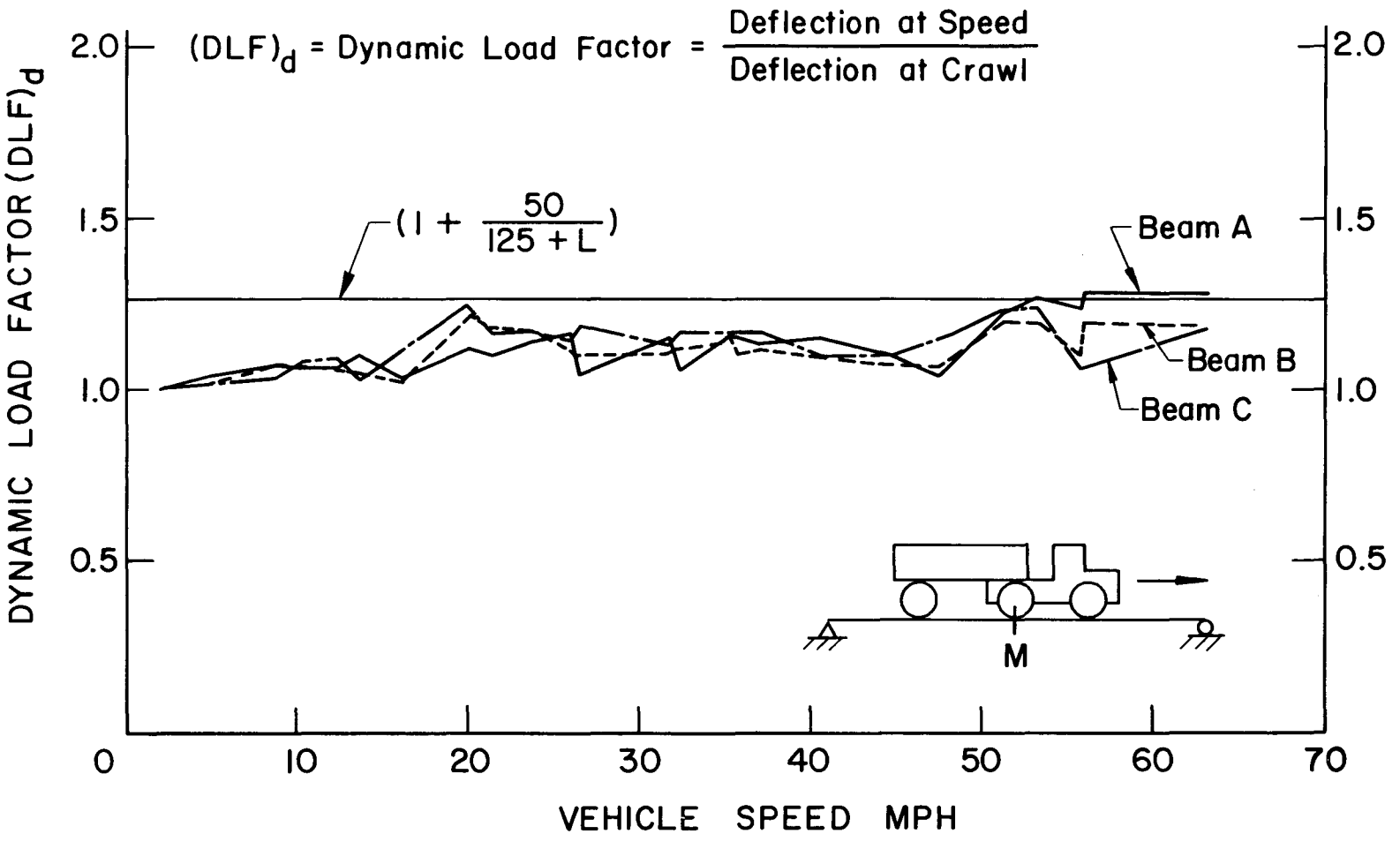

Fig. 32 Dynamic Load Factors Based on Deflections - Single Beam Effect
Truck in Lane 2, Section M

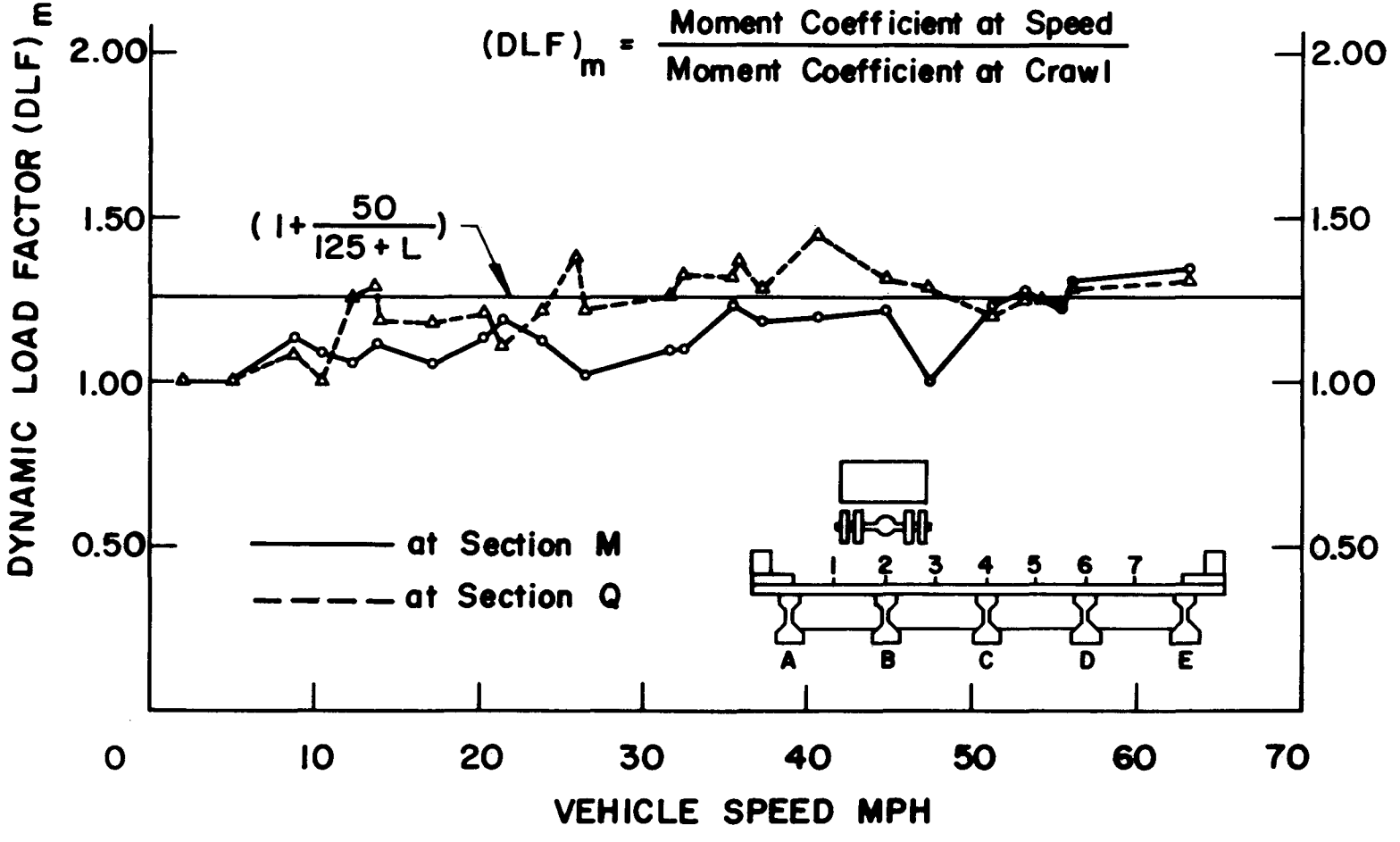

Fig. 33 Amplification of Moment Coefficient for Beam A
Truck in Lane 2

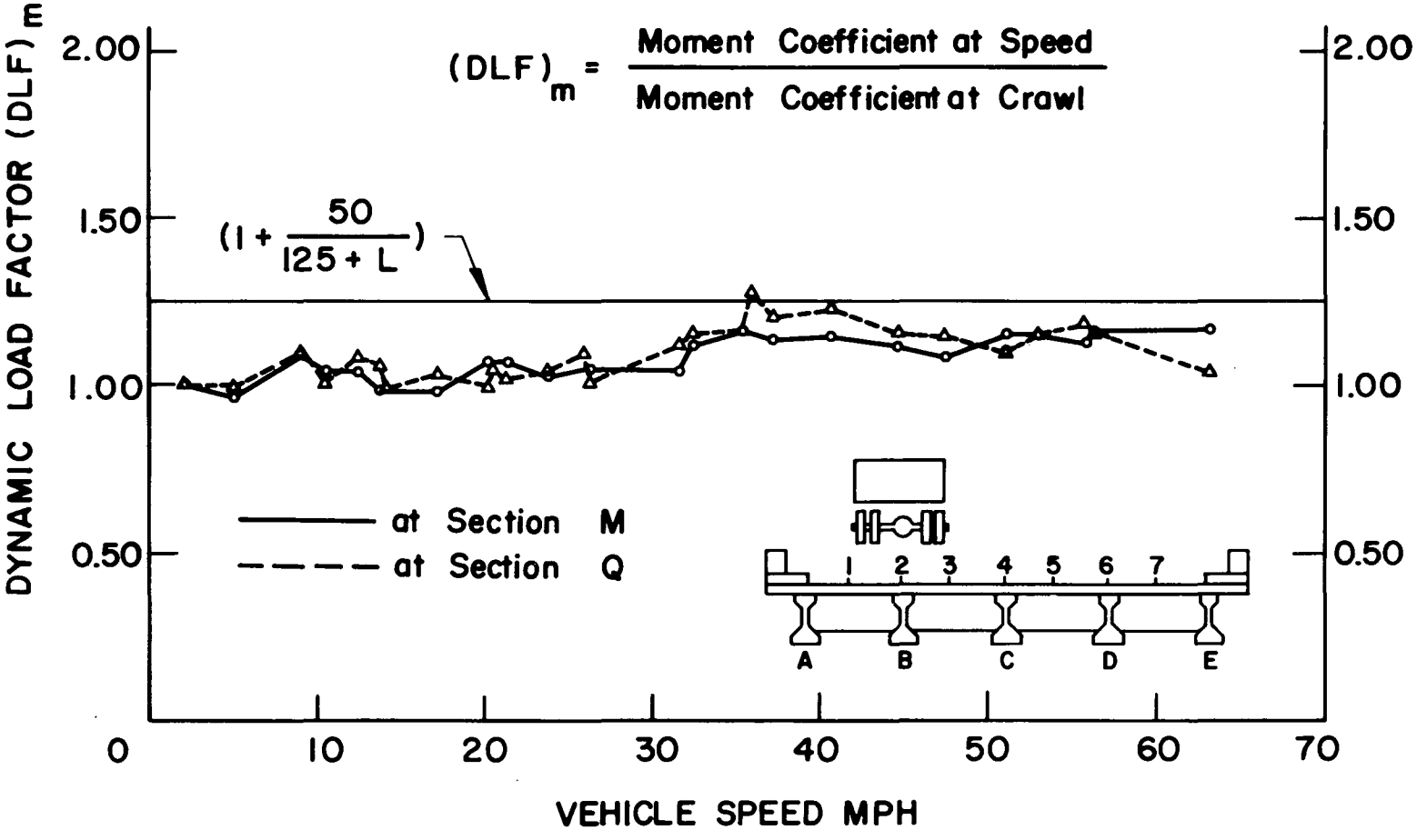

Fig. 34 Amplification of Moment Coefficient for Beam B
Truck in Lane 2

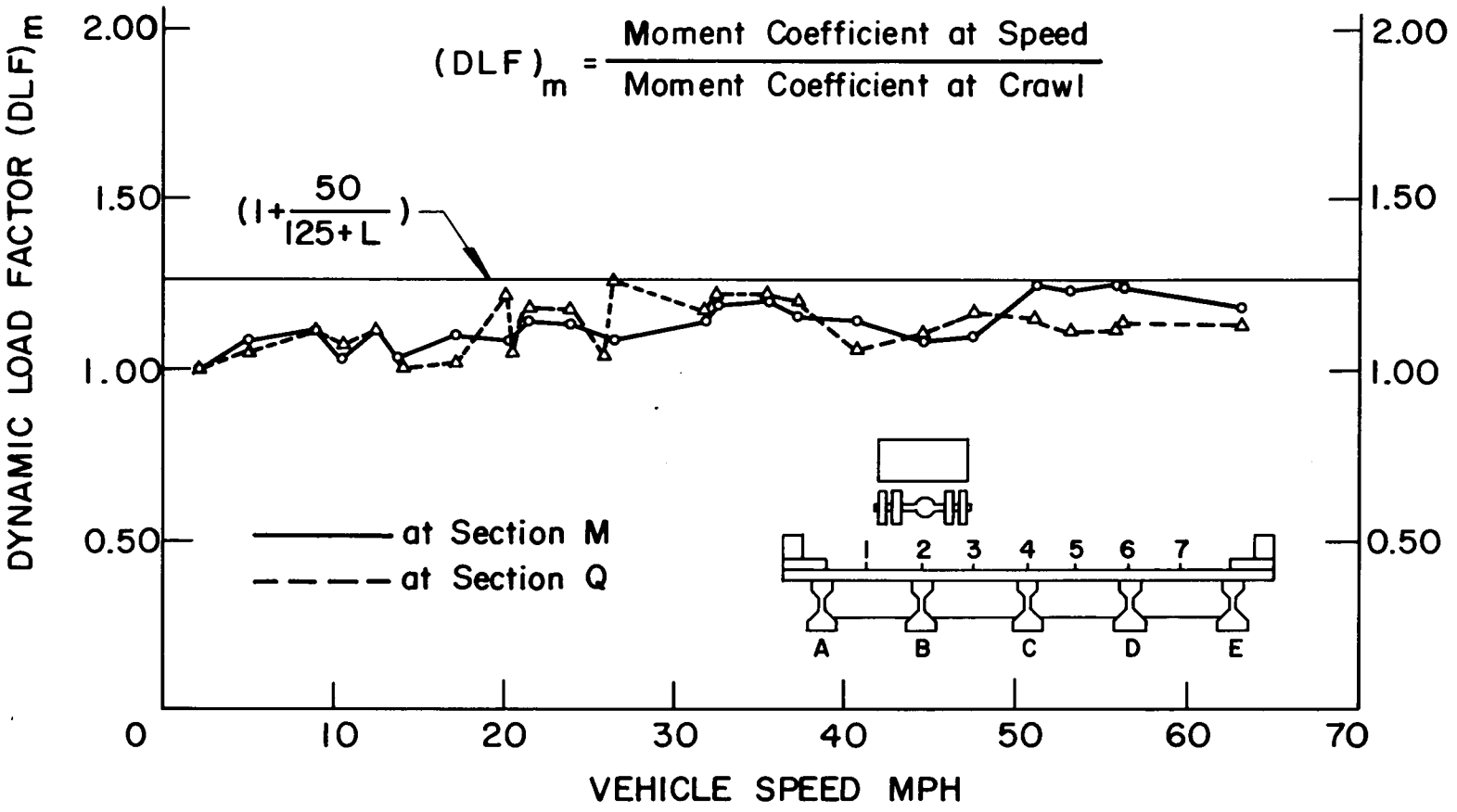

Fig. 35 Amplification of Moment Coefficient for Beam C
Truck in Lane 2

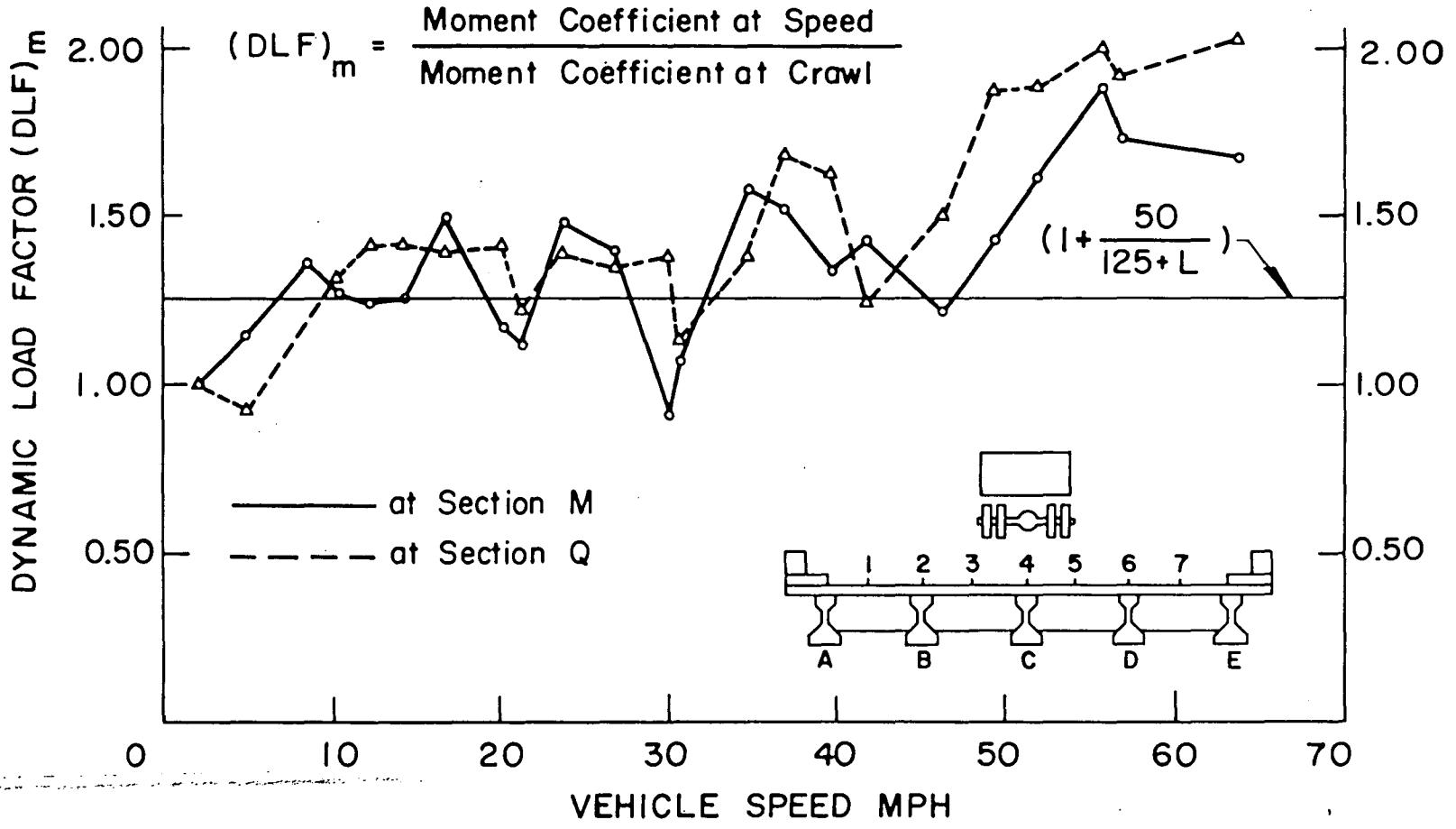

Fig. 36 Amplification of Moment Coefficient for Beam A
Truck in Lane 4

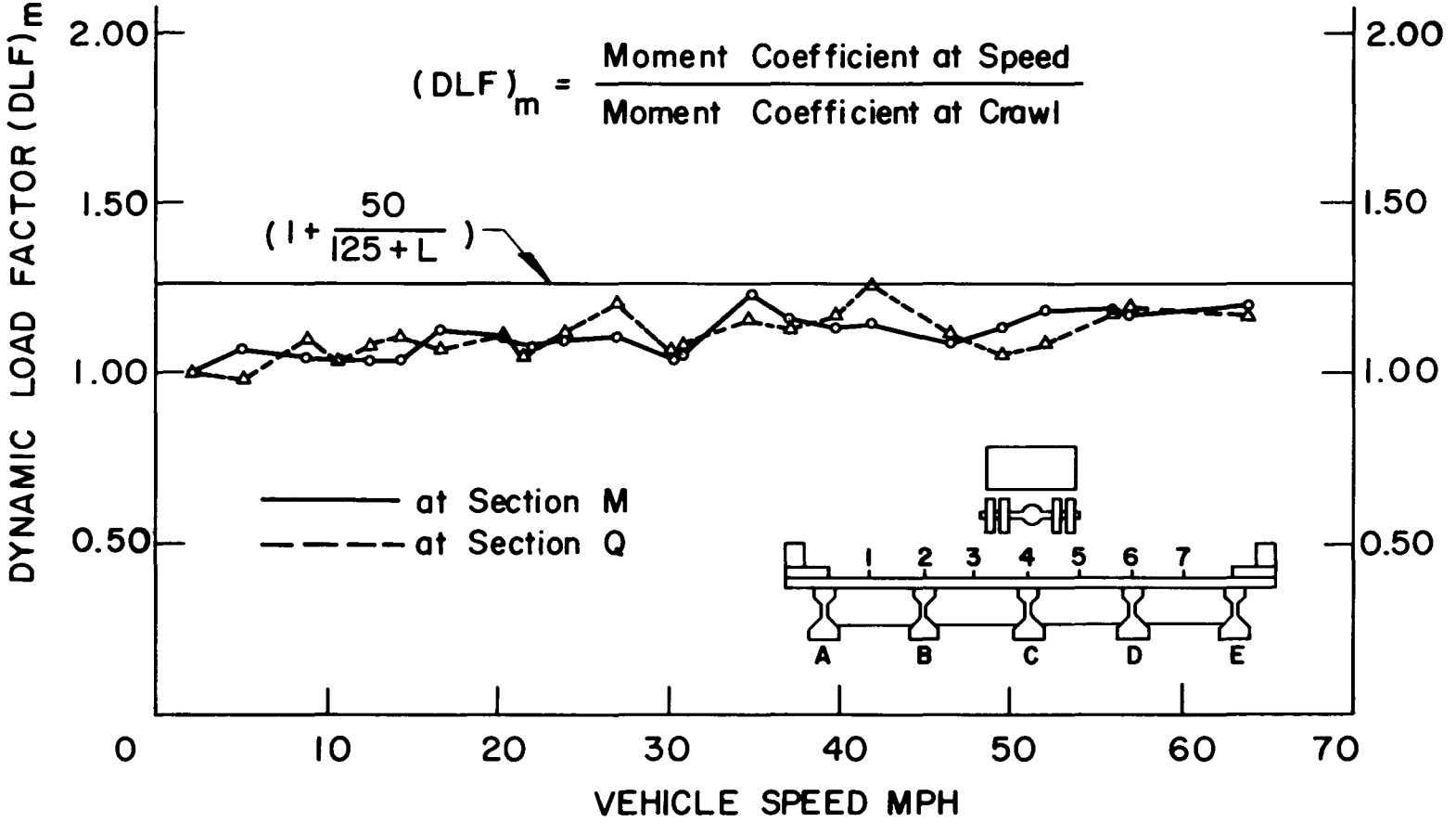

Fig. 37 Amplification of Moment Coefficient for Beam B
Truck in Lane 4

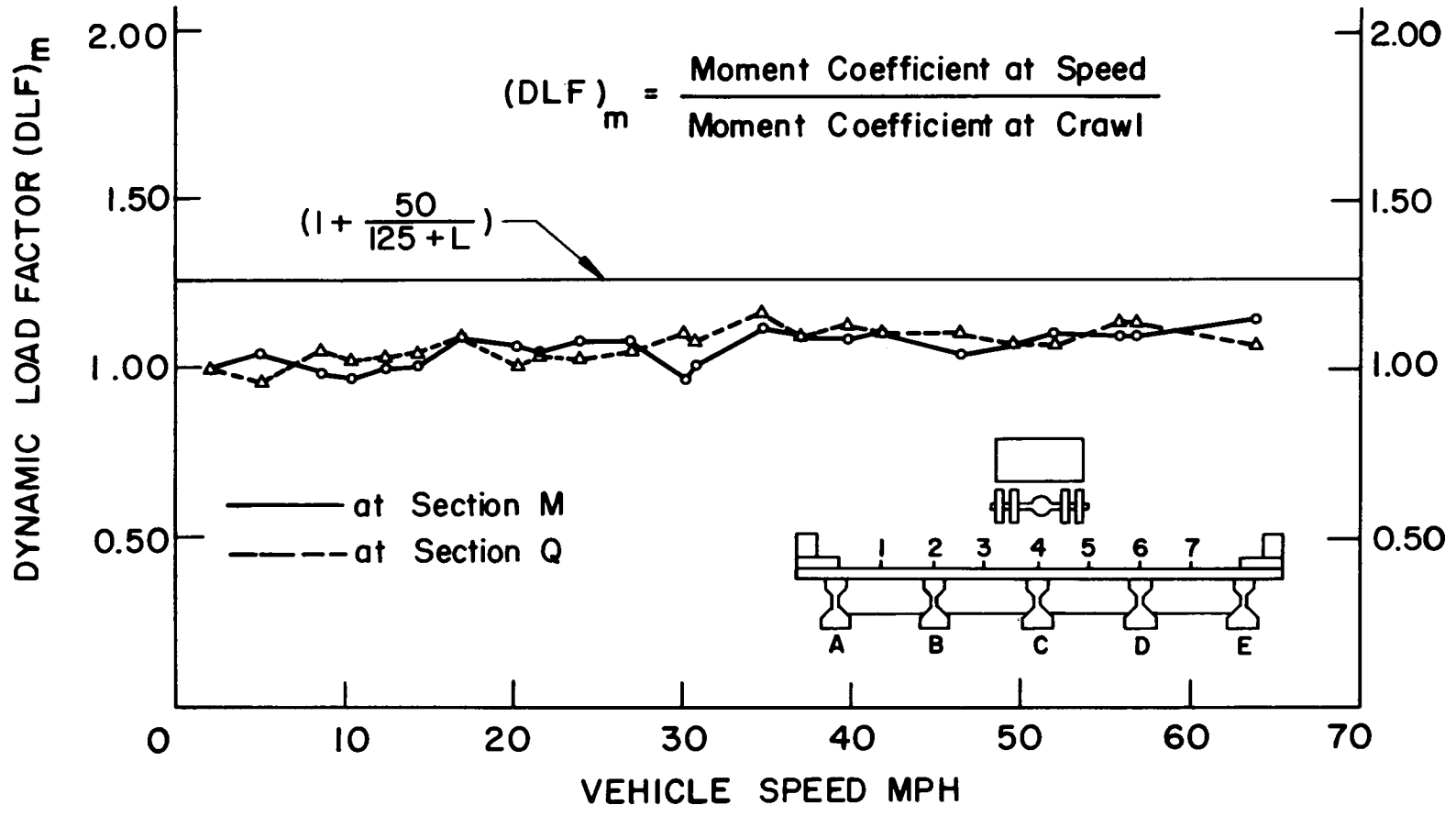

Fig. 38 Amplification of Moment Coefficient for Beam C
Truck in Lane 4

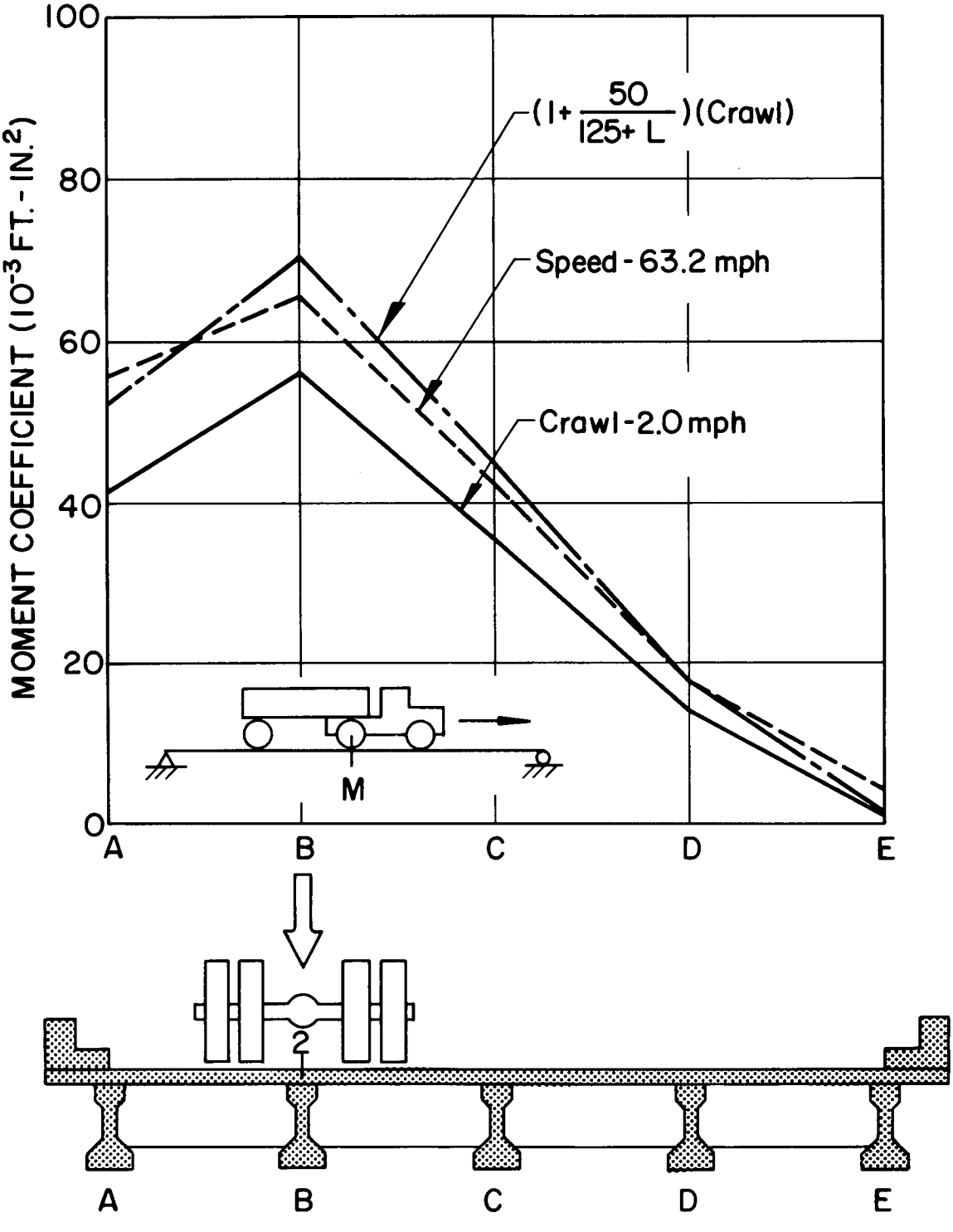

Fig. 39 Amplification of Girder Moment Coefficients at Section M, Truck in Lane 2

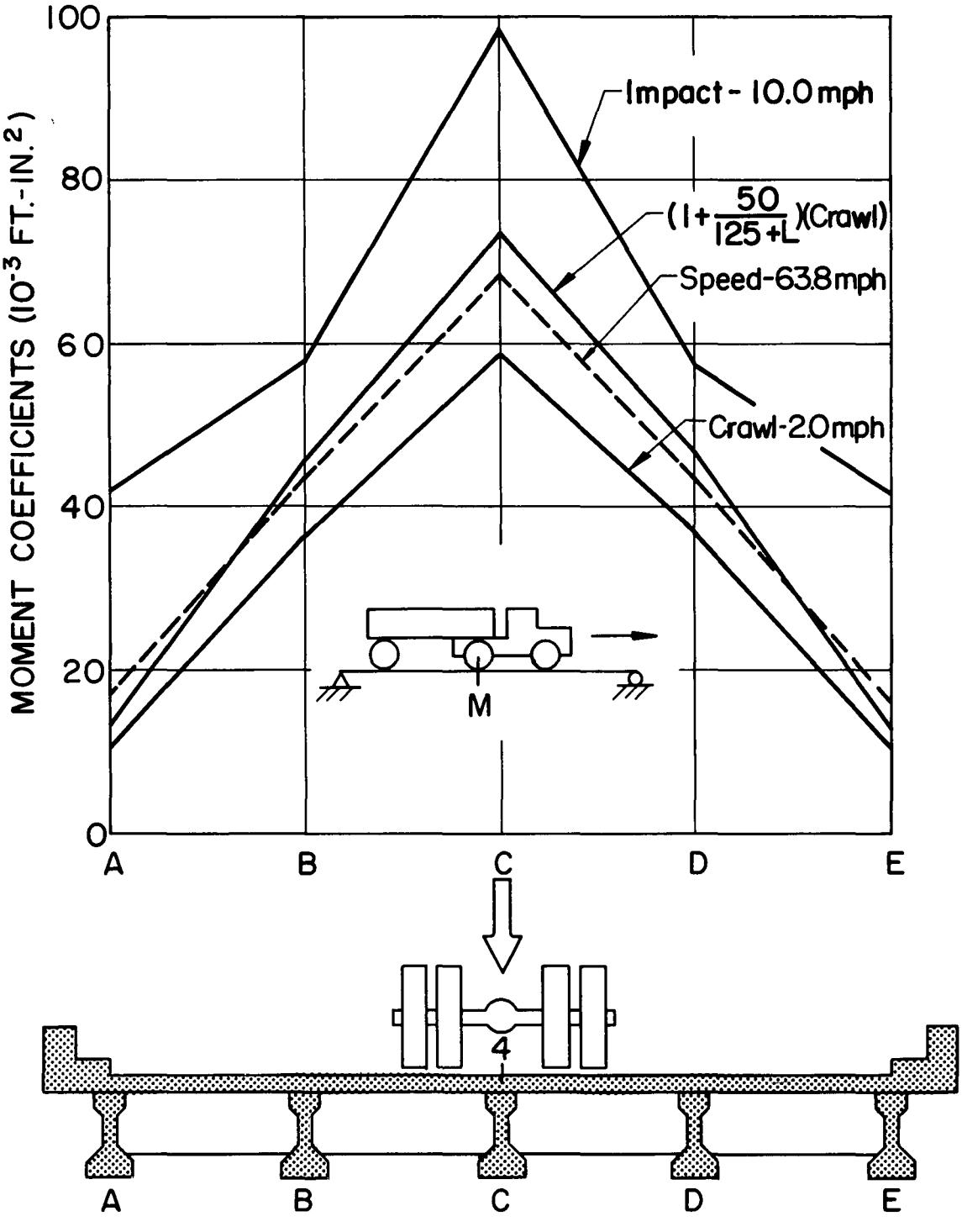

Fig. 40 Amplification of Girder Moment Coefficients at Section M, Truck in Lane 4

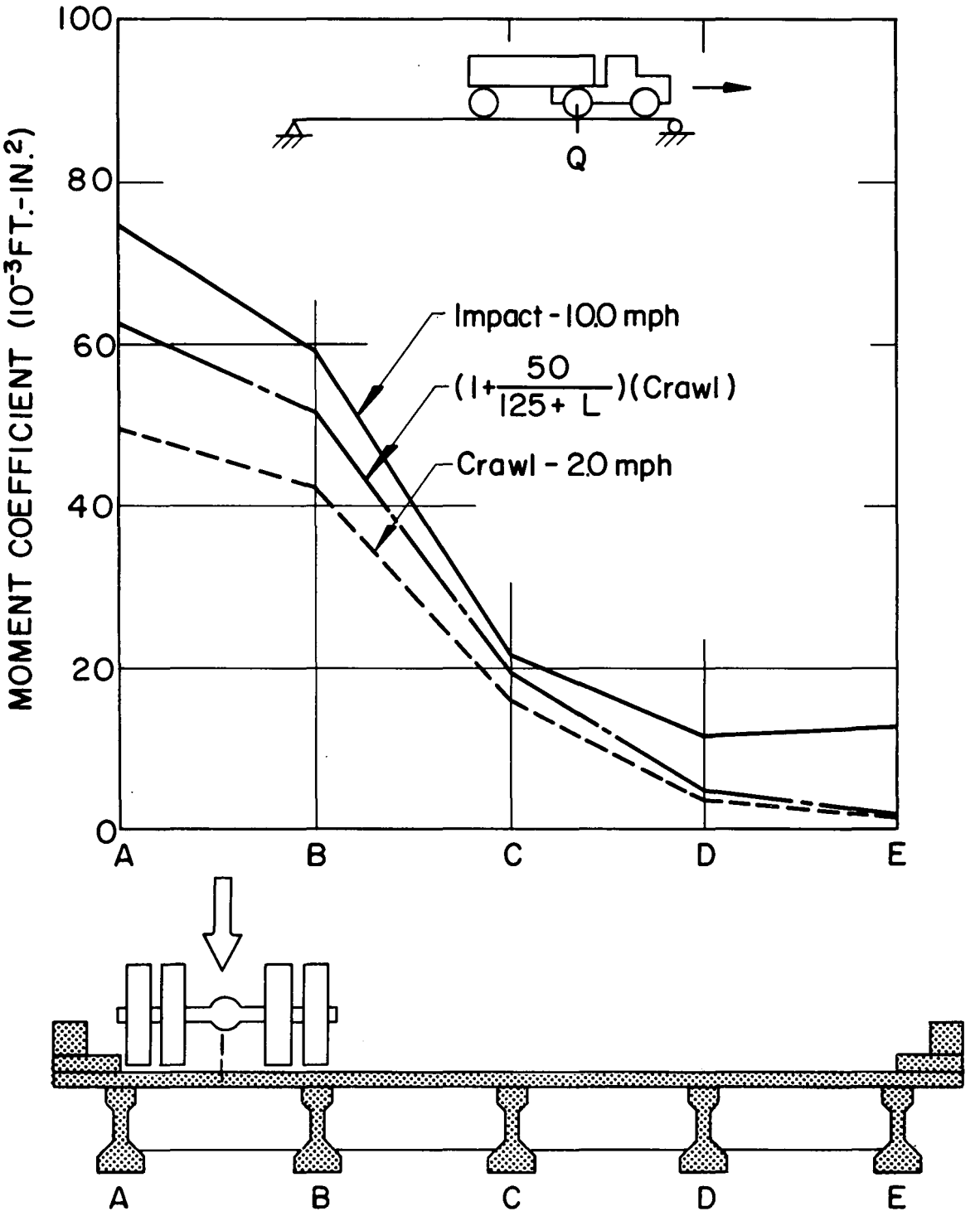

Fig. 41 Amplification of Girder Moment Coefficients at Section Q, Truck in Lane 1

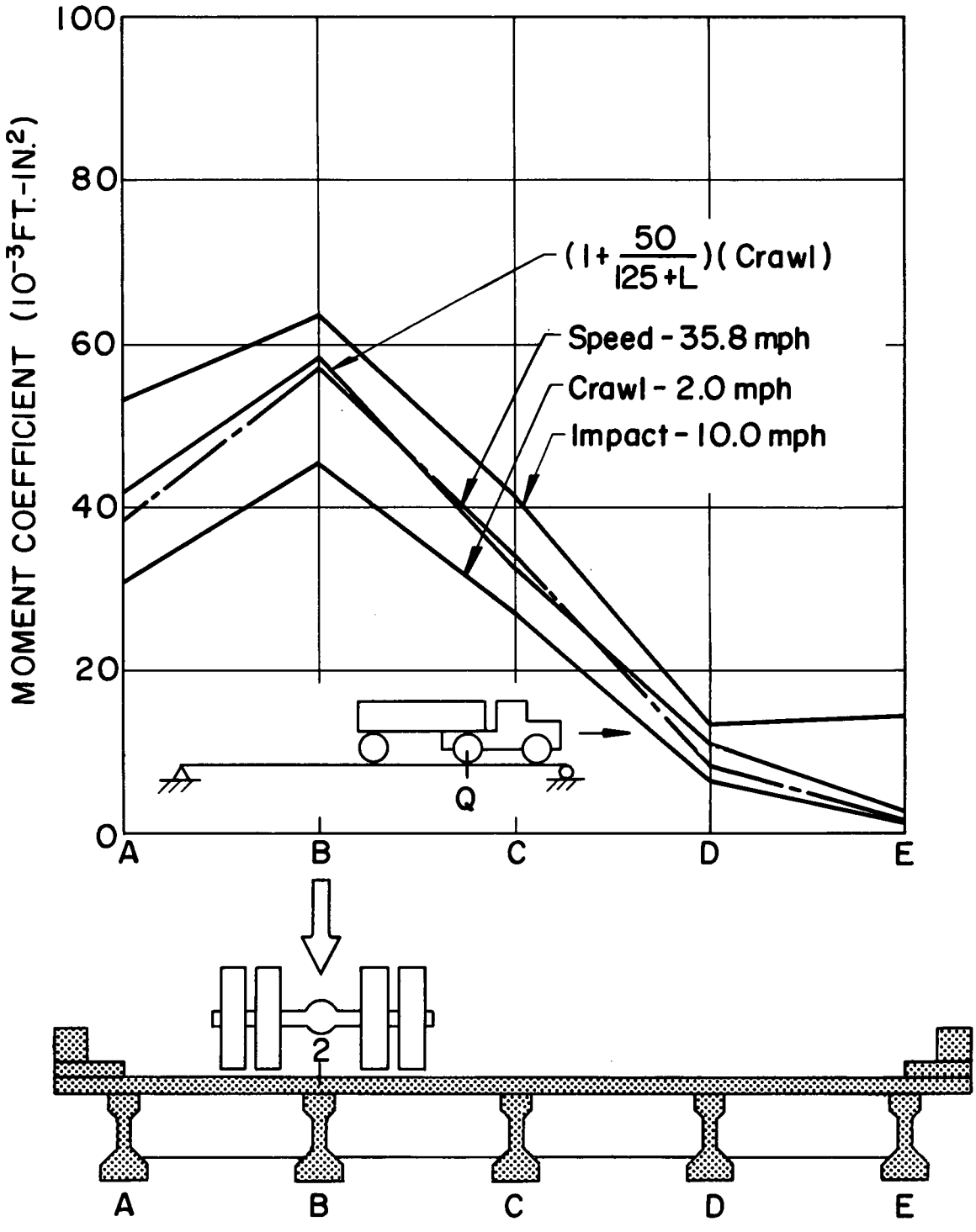

Fig. 42 Amplification of Girder Moment Coefficients at Section Q, Truck in Lane 2

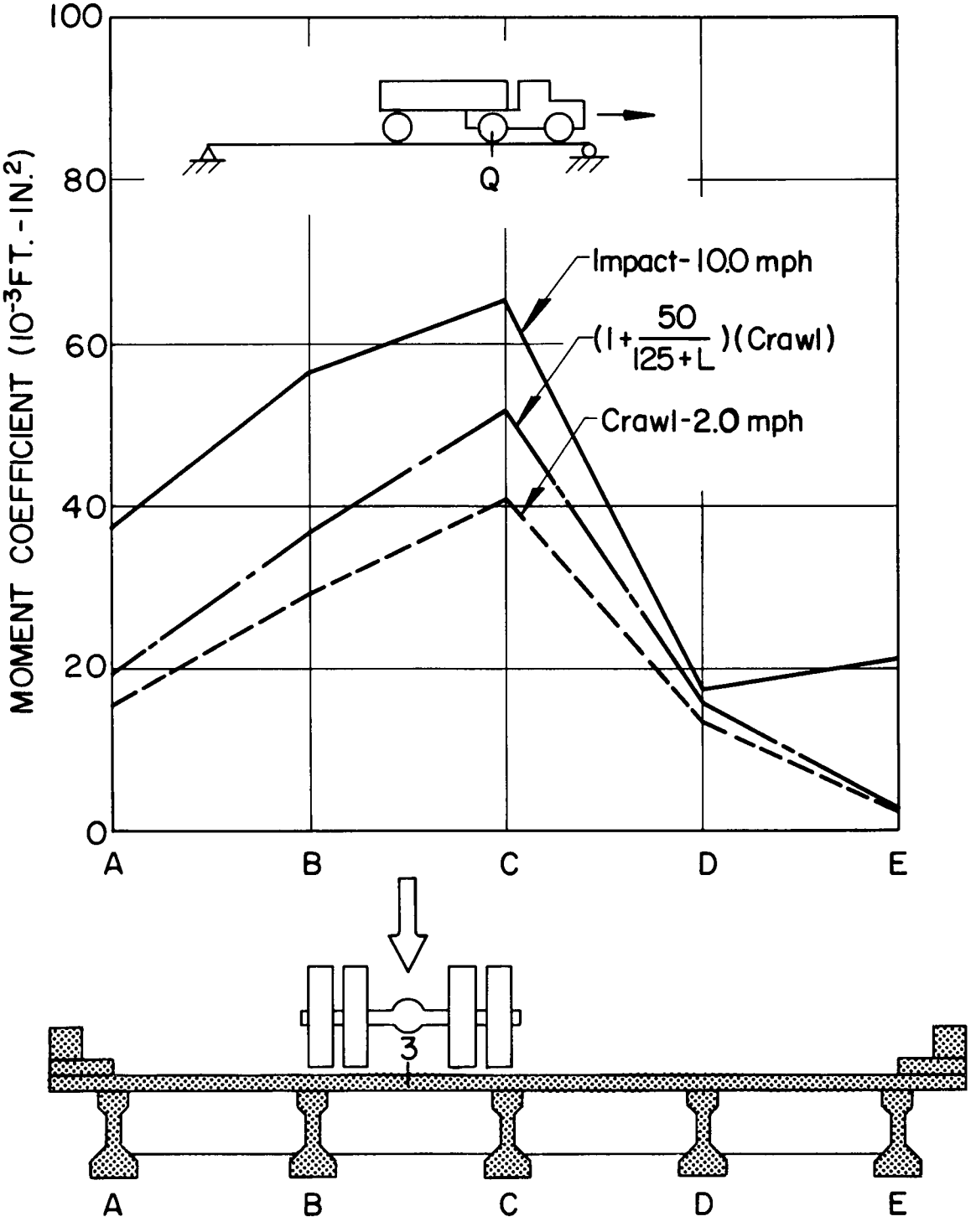

Fig. 43 Amplification of Girder Moment Coefficients at Section Q, Truck in Lane 3

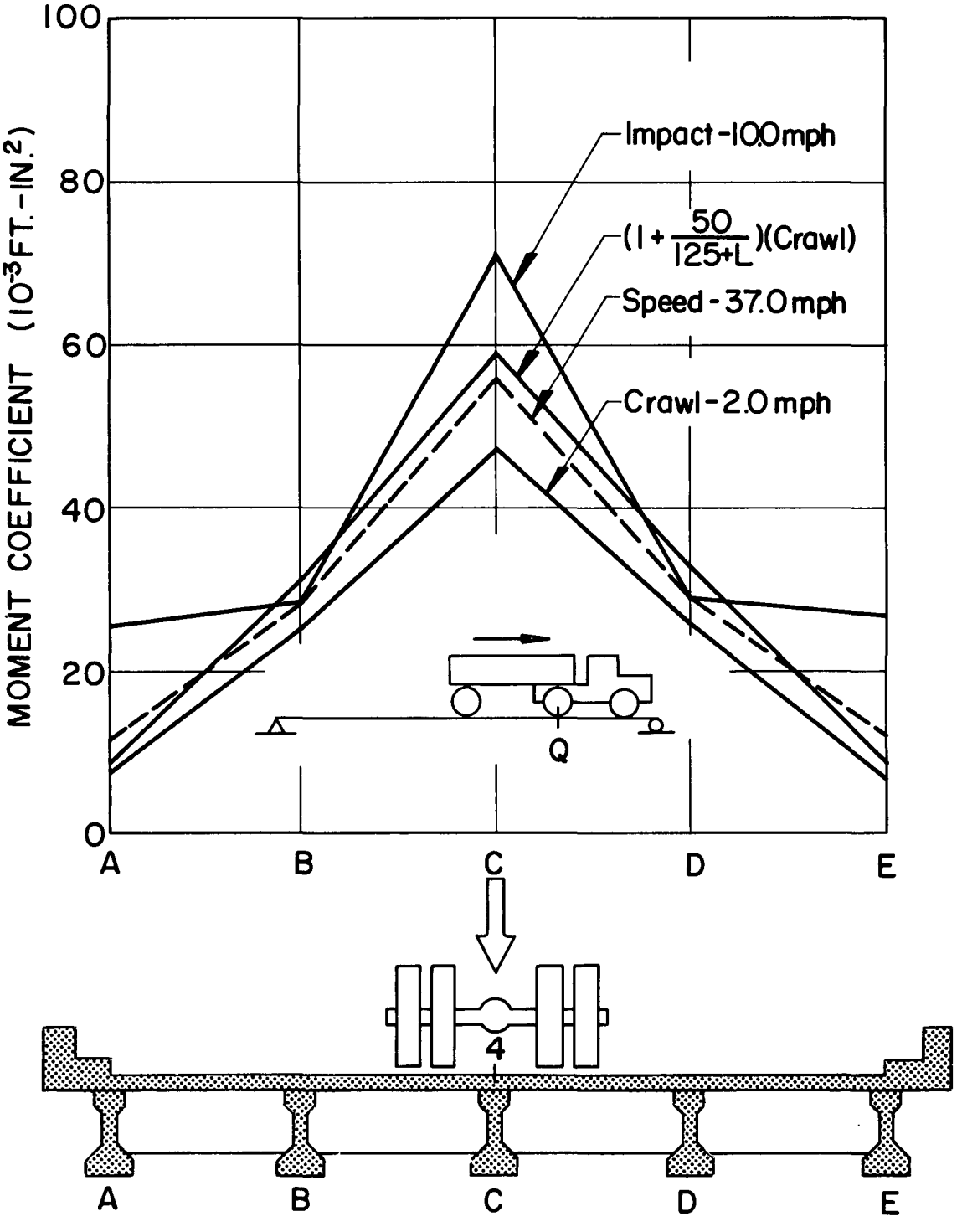

Fig. 44 Amplification of Girder Moment Coefficients at Section Q, Truck in Lane 4

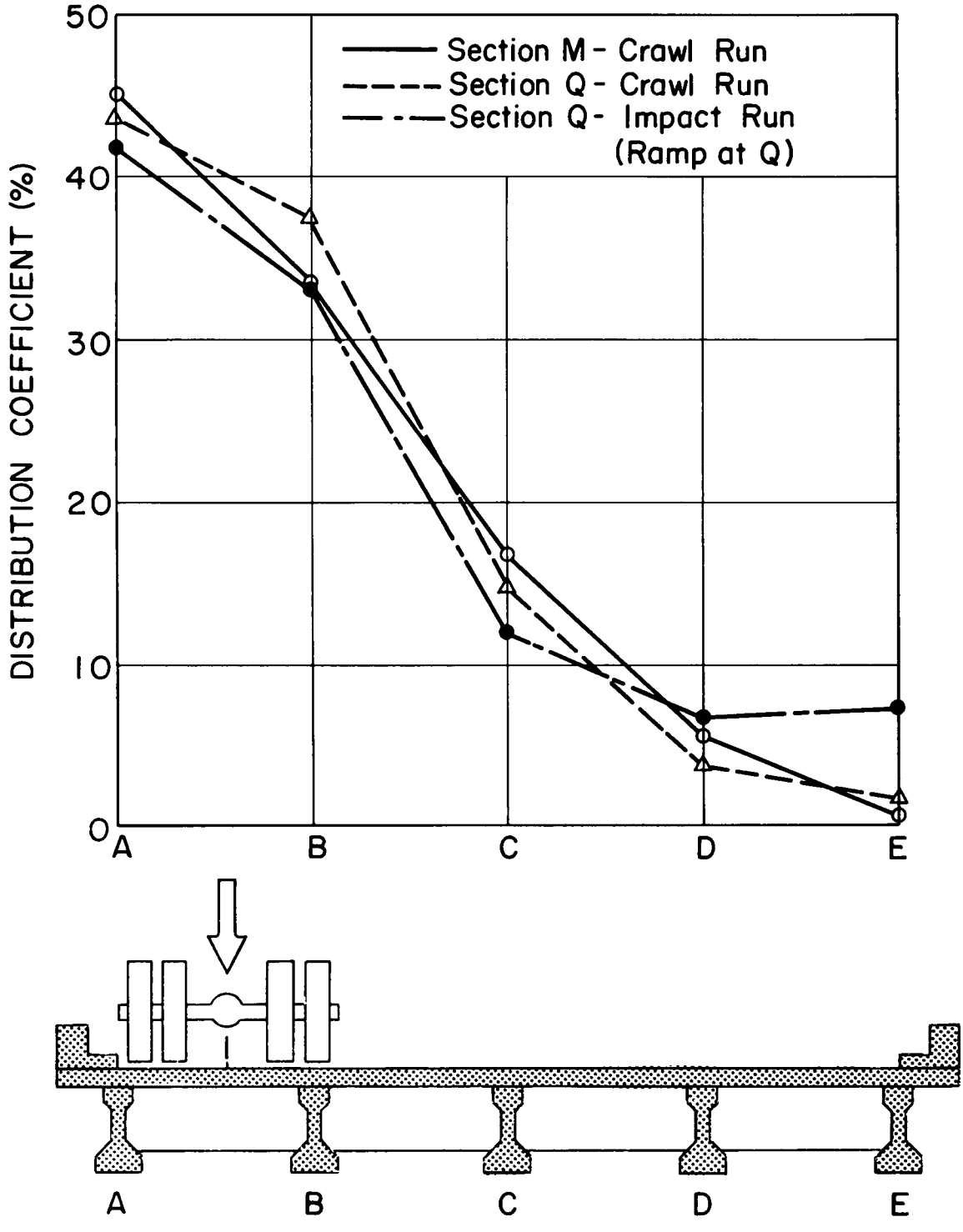

Fig. 45 Comparisons of Distribution Coefficients for Crawl Runs and Impact Runs, Lane 1

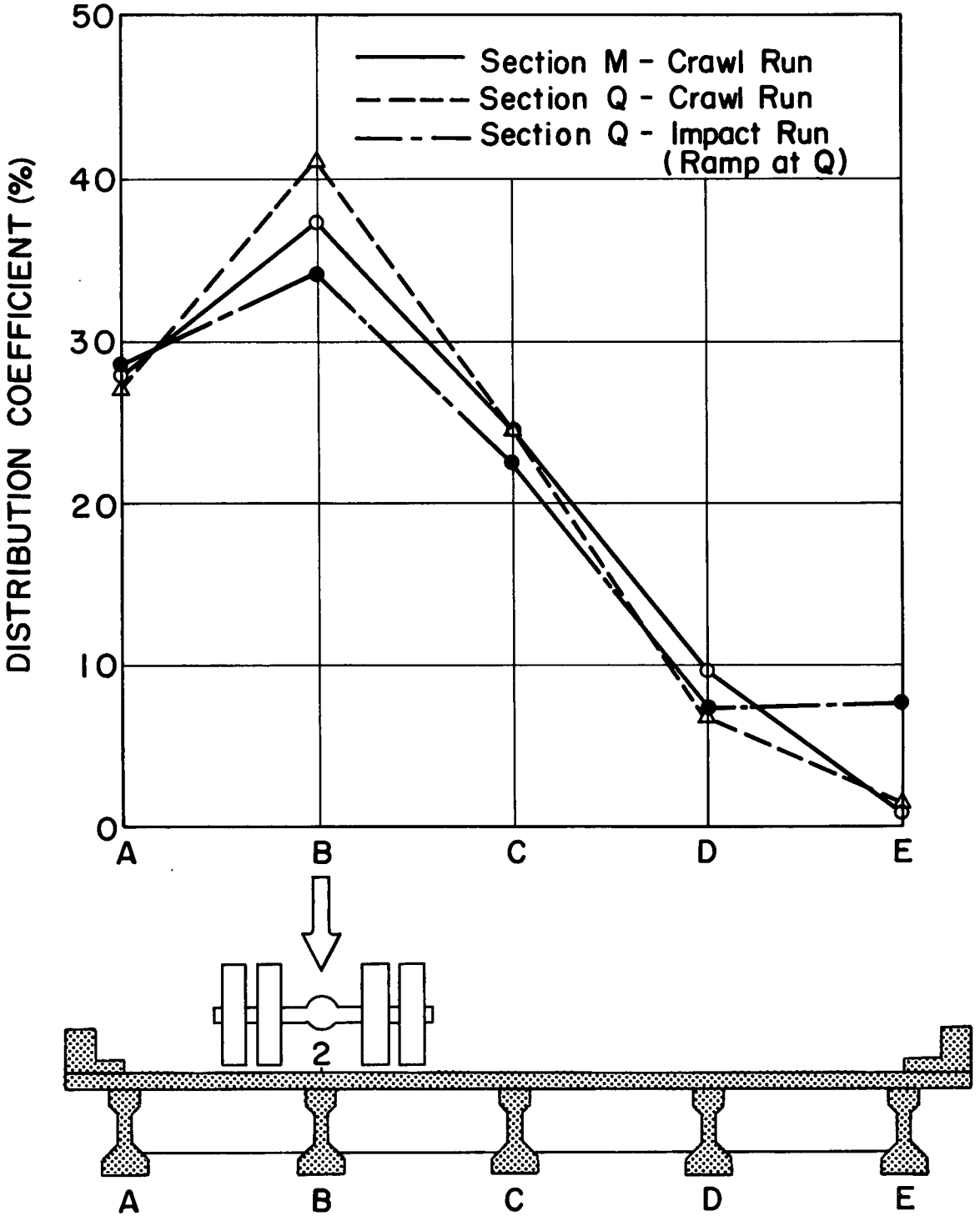

Fig. 46 Comparisons of Distribution Coefficients for Crawl Runs and Impact Runs, Lane 2

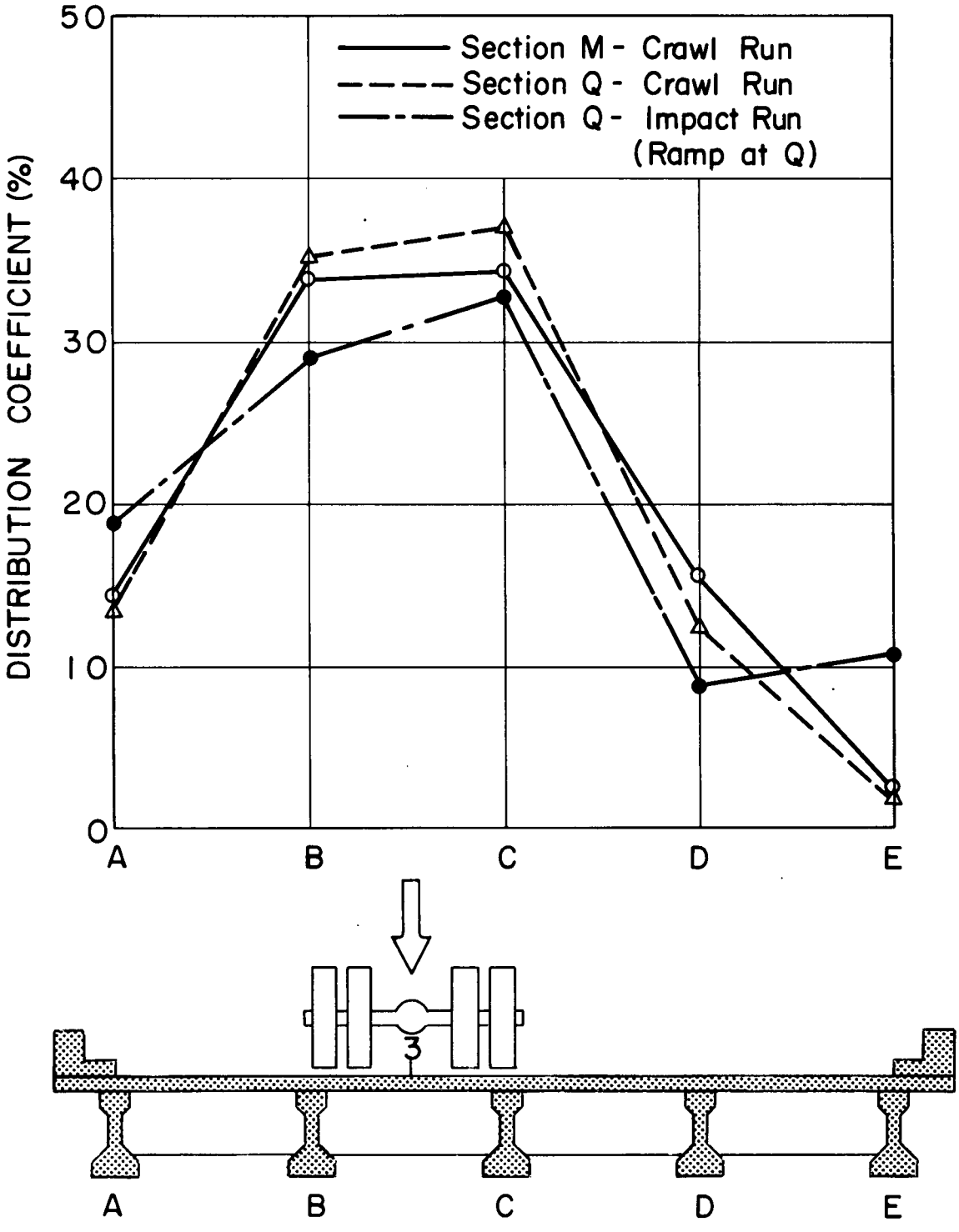

Fig. 47 Comparisons of Distribution Coefficients for Crawl Runs and Impact Runs, Lane 3

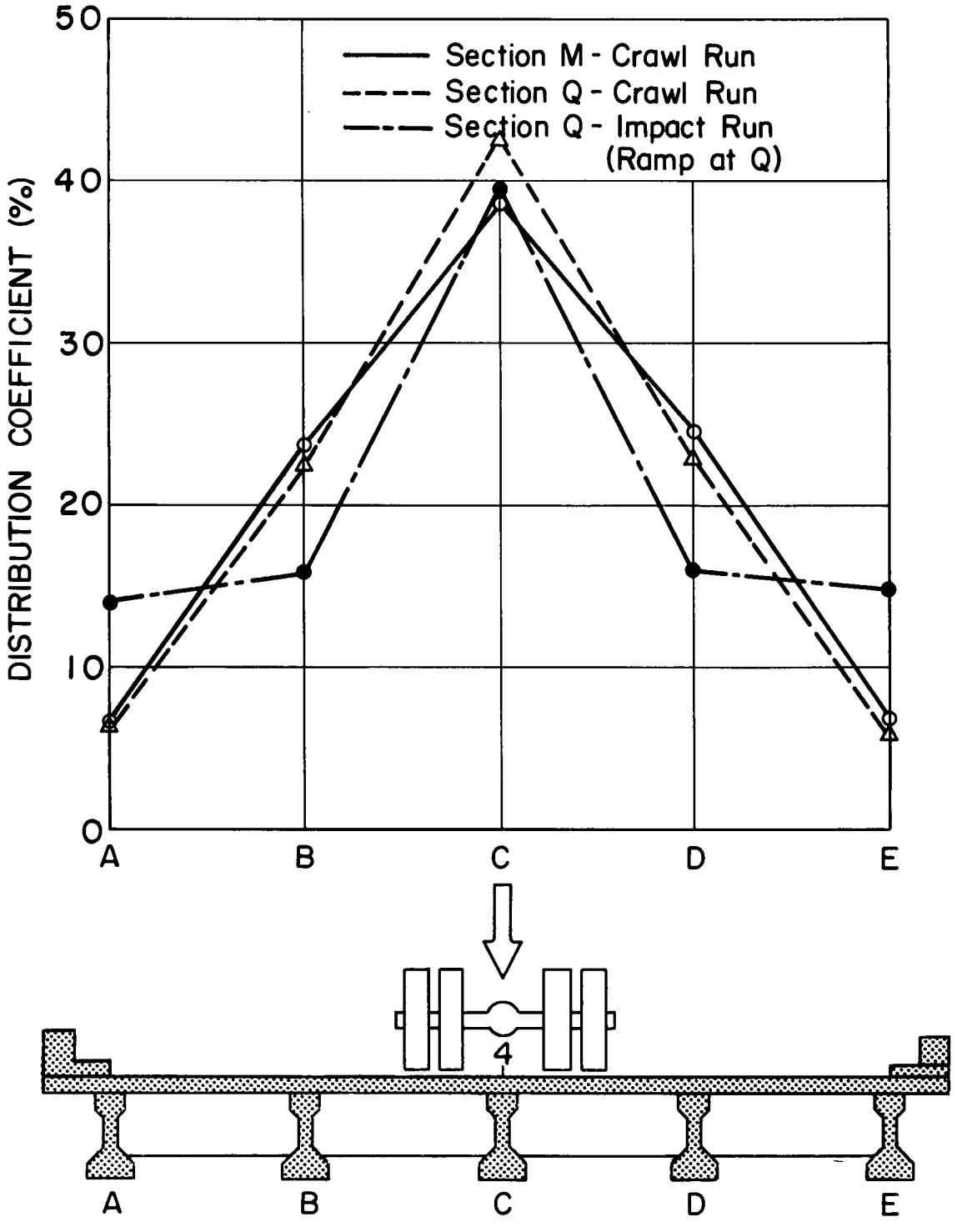

Fig. 48 Comparison of Distribution Coefficients for Crawl Runs and Impact Runs, Lane 4

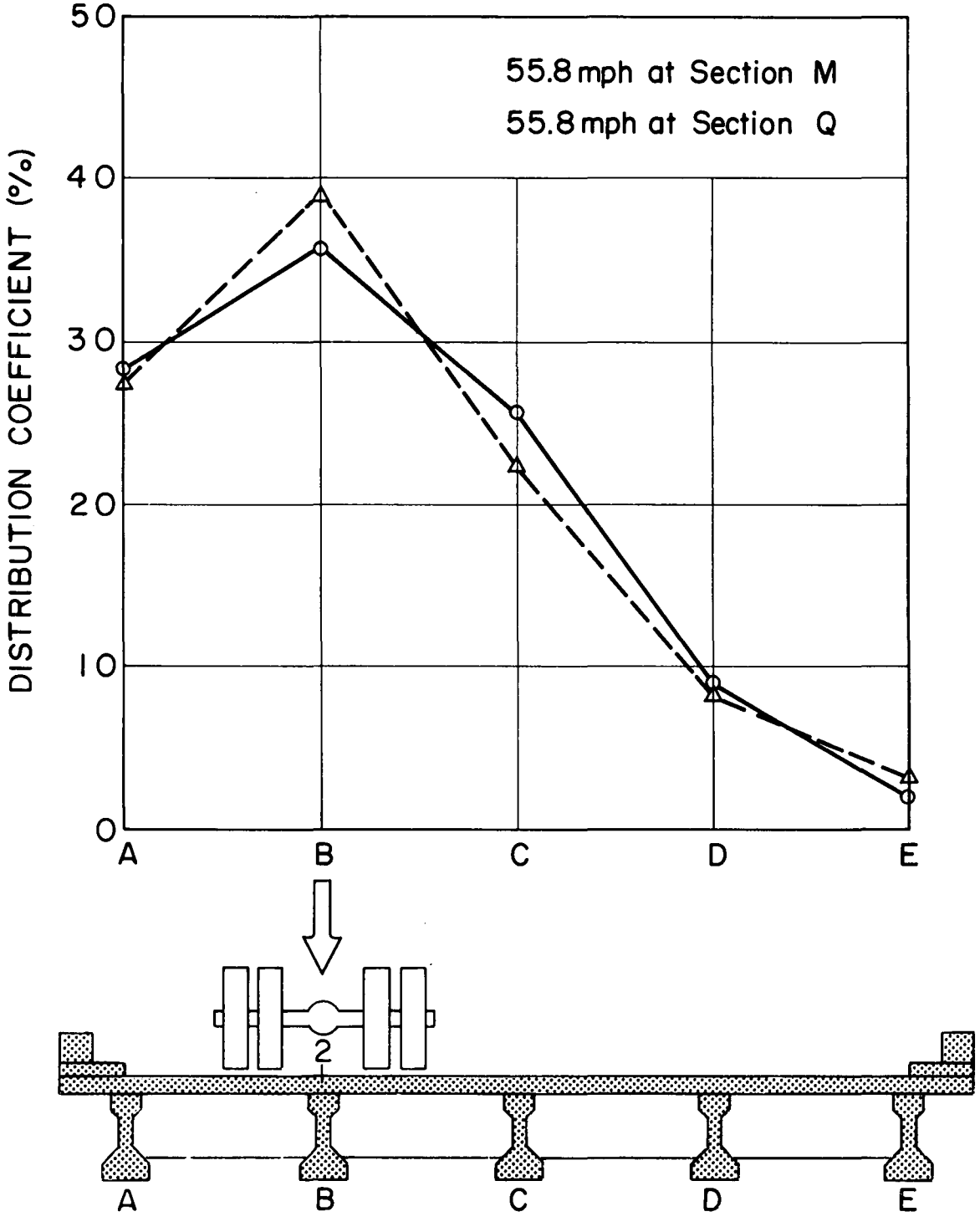

Fig. 49 Comparison of Distribution Coefficients for Speed Runs, Lane 2

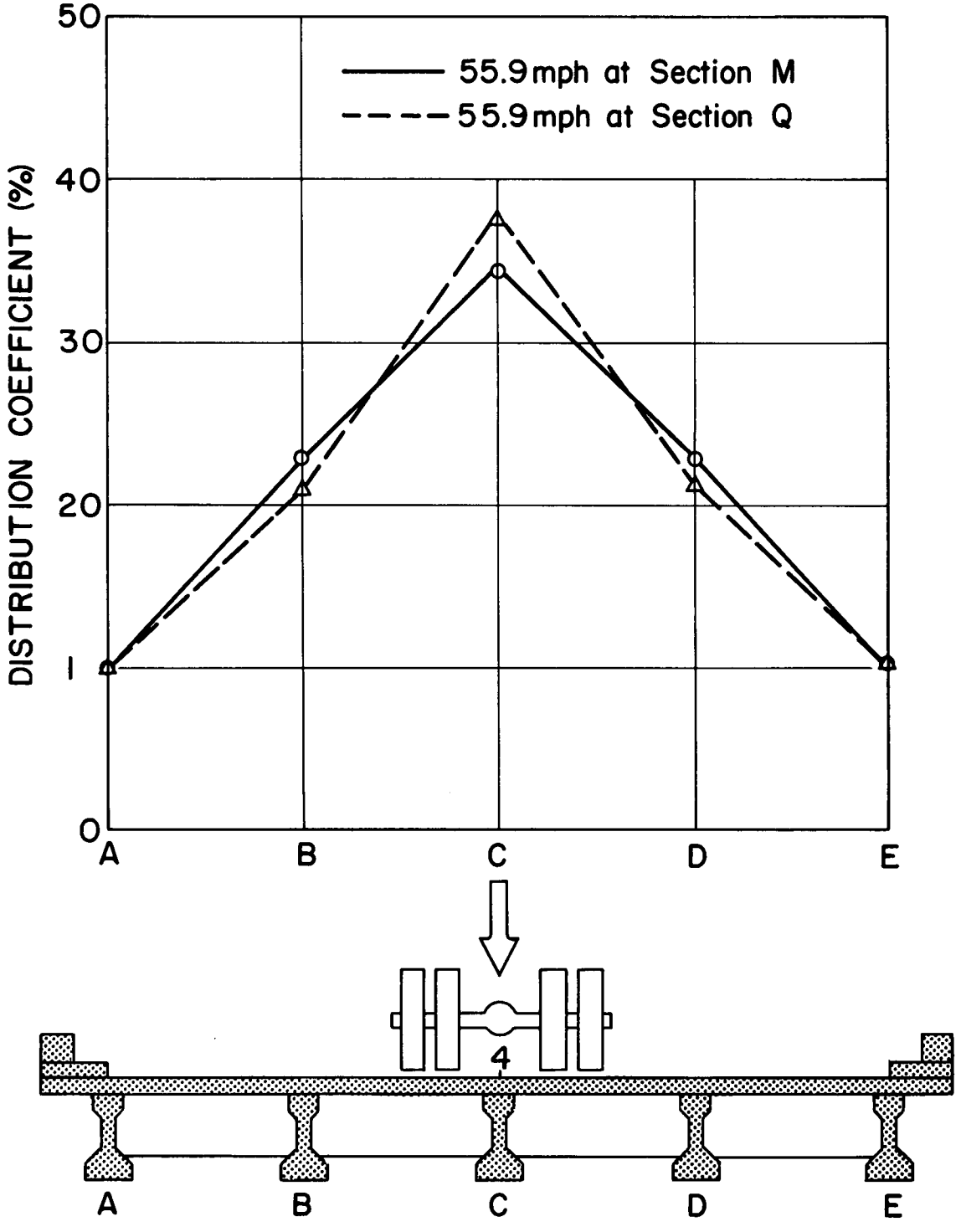

Fig. 50 Comparisons of Distribution Coefficients for Speed Runs, Lane 4

10. REFERENCES

1. Pennsylvania Department of Transportation, Bridge Division, STANDARDS FOR PRESTRESSED CONCRETE BRIDGES, 1960.

2. American Association of State Highway Officials STANDARD SPECIFICATIONS FOR HIGHWAY BRIDGES, Tenth Edition, Washington, D. C., 1969.

3. Douglas, W. J. and VanHorn, D. A. LATERAL DISTRIBUTION OF STATIC LOADS IN A PRESTRESSED CONCRETE BOX-BEAM BRIDGE, Fritz Engineering Laboratory Report 315.1, August, 1966.

4. Guilford, A. A. and VanHorn, D. A. LATERAL DISTRIBUTION OF DYNAMIC LOADS IN A PRESTRESSED CONCRETE BOX-BEAM BRIDGE - DREHERSVILLE BRIDGE, Fritz Engineering Laboratory Report 315.2, February, 1967.

5. Guilford, A. A. and VanHorn, D. A. LATERAL DISTRIBUTION OF VEHICULAR LOADS IN A PRE-STRESSED CONCRETE BOX-BEAM BRIDGE - BERWICK BRIDGE, Fritz Engineering Laboratory Report 315.4, October, 1967.

6. Schaffer, T. and VanHorn, D. A. STRUCTURAL RESPONSE OF A 45° SKEW PRESTRESSED CONCRETE BOX-GIRDER HIGHWAY BRIDGE SUBJECTED TO VEHICULAR LOADING - BROOKVILLE BRIDGE, Fritz Engineering Laboratory Report 315.5, October, 1967

7. Lin, Cheng-Shung and VanHorn, D. A. THE EFFECT OF MIDSPAN DIAPHRAGMS ON LOAD DISTRIBUTION IN A PRESTRESSED CONCRETE BOX-BEAM BRIDGE - PHILADELPHIA BRIDGE, Fritz Engineering Laboratory Report 315.6, June, 1968.

8. VanHorn, D. A. STRUCTURAL BEHAVIOR CHARACTERISTICS OF PRESTRESSED CONCRETE BOX-BEAM BRIDGES, Fritz Engineering Laboratory Report 315.8, June, 1969.

9. Linger, D. A. and Hulsbos, C. L.
DYNAMICS OF HIGHWAY BRIDGES, Joint Publication Bulletin No. 188, Iowa Engineering Experiment Station Bulletin No. 17, Iowa Highway Research Board.

10. Rowe, R. E.
CONCRETE BRIDGE DESIGN, John Wiley and Sons, Inc., 1962.

11. Rowe, R. E.
SUPPLEMENT TO CONCRETE BRIDGE DESIGN, John Wiley and Sons, Inc., 1962.

12. Motarjemi, D. and VanHorn, D. A.
THEORETICAL ANALYSIS OF LOAD DISTRIBUTION IN PRE-STRESSED CONCRETE BOX-BEAM BRIDGES, Fritz Engineering Laboratory Report 315.9, October, 1969.

13. Biggs, John M.
INTRODUCTION TO STRUCTURAL DYNAMICS, McGraw-Hill Book Company, 1964.

14. Lin, T. Y.
DESIGN OF PRESTRESSED CONCRETE STRUCTURES, June, 1963.

15. ACI Building Code
ACI STANDARD BUILDING CODE REQUIREMENTS FOR REINFORCED CONCRETE, June, 1963.

16. Sanders, W. W. and Elleby, H. A.
DISTRIBUTION OF WHEEL LOADS ON HIGHWAY BRIDGES, National Cooperative Highway Research Program Report 83, Iowa State University, Ames, Iowa, 1970.

17. Fang, S. J., Macías Rendón, M. A. and VanHorn, D. A.
ESTIMATION OF BENDING MOMENTS IN BOX-BEAM BRIDGES USING CROSS-SECTIONAL DEFLECTIONS, Fritz Engineering Laboratory Report 322.2, June, 1968.

18. Macias Rendon, M. A. and VanHorn, D. A.
A STRUCTURAL MODEL STUDY OF LOAD DISTRIBUTION IN BOX-BEAM BRIDGES, Fritz Engineering Laboratory Report 322.1, May, 1968.

19. Biggs, J. M., Suer, H. S. and Louw, J. W.
VIBRATION OF SIMPLE-SPAN HIGHWAY BRIDGES, Transactions of American Society of Civil Engineers, Vol. 124, 1959.

20. Aktas, Z. and VanHorn, D. A.
BIBLIOGRAPHY ON LOAD DISTRIBUTION IN BEAM-SLAB HIGHWAY BRIDGES, Fritz Engineering Laboratory Report No. 349.1, September, 1968.

21. Chen, Y. and VanHorn, D. A.
STRUCTURAL BEHAVIOR OF A PRESTRESSED CONCRETE BOX-BEAM BRIDGE, HAZLETON BRIDGE, Fritz Engineering Laboratory Report No. 315A.1, December, 1970.